MOLECULAR RESPONSES OF LUNG CANCER TO IONIZING RADIATION: INVESTIGATION OF THE BIGUANIDE METFORMIN IN COMBINATION WITH IONIZING RADIATION.

YARYNA STOROZHUK, B.Sc.

A Thesis Submitted to the

School of Graduate Studies

In Partial Fulfillment of the Requirements

For the Degree

Masters of Science

McMaster University

Yaryna Storozhuk- McMaster University Masters of Health Science (2012). Hamilton, Ontario (Medical Science)

TITLE: MOLECULAR RESPONSES OF LUNG CANCER TO IONIZING RADIATION: INVESTIGATION OF THE BIGUANIDE METFORMIN IN COMBINATION WITH IONIZING RADIATION

AUTHOR: Yaryna Storozhuk, B.Sc. (Honours Biology Program) (McMaster University)

SUPERVISOR: Dr. Theodoros Tsakiridis, MD, Ph.D.

NUMBER OF PAGES: vi, 137

ABSTRACT

Lung cancer (LC) remains a leading cause of cancer mortality. More than 80% of LC patients are affected by non-small cell LC (NSCLC). Despite high dose conventional radiotherapy in combination with chemotherapy, NSCLC shows poor local response, indicating a need to develop new effective and well tolerated adjuncts to radiotherapy.

Radiotherapy (RT) is a common therapeutic modality for the treatment of epithelial tumors of lung, prostate, and breast origin but these tumours demonstrate resistance to ionizing radiation (IR), fail to arrest cell cycle to repair DNA damage, and continue to proliferate under genotoxic stress. IR-induced double strand DNA breaks (DSB)s lead to activation of the kinase Ataxia Telangiectasia Mutated (ATM), which phosphorylates in the nucleus histone H2Ax (γH2Ax), a signal for recruitment of molecular DNA repair complexes. ATM stimulates IR-induced cycle arrest through activation of checkpoint kinases (Chks), p53, and cyclin-dependent kinase inhibitors (CDKI)s such as $p21^{cip1}$ and $p27^{kip1}$. Additionally, ATM regulates the pro-survival and radio-resistance pathway of Akt - mammalian target of rapamycin (mTOR), which controls gene transcription, and translation and cell survival.

Previous research from our laboratory showed that in cancer cells IR activates the energy sensor AMP-activated kinase (AMPK) pathway a key, evolutionally preserved, kinase that regulates the expression of p53, $p21^{cip1}$ and $p27^{kip1}$ and mediates a cell cycle checkpoint under conditions of metabolic stress. Our work suggested that AMPK is also a sensor of genomic stress and showed that IR activates AMPK acutely in epithelial cancer cell cultures to transduce signals through a DNA damage response (DDR)-mediated ATM-AMPK-p53-$p21^{cip1}$ axis and mediate cell cycle arrest and radio-sensitization.

The first part of my laboratory work aimed to verify the role of AMPK in the propagation of DDR signals using genetically modified cell models lacking the catalytic subunit of AMPK (AMPK$\alpha^{-/-}$ mouse embryonic fibroblasts (MEFs). I observed that lack of AMPK causes deregulated stimulation of both ATM and Akt-mTOR indicating that AMPK plays vital role in normal propagation of DDR and growth pathways stabilizing the expression and activity of both upstream (ATM) and downstream (p53/p21^{cip1} and Akt-mTOR) signals.

Work of other members of our laboratory showed that AMPK expression is tightly regulated by radiation in cancer cells. Based on that and the results of the above studies, I examined the chronic regulation of ATM-AMPK-p53/p21^{cip1} pathway in human lung tumour xenografts. I observed significant stimulation of expression and activity of this pathway in radiated tumours that is sustained for a long time (up to 8 weeks) following treatment.

Given its widely reported anti-cancer properties and evidence that metformin (MET) inhibits tumour growth likely through modulation of the AMPK and mTOR signaling pathways, we examined whether this biguanide can enhance radiation responses in lung cancer cells and whole tumours. MET inhibited survival of various human cancer cell lines of breast, prostate and lung origin. However, lung cancer cell lines portrayed significantly higher sensitivity to the cytostatic actions of this agent at doses that can be clinically achievable and well tolerated in humans. MET enhanced sensitivity of lung cancer cell lines to clinical doses of IR in a dose dependent manner, while combination treatment of MET and IR produced highest inhibition of lung cancer tumour growth compared to either treatment alone. MET simultaneously inhibited Akt and up-regulated AMPK and ATM activity, while propagation of those pathways was further enhanced by combined MET and IR treatment. Further, the combined MET+IR induced

higher expression of apoptosis markers and the greater inhibition angiogenesis in lung tumours compare to each treatment alone.

Overall, we concluded that:

i. **IR leads to long-term up regulation of AMPK-p53-p21cip axis while inhibiting Akt-mTOR pro-survival pathway. Functional AMPK is required for propagation of DNA damage response pathways upon exposure to IR.**

ii. **MET has a strong potential to act as an effective adjuvant to radiotherapy in treatment of human lung cancer.**

ACKNOWLEDGMENTS

I would first like to thank my supervisor, Dr. Theodoros Tsakiridis for his guidance in this project and support throughout the two years. I would also like to thank my supervisory committee members, Dr. Gurmit Singh and Dr. Hal Hirte for their suggestions and ideas on carrying out the experiments effectively. I would also like to express my appreciation for Dr. Evangelia Tsiani and Carly Barron from Brock University for their help and collaboration.

I want to thank all staff and students on the 4th floor of Juravinski Cancer Centre for their guidance in techniques and support in carrying out the experiments. A big thank you to radiology technician staff in the clinical unit 21-I in the cancer centre for their help with performing radiation on cells and on animals- their help and collaboration was an integral part of this research project.

Lastly, I would want to express the biggest gratitude towards my family, for their never-ending love and support and constant belief in my abilities to achieve the goals I put in front of me. My parents have always believed in me and my successful career as a scientist, and for that- I am forever grateful.

TABLE OF CONTENTS

CHAPTER 2

LIST OF ABBREVIATIONS

4E-BP1 Eukaryotic Initiation Factor 4E Binding Protein 1
ACC Acetyl Coenzyme-A Carboxylase
ADP Adenosine diphosphate
AICAR 5-aminoimidazole-4-carboxamide riboside
ANOVA Analysis of variance
AMP Adenosine monophosphate
AMPK AMP-Activated Protein Kinase
AMPK-/- AMP-Activated Protein Kinase α1/α2 Knockout
AT Ataxia Telangiectasia
ATCC American Type Culture Collection
ATM Ataxia Telangiectasia Mutated
ATP Adenosine Triphosphate
ATR Ataxia Telangiectasia and Rad3 Related
BER Base Excision Repair
Ca2+ Calcium Ion
CaMKK Calmodulin-Dependent Protein Kinase Kinase
CC Compound C
CC3 Cleaved Caspase 3
CDK Cyclin-Dependent Kinase
CDKI Cyclin-Dependent Kinase Inhibitor
Chk 1/2 Check Point Kinases 1/2
CPT-1 Carnitine-Palmitoyl Transferase-1
60Co Cobalt Radiotherapy Unit
C02 Carbon Dioxide
DMEM Dulbecco's Modified Eagle's Medium
DMSO Dimethyl Sufoxide
DNA Deoxyribonucleic Acid
DNA-PK DNA Protein Kinase
DSB Double Strand Break
EEF2K Eukaryote Elongation Factor 2 Kinase
EGF Epidermal Growth Factor
EGFR Epidermal Growth Factor Receptor
ERK Extracellular Signal-Regulated Kinase
FAS Fatty Acid Synthase
FBS Fetal Bovine Serum
FoxOForkhead Family of Transcription Factor
GADD Growth Arrest and DNA Damage Gene
Gy Gray
H2AX Histone H2A Family Member
H+ Hydrogen Ion
HIF-1α Hypoxia-Inducible Factor-1α
HR Homologous Recombination
HMG-CoA Hydroxy-3-Methyl-Glutaryl-CoA Reductase
IGF-I Insulin-like Growth Factor-I

IR Ionizing Radiation
JNK c-Jun N-terminal Kinase
LKB1 Liver Kinase B1
NAD+ Nicotinamide Adenine Dinucleotide
MAPK Mitogen-Activated Protein Kinase
MAPKKK Mitogen-Activated Protein Kinase KinaseKinase
MEF Mouse Embryo Fibroblasts
MET Metformin
MMR Mismatch Repair
MO25 Scaffolding Mouse 25 Protein
MRE11 Meiotic Recombination 11
mSIN1 Mammalian Stress-Activated Protein Kinase InteractingProtein 1
mTOR Mammalian Target of Rapamycin
NBS1 Nijmegen Breakage Syndrome 1
NER Nucleotide Excision Repair
NHEJ Non-Homologous End-Joining
NSCLC Non-Small Cell Lung Cancer
PBS Phosphate Buffered Saline
PGC 1α Peroxisome Proliferator-Activated Receptor GammaCo-activator 1-Alpha
Pi Phosphate Group
PI Propidium Iodide
PI3K Phosphoinositide-3 Kinase
PIKK Phosphoinositide 3-Kinase Related Protein Kinase
PIP Phosphatidylinositol/Phosphoinositide Phosphate
PTEN Phosphate and Tensin Homolog
PVDF PolyvinylideneDifluoride
TBS Tris Buffered Saline
TBS-T Tris Buffered Saline-Tween 20
Rb Retinoblastoma Protein
ROS Reactive Oxygen Species
RPMI Roswell Park Memorial Institue Media
S6K p70-S6 Kinase
SCLC Small Cell Lung Cancer
SDS Sodium Dodecyl Sulfate
SDS-PAGE SDS-Polyacrylamide Gel Electrophoresis
SSB Single Strand Break
STRAD Ste20-Related Adaptor Protein
TCA Tricarboxylic Acid Cycle
TAK1 Transforming Growth Factor β Activated Kinase
TSC Tuberous Sclerosis Complex
ULK1 Unc-51-Like Kinase 1
WT Wild Type

FIGURE LEGEND

Hypothesis and Objectives

"AMP-activated protein kinase (AMPK) is a mediator of acute and long-term radiation responses in lung cancer. AMPK responses to radiation treatment are further enhanced by biguanide agent metformin, which modulates molecular pathways of DNA damage repair, metabolic stress and tumour growth in human lung cancer cells and tumours".

Specific objectives:

1) To investigate in lung cancer cells the role of AMPK in the response of molecular pathways of DNA damage and survival to ionizing radiation.

2) To evaluate the chronic regulation of AMPK and its effector pathways by ionizing radiation in human lung cancer xenografts.

3) To examine the response of lung cancer cells to clinically relevant doses of metformin.

4) Evaluate the ability of metformin to enhance radiation responses in lung cancer cells and tumours.

CHAPTER 1

INTRODUCTION

Lung Cancer: Etiology and Statistics

Lung cancer has been the most common cancer worldwide since 1985, both in terms of incidence and mortality. Globally, lung cancer is the largest contributor to new cancer diagnoses (1,350,000 new cases and 12.4% of total new cancer cases) and to death from cancer (1,180,000 deaths and 17.6% of total cancer deaths) (Wilkinson et al, 2010). The five year survival rate for lung cancer is 15.6% in Canada, and although there has been some improvement in survival during the past few decades, the survival advances that have been realized in other common malignancies have yet to be achieved in lung cancer. There has been a large relative increase in the numbers of cases of lung cancer in developing world, accounting for 49% of globally diagnosed lung cancer incidences (Wilkinson et al, 2010)

The main risk factor for developing lung cancer is tobacco exposure through smoking, while numerous occupational hazards and environmental pollutants, such as radon radiation exposure, asbestos, zinc, iron oxides, chromium and uranium exposures also play a significant role in lung tumorigenesis (Buchagen, 1991).

Lung tumours are carcinomas that originate in respiratory epithelium and are histologically subdivided into two main types: non-small cell lung carcinomas (account for 75% of diagnosed lung cancer cases), while 10-15% of cases are comprised of small cell lung carcinomas (Wilkinson et al, 2010).

1.1 Non- small cell lung carcinoma

Seventy five percent of all lung tumours are non-small cell lung cancers (NSCLC) which usually lack the neuroendocrine features that characterize the SCLC tumors and are classified according to their cell of origin (Wilkinson et al, 2010).

The three main subtypes of NSCLC include: adenocarcinomas, squamous cell carcinomas and large cell carcinomas. As an overall class of lung cancer, NSCLCs are relatively insensitive to chemotherapy and radiation therapy compared with SCLC (Wilkinson et al, 2010).

Squamous cell or epidermoid carcinomas account for 25% to 30% of all diagnosed lung cancer cases. These cancers start in cells at early stages of developing the squamous cell phenotype, which are flat cells that line lumen of the lung airways (Wilkinson et al, 2010). They are often linked to a history of smoking and present frequently in the lumen of main airways in the lung hilum but are also found in lung periphery occasionally associated with cavitations of lung parenchyma (lung bullae).

Adenocarcinomas comprise nearly 40% of lung cancers, which arise in major bronchi and consist of mucin – containing and secreting cells (Travis, 2011). This type of lung cancer occurs in smokers (or previous smokers), however, adenocarcinomas are also the most common type of lung cancer seen in non-smokers.

Large cell carcinomas account for about 10% to 15% of lung cancers, and usually appear in any part of the lung. Large cell carcinomas tend to have a significantly faster growth and rate and higher metastatic potential, making this type of cancer highly resistant to conventional treatment options employed in lung cancer therapy (Travis, 2011).

1.1.2 Small Cell Lung Cancer

Approximately 15% of all lung cancer cases are comprised of small cell lung carcinomas. Unlike non-small cell lung carcinomas, small cell lung cancer (SCLC) often starts in the bronchi near the center of the chest develop mainly in the large airways and tend to metastasize early in the course of the disease (Travis, 2011). These cancer cells have significantly faster proliferation rate and increased metastatic potential in comparison to NSCLC. They usually spread early lymph nodes and other organs, such as the bones, brain, adrenal glands, and liver. Due to high metastatic potential, surgical resection or localized radiotherapy is rarely employed in patients with SCLC, and either treatment provides poor outcomes (Travis, 2011).

1.2 Molecular Signalling Alterations and Development of Lung Cancer

Lung carcinogenesis, similarly to any tumorigenic progression, is a multistage process involving alterations in multiple genes and diverse pathways. Inherited polymorphisms in a variety of genes, most notably the carcinogen metabolism genes, may affect the susceptibility of an individual to develop lung cancer, particularly in combination with environmental exposures. Genes involved with DNA repair, cell growth, signal transduction, and cell cycle control may all be damaged at different stages of lung tumor progression. Mutational activation of oncogenes and inactivation of tumor suppressor genes, and subsequent increased genetic instability are major genetic events in lung carcinogenesis (Massion et al, 2003). The most common early genetic alterations in non-small cell lung cancer involve loss of genomic regions of chromosomes 3p and 9p, deletions of chromosomal arm on 5p and mutations of p53 and K-Ras oncogene activation (Massion et al, 2003).

It is now generally accepted that transformation of lung epithelial cells requires inactivation of multiple tumor suppressor genes. One of the main tumour suppressor genes altered in lung cancer progression is p53 protein, which has been well established as the guardian of cellular genomic stability. Recently published studies have concluded that mutations or alterations in functions of p53 protein are found in 80-90% of SCLC and in up to 70% of NSCLC depending on the histological types examined (Massion et al, 2003).

1.2.1. Ras superfamily and K-Ras oncogenic mutations

Ras is a membrane-associated guanine nucleotide-binding protein that is normally activated in response to the binding of extracellular signals, such as growth factors, RTKs (Receptor Tyrosine Kinases), TCR (T-Cell Receptors) and PMA (Phorbol-12 Myristate-13 Acetate). Ras signalling affects many cellular functions, which includes cellular proliferation, apoptosis, migration, fate specification, and differentiation (Riley et al, 2012).

Ras acts as a binary signal switch cycling between ON and OFF states, which are characterized in terms of a small molecule, a guanine nucleotide, bound to the protein. In the resting cell, Ras is tightly bound to GDP (Guanosine Diphosphate), which is exchanged for GTP (Guanosine Triphosphate) upon binding of extracellular stimuli to cell membrane receptors (Romeo et al, 2012). In the GTP-bound form, Ras interacts specifically with so-called effector proteins, thereby initiating cascades of protein-protein interactions that may finally lead to cell proliferation. To return to the inactive OFF state, Ras cleaves off the terminal phosphate moiety, the Gamma-Phosphate, of GTP in an enzymatic process, the intrinsic GTPase reaction. The remaining GDP-bound Ras is no longer able to interact with effectors; it is switched OFF (Romeo et al, 2012).

Ras is thought to activate a number of signalling pathways, including the Raf/MEK/ERK (Extracellular Signal-Regulated Kinases) pathway, the MEKK/SEK/JNK (Jun N-terminal Kinases) pathway, a PI3K (Phosphatidylinositol 3-Kinase)/Akt/NF-Kappa B (Nuclear Factor-Kappa B) pathway, a p120-GAP/p190-B/Rac/NF-KappaB pathway, and a Raf/MEKK1/IKK (I-KappaB Kinase)/I-KappaB/NF-KappaB pathway (Romeo, 2012).

Reactive free radicals and cellular redox stress have been proposed to directly activate Ras. NO (Nitric Oxide) promotes the direct post translational modification of Ras by single S-nitrosylation at Cys118 (Mansi et al, 2011). These results in stimulation of guanine nucleotide exchange, possibly by destabilization associates with other effectors, leading to transduction of Ras mediated signals through multiple pathways. In addition to Raf, PI3K and RalGDS other Ras effectors have been proposed, including p120GAP, PKC-zeta, Rin1, AF6, and NF1 GAP (Figure 1) (Mansi et al, 2011).

The Raf protein kinase family controls the activation of the MAPK (Mitogen-Activated Protein Kinases) pathway and plays a major role in controlling proliferation and differentiation. The PI3K mediates some of the Ras-dependent actin cytoskeleton remodelling and protection against apoptosis. The Ras-Raf-MEK-ERK pathway features several oncogenes and is deregulated in approximately 30% of human lung adenocarcinomas and large cell carcinomas, but infrequently in squamous cell carcinomas and only rarely in small cell lung cancer (SCLC) (Mansi et al, 2011).

The K-Ras proto-oncogene, one of the first genes found to be altered in lung cancers, is activated by point mutation in about 30% of human lung adenocarcinomas and large cell

carcinomas, but infrequently in squamous cell carcinomas and only rarely in small cell lung cancer (SCLC) . The predominant K-Ras mutation detected in human lung adenocarcinomas is a GC to TA transversion in the first base of codon 12 (Zhang and Wang, 2011).

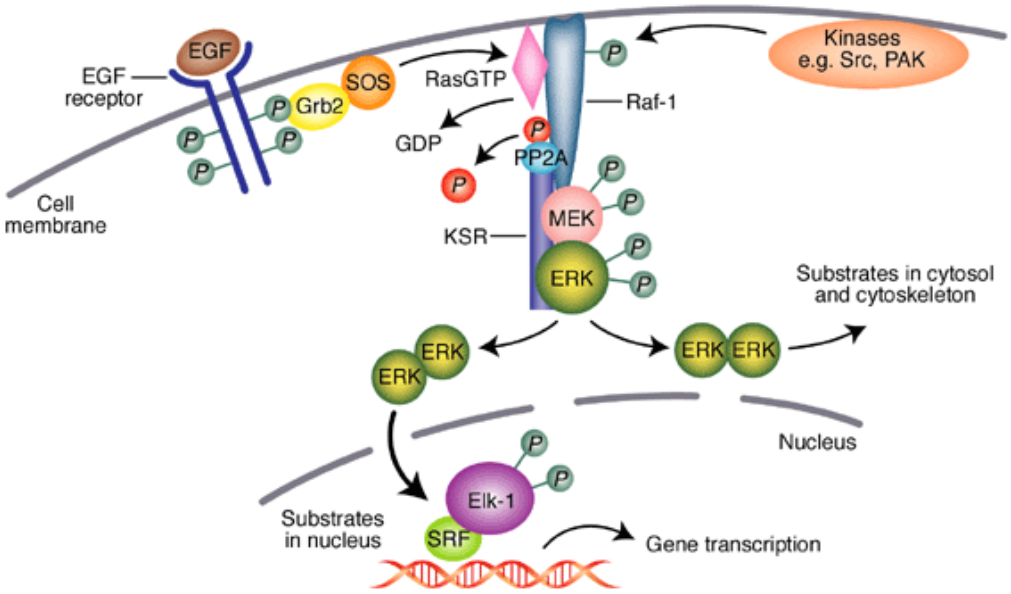

Adapted from Kolch, 2002

Figure 1. Most growth factors that signal through receptor tyrosine kinases (RTKs) or heterotrimeric GPCR (G-Protein Coupled Receptors) stimulate Ras by recruiting the GEF (Guanine-Nucleotide Exchange Factor) to the membrane. GTP-bound Ras recruits and activates Raf, initiating a cascade of protein phosphorylation by first phosphorylating MEKs, followed by ERK. Phosphorylated ERK moves from the cytoplasm into the nucleus where it subsequently phosphorylates a number of transcription factors and up regulates gene expression involved in cell growth and survival. In addition to RAF pathway, Ras kinase also activates PI3K-Akt pathway, activation of which leads to subsequent signal propagation, resulting in cell proliferation and survival.

1.3 PI3K/Akt Pro- Survival Pathway

The PI3K signalling pathway regulates the activities of a broad range of downstream molecular effectors, which in turn act synergistically to mediate a number of cell behaviours and properties in both normal and pathological conditions.

There are three classes of PI3Ks that differ in structure and function. The class I is the most intensely studied and includes p110α, β, γ, and δ catalytic isoforms, which are controlled by coupling with their proper regulatory isoforms (p85 and p101) to affect their lipid kinase activity (Sheppard et al, 2012). The PI3K activation in terms of signalling response varies according to the type of stimulus. For example, p110α and δ are recruited and activated at the plasma membrane upon activation of tyrosine kinase receptors (TKRs) whereas p110γ requires engagement of G-protein-coupled receptors (GPCR). Conversely, p110β can be activated by both TKRs and GPCR (Markman, 2010).

The PI3K signalling pathway can be activated by growth-factor stimulation of various receptor tyrosine kinases, including EGF receptors, human EGF receptor 2 and IGF-1 receptors among many others (Sheppard et al. 2012). Activation of these receptor tyrosine kinases leads to the formation of secondary adaptor complexes, recruitment of PI3K to the plasma membrane through the binding of the SH2 domain of p85 to the phosphotyrosine residues on adaptor proteins, and the release of the p110 catalytic subunit from inhibition by the regulatory subunit (McNamara and Degterev, 2011). Once activated, PI3K enzymes catalyze the phosphorylation in position 3 of the inositol ring of phosphoinositides, resulting in the generation of 3-phosphoinositides, mainly the phosphatidylinositol-3-trisphosphate (PIP3). These lipids act as docking sites for the recruitment at plasma membrane of protein-bearing pleckstrin homology

(PH) domain such as Akt/PKB, PDK1, BTK, and PLCγ (McNamara and Degterev, 2011). Once bound to PIP3 lipids, these proteins turn activated and signal to a wide array of downstream effectors that ultimately leads to multiple cellular responses (Sheppard et al, 2012). This signalling cascade can be antagonized by the action of the phosphatase and tensin homolog (PTEN), a widely recognized tumor suppressor which dephosphorylates the PIP3 (Sheppard et al, 2012).

Multiple mechanisms contribute to the regulation of cell function by PI3K effectors, however, the two best studied proteins that respond to the PIP3 generation are Akt kinase (protein kinase B) and phosphoinositide-dependent kinase 1 (PDK1) (Figure 2) (Zhu and Zhou, 2010). Both of these proteins contain PH domains and accumulate at the membrane after PI3K activation. Their localization to the plasma membrane brings these enzymes into close proximity with one another, promoting Akt phosphorylation by PDK1 (Zhu and Zhou, 2010).

1.3.1 Akt

Akt, a serine/threonine kinase, is the central mediator of the PI3K pathway with multiple downstream effectors that influence key cellular processes. Three Akt isoforms are expressed in humans (Akt 1-3). All Akt family members share a similar domain structure with an N-terminal plekstrin homology domain, a linker domain, a central kinase domain, and a C-terminal hydrophobic domain. In order to be fully activated, Akt requires phosphorylation at two specific amino acid residues, threonine 308 and serine 473, located in the kinase domain and C-terminal hydrophobic domain, respectively (Chen and Li, 2010). Phosphorylation is achieved by the action of two independent protein kinases: phosphatidylinositol-dependent kinase 1 (PDK1), which

phosphorylates threonine 308 and the mammalian target of rapamycin complex-2 (mTORC2), which phosphorylates serine 473 (Chen and Li, 2010).

Upon phosphorylation and activation of kinase, Akt then phosphorylates a variety of downstream targets in the cytoplasm including glycogen synthase kinase (GSK), Bad, forkhead family of transcription factor (FoxO), PAK1, cAMP response element-binding protein (CREB), p27, and Mdm2 (Brazil et al., 2004). Akt stimulates protein synthesis and cell growth by activating mTOR (as part of the mTOR-raptor or mTORC1 complex) through effects on the intermediary tuberous sclerosis (TSC) 1/2 complex. The enzyme influences cellular proliferation by inactivating cell cycle inhibitors $p27^{kip1}$ and $p21^{cip1}$ and promoting activation of cell cycle proteins (c-Myc and cyclin D1) (Shimura, 2011). Phosphorylation of downstream targets by Akt has been shown to increase cell proliferation, motility, protein synthesis, and gluconeogenesis as well as inhibit apoptosis. Akt has also been shown to target nuclear proteins directly, including transcription factors and nuclear receptors leading to a unique signalling network (Trotman et al., 2006) (Figure 2). Akt signalling is extinguished by phosphatases, including PHLPP1 (Gao et al., 2005) and PP2A (Trotman et al., 2006).

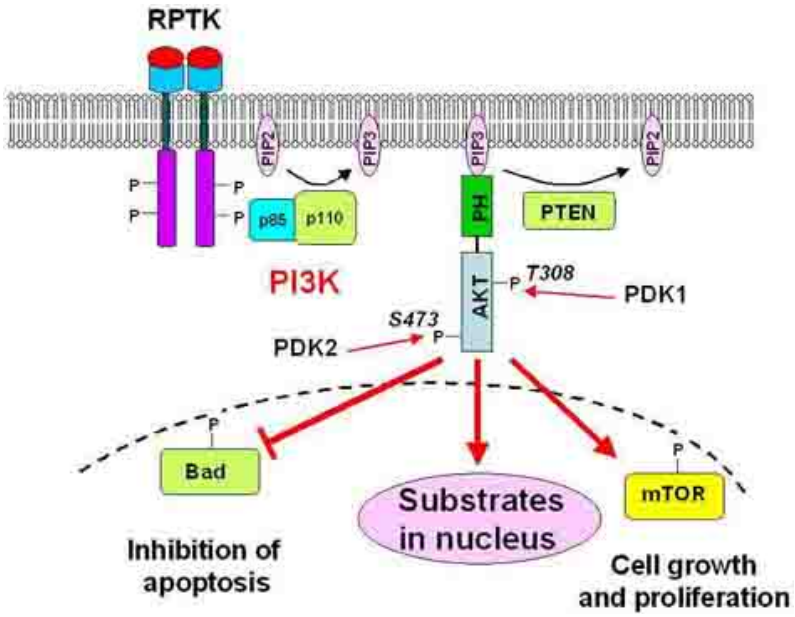

Adapted from Meier et al, 2005.

Figure 2. Schematic representation of the PI3K-AKT (AKT) signalling pathway. An extracellular factor such as a growth factor interacts with its receptor protein tyrosine kinase (RPTK) resulting in autophosphorylation of tyrosine residues. Phosphatidylinositol-3 kinase (PI3K) consisting of an adaptor subunit p85 and a catalytic subunit p110 is translocated to the cell membrane and binds to phosphotyrosine consensus residues of the RPTK through its adaptor subunit. This results in allosteric activation of the catalytic subunit leading to production of phosphatidylinositol-3,4,5-triphosphate (PIP3). PIP3 recruits signalling proteins with pleckstrin homolgy (PH) domains to the cell membrane including AKT. PTEN (phosphatase and tensin homologue deleted from chromosome 10) is a PIP3 phosphatase and negatively regulates the PI3K-AKT pathway. The interaction of PIP3 with the PH domain of AKT likely induces conformational changes in AKT, thereby exposing the two main phosphorylation sites at T308 and S473. T308 and S473 phosphorylation by protein serine/threonine kinase 3'-phosphoinositide-dependent kinases 1 and 2 (PDK1 and PDK2) is required for maximal AKT activation. Activated AKT translocates to the nucleus and mediates the activation and inhibition of various targets resulting in cellular survival and cell growth and proliferation.

1.3.2. AKT involvement in cell cycle regulation

Deregulated cell cycle progression has been implicated in development of numerous cancers. Various researchers have concluded a positive link between PI3K/Akt signalling and deregulation of cell cycle progression by affecting key cell cycle progression proteins such as $p21^{Cip1}$, $p27^{Kip1}$, and Cyclin D1 (Shimura et al, 2011).

Recently, it has been shown that Akt has the ability to control $p21^{Cip1}$ protein stability by marking the effector for degradation through ubiquitin-mediated or ubiquitin-independent pathways (Chang et al, 2003). Moreover, The PI3K/Akt pathway has also been implicated in altering $p27^{Kip1}$ activity. Expression of dominant negative mutations in Akt in mesenchymal cells causes transcriptional induction of $p27^{Kip1}$, which leads to the inhibition of both Cdk2 activity and DNA synthesis. However; these effects were not observed in an endothelial cell model (Chang et al, 2003).

The forkhead family of transcription factors (TFs) has recently been categorized into the forkhead box factor (FOX) family. The FOX family includes AFX/FOXO4, FKHR/FOXO1, and FKHR-L1/FOXO3a. Akt can inactivate FOX TFs through direct phosphorylation of multiple S/T residues (Yang and Hung, 2011). As a result of these phosphorylation events, pro-apoptotic genes induced by FOX family transcription factors are down regulated, including both $p27^{kip1}$ and Fas (Shimura, 2011; Yang and Hung, 2011). Thus, the PI3K/Akt pathway prevents cell death by both inducing and repressing gene expression.

The PI3K/Akt pathway is also a strong activator of cyclin D1, a critical player in cell cycle progression. Cyclin D1 degradation occurs mainly through the ubiquitin-dependent proteolysis pathway triggered by phosphorylation. In order to be recognized by ubiquitin-conjugating

enzymes E1 and E2 for proteolysis, cyclin D1 must be phosphorylated at T286 near its carboxyl terminus (Shimura et al, 2011). GSK-3 is the primary kinase that phosphorylates cyclin D1 at this residue. Moreover, cyclin D1 phosphorylation at T286 by GSK-3 is also associated with the translocation of cyclin D1 from the nucleus to the cytoplasm. Rapid cyclin D1 degradation induced by GSK-3 is inhibited by activation of PI3K/Akt pathway because Akt directly phosphorylates and inactivates GSK-3 (Shimura et al, 2011).

1.3.3. Akt Activation and Radioresistance

The PI3-K/AKT pathway is frequently over-activated in many solid tumors such as NSCLC. PI3-K/AKT activation triggers a cascade of responses, which has consequences for all major cancer-cell growth mechanisms: survival, proliferation, and cell growth. Additional effects involve DNA double strand break repair and tumor angiogenesis through hypoxia-inducible factor 1α (HIF-1α) and vascular endothelial growth factor (VEGF) (Graves et al, 2010).

Ionizing radiation has been previously shown to rapidly activate kinases, and contributes to tumor cell viability. Sensitivity of tumor cells to radiation therapy is a critical determinant of the probability of local control and, ultimately, of cure (Tannock and Hill, 1998).

In some cell types, the antiapoptotic effects of EGFR receptor signalling have been attributed to activation of the PI3K/AKT pathway (Kainulainen et al., 2000). EGFR signalling to PI3K/AKT has been proposed to enhance the expression of the mitochondrial anti-apoptosis proteins Bcl-xL and Mcl-1 and caspase inhibitor proteins such as c-FLIP isoforms (Leverrier et al., 1999; Kuo et al., 2001; Panka et al., 2001).

1.3.4. Akt and Apoptosis

Programmed cell death or apoptosis is a tightly regulated mechanism within the cell. The Bcl-2 family of proteins are structurally and functionally related effectors that play a central role in apoptosis regulation, with molecules such as Bad and Bax acting as apoptosis promoting proteins, while Bcl-2 and Bcl-XL are regarded as antiapoptotic agents (Li at el, 2011).

Akt kinase is involved in promotion of cell survival by inhibiting actions of pro-apoptotic proteins. As an example, Akt is known to down regulate Bad activity by phosphorylating the protein on S112 residue (Chang et al, 2003). When Bad becomes phosphorylated, the marker is unable to form dimers with Bcl-2 protein; the dissociation of Bad-Bcl-2 complex leads to promotion of cell survival (Chang et al, 2003) (Figure 2).

1.3.5. mTOR

mTOR (the mammalian target of rapamycin), also known as FRAP is a 289 kDA serine/threonine kinase that belongs to the PI3K- related protein kinase (PIKKs) family. The protein encompasses two functionally distinct protein complexes: mTOR complex 1 (mTORC1) and mTOR complex 2 (mTORC2). mTORC1 consists of mTOR, raptor, mLST8, and two negative regulators PRAS40 and DEPTOR, while mTORC2 consists of mTOR, rictor, MLST8, mSIN1, and novel components Protor, Hsp70, and DEPTOR (Populo et al, 2012).

Complex I of the mTOR protein is activated by the PI3K/Akt kinase pathway and is mainly responsible for ribosomal biogenesis through phosphorylation of S6K and stimulation of protein synthesis by phosphorylation and inhibition of eukaryotic initiation factor 4E (eIF4E) binding protein 1 (4E-BP1) (Keith et al, 1995). P70S6K1 undergoes phosphorylation on Thr389 residue by mTORC1, leading to phosphorylation of 40S ribosomal protein S6, enhanced mRNA

translation and increased expression of ribosomal proteins, elongation factors as well as insulin growth factor 2 (Populo et al, 2012).

Unlike P70S6K1 kinase, 4EBP1 protein mainly functions as a repressor of protein translation. 4EBP1 inhibits the initiation of protein translation upon binding and inactivating elF4E (eukaryotic translation initiation factor 4E). When phosphorylated by mTORC1, 4EBP1 becomes dissociated from elF4E, allowing the cell to translate mRNAs into proteins and undergo G1-S transition of the cell cycle (Figure 3) (Populo et al, 2012).

In addition to main downstream targets, mTORC1 is known to regulate several crucial factors responsible for carcinogenic development, such as HIF-1α, $p21^{cip1}$ and $p27^{Kip1}$ cyclin-dependent kinase inhibitors, Rb and STAT 3 proteins (Huang et al, 2001; Nourse et al, 1994; Yokogami et al, 2000).

Complex II of the mTOR is activated by various growth factors, such as EGF, IGF, VEGF and PDGF, with the activated complex leading to phosphorylation of PKC-α and Ser473 residue of Akt protein (Sarbassov et al, 2004). Unlike mTORC1, complex II is highly resistant to macrolide fungicide and the widely used mTOR inhibitor rapamycin.

1.3.6. mTOR Activation

mTORC1 signalling cascade is activated upon phosphorylation of Akt kinase on Thr308 and Ser473 residues (Populo et al, 2012). Upon activation, Akt phosphorylates TSC2, which prevents formation of TSC1/TSC2 inhibitory complex allowing for activation of small GTPase protein Rheb. GTP-bound Rheb in turn leads to activation of mTORC1 through phosphorylation on Ser 2448 residue (Populo et al, 2012).

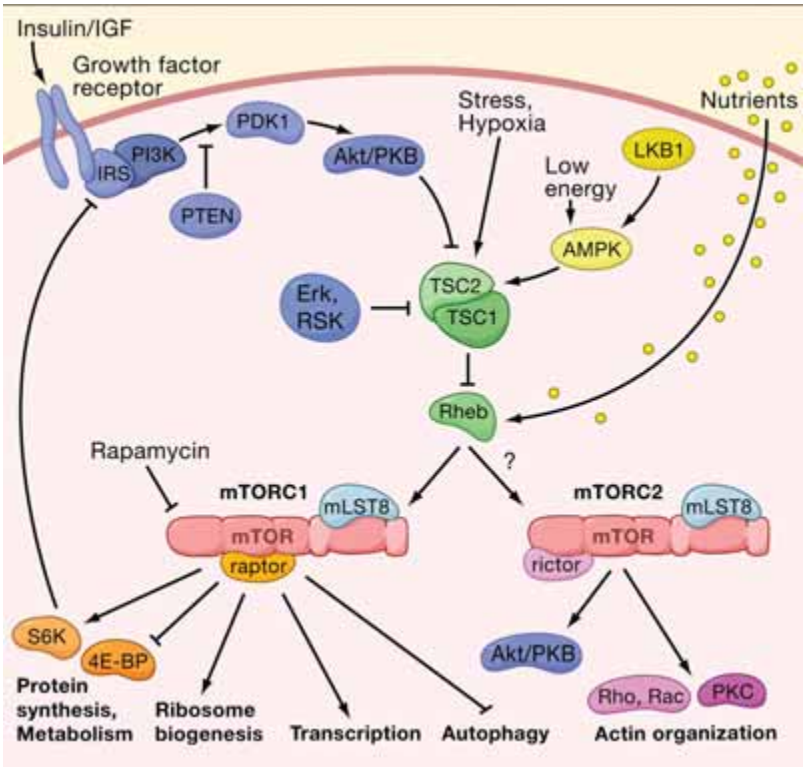

Adapted from Secko, 2006.

Figure 3. Activation and Regulation of mTOR pathway. mTOR kinase is composed of two distinct complexes: mTORC1 (mTOR, Raptor and mLST8) and mTORC2 (mTOR, rictor, MLST8). mTOR is activated by growth factor and hormone signalling (IGF) or through nutrient sensing. mTOR activation includes de-phosphorylation of TSC1/TSC2 complex by Akt pathway, while phosphorylation of TSC2 by AMPK inhibits activation. When activated, mTORC1 phosphorylates downstream targets S6K and 4E-BP1 proteins, involved in protein synthesis, translation, transcription and ribosome angiogenesis, while mTORC2 leads to phosphorylation of Akt pathway, resulting in positive feedback loop of the pathway.

1.4 Tumour Suppressors and Progression of NSCLC

1.4.1. P53

The TP53 tumor suppressor gene is located at the short arm of chromosome 17 (17p13). It contains 11 exons spanning 20 kilobases and encodes a nuclear phosphor-protein of 53kDa (Böhlig and Rother, 2010). The TP53 protein contains distinct functional domains: the N-terminus transactivation domain, the sequence-specific DNA-binding domain, the oligomerization domain, and the C-terminus negative regulatory domain (Miliani de Marval and Zhang, 2011). The TP53 gene has been implicated in a growing number of biological processes, including DNA repair, cell-cycle arrest, apoptosis, autophagy, senescence, metabolism, and aging (Zheltukhin and Chumakov, 2011).

The transcription factor TP53 can activate the transcription of numerous downstream genes, such as $p21^{cip1}$ and MDM2, by binding to specific sequences, which often mediates their biological functions. The induction and activation of p53 in response to cellular stresses have been shown to be largely regulated at posttranslational level through multiple mechanisms. Upon cellular stresses, p53 is phosphorylated at Ser-15, Ser-20, and Ser-46 residues, where NH2-terminal phosphorylation of p53 stabilizes the protein and converts it to an active form. On the other hand, protein phosphatases PP-1 and PP2A had an ability to dephosphorylate p53 and negatively modulated its activity (Maddocks and Vousden, 2011). Ser-15 has been shown to be phosphorylated by upstream kinases such as ATM (ataxia-telangiectasia mutated), ATR (ataxia-telangiectasia mutated and Rad3-related), Chk1 (checkpoint kinase 1), and DNA-PK (DNA-dependent protein kinase) (Zheltukin and Chumakov, 2011). The p53 suppressor gene is mutated commonly in human cancer, and inactivation of p53 protein tumor-suppressor activity seems to

be one of the most common molecular steps in the development of cancer. P53 mutations have been identified frequently in human lung cancers; the prevalence was reported to be highest in small cell carcinomas (>70%) and lowest in adenocarcinomas (33%) (Mogi and Kuwano, 2011).

The main transcription target of p53, which regulates G1/S arrest, is protein $p21^{cip1}$, which together with $p27^{kip1}$ and p57 creates family of proteins sharing the ability to inhibit a wide range of cyclin-dependent kinases (Cdk) and thus they can induce the cell cycle arrest. G1/S checkpoint is controlled by interaction of E2F protein (a member of essential transcription factors family) with pRb (retinoblastoma susceptibility protein). When $p21^{cip1}$ is not up-regulated, it does not inhibit cdk4 and cdk6, which in turn react with D-type cyclins and induce phosphorylation of pRb. This, in turn, leads to dissociation of pRb from the complex with E2F and the cell cycle can progress (Pollard et al, 2001). Thus, the main function of p21 is induction of cell cycle arrest. Moreover, it possesses other anti-proliferative functions as maintenance of differentiation and senescence and it is also capable of modulation of apoptosis by interaction with caspase-3 (Suzuki et al, 1998)

1.4.2. ATM

The ATM protein is a serine/threonine protein kinase and a member of the phosphoinositide 3-kinase-related protein kinase (PIKK) family (Flynn and Zou, 2011). All members of the PIKK family are large serine/threonine protein kinases involved in signalling following cellular stress. The other members of the PIKK family include ATR (ATM and Rad3 related protein kinase), DNA-PKcs (DNA-dependent protein kinase catalytic subunit), mTOR (mammalian target of rapamycin), and hSMG1 (Tichy et al, 2010). The protein was first identified in patients suffering from A-T disorder, an autosomal recessive disorder characterized

by progressive cerebellar ataxia, neurodegeneration, radiosensitivity, cell-cycle checkpoint defects, genome instability, and a predisposition to cancer (Lovejoy and Cortez, 2009). Cells isolated from A-T patients displayed abnormal telomere formations, defects in cell cycle progression and fusion of chromosomal ends (Lovejoy and Cortez, 2009).

ATM exists in an inactive dimer in undamaged cells, but following induction of DNA damage, or treatment with agents that alter chromatin structure, ATM undergoes an intermolecular auto phosphorylation on S1981 resulting in disassociation of the dimer into active monomer. Following DNA damage, ATM is rapidly recruited to sites of DNA double strand breaks (Derheimer and Kastan, 2010).

In addition to playing a central role in recruitment of repair machinery proteins to the sites of DNA double stranded breaks, ATM plays an important role in regulation of cell cycle progression. Following the induction of DNA double strand breaks in S-phase, ATM is known to activate CHK2 protein by phosphorylation on threonine-68, which leads to the phosphorylation of phosphatase CDC25A, resulting in its degradation and the inability to load Cdc45 on to replication origins necessary for the initiation of DNA replication (Lin and Liyang, 2010). The decrease in CDC25A following DNA damage results in an increase phosphorylation level of CDK2 resulting in degradation of CDK2 and thus delayed entry and progression through S-phase (Reinhardt and Yaffe, 2009).

The CHK2-mediated inhibition of the CDC25 family of phosphatases is also important for the activation of the G2/M checkpoint. In addition to the inhibition of the CDC25 family members, phosphorylation of Rad17 is critical to the induction of the G2/M checkpoints following exposure to ionizing radiation (Reinhardt and Yaffe, 2009).

1.4.3. Liver Kinase 1 (LKB1)

LKB1 is a serine/threonine kinase (formerly known as STK11) that contains two nuclear localization sequences, a central kinase domain, and a C-terminal farnesylation motif, where the N- and C-terminal non-catalytic regions share no similarities with other proteins. LKB1 activity is regulated by the pseudo kinase STE20-related kinase adaptor alpha (STRADα) and the scaffolding protein mouse protein 25 alpha (MO25) through a phosphorylation-independent mechanism (Ollia and Mäkelä, 2011). The canonical target of LKB1 is the energy regulated AMP-activated protein kinase (AMPK), though LKB1 phosphorylates other AMPK family members such as MAP/microtubule affinity-regulating kinases 1-4 and Snf1-like kinases (NUAK) 1 and 28 (Fan et al, 2009).

LKB1 functions as a tumour suppressor that regulates cell polarity, differentiation, and metastasis as well as responds to energy status to regulate cell metabolism (Alessi et al, 2006). One function of LKB1 directly linked to lung cancer is the phosphorylation, ubiquitination, and the degradation of polyomavirus enhancer activator 3 (PEA3). Mutant LKB1 increases the stability of PEA3, which, in turn, increases transcription of genes involved in metastasis, including COX-2, MMP-9, and MMP-14 (Upadhyay et al, 2006; Cowden Dahl et al, 2007).

1.5 AMP-activated protein kinase (AMPK)

AMP-activated protein kinase (AMPK) is a heterotrimeric enzyme that functions as a sensor of energy status that maintains cellular energy homeostasis. Recent work shows that the kinase is activated by increases not only in AMP, but also in ADP. Although best known for its effects on metabolism, AMPK has many other functions, including regulation of mitochondrial biogenesis and disposal, autophagy, cell polarity, and cell growth and proliferation.

Mammals have seven genes encoding AMPK; i.e., two isoforms of α (α1 and α2), two of β, (β1 and β2), and three of γ (γ1, γ2, and γ3). The subunits contain a typical serine/threonine kinase domain at the N terminus; as for many protein kinases, these only have significant activity when phosphorylated by upstream kinases at a conserved threonine residue within the activation loop (Thr 172 in human α1) (Hawley et al. 1996; Stein et al. 2000). The γ subunits contain the regulatory adenine nucleotide-binding sites and are composed of four tandem repeats of a sequence known as a CBS motif.

The major upstream kinase phosphorylating Thr 172, and thus activating AMPK, in most mammalian cells is a complex between the tumor suppressor kinase LKB1 and two accessory subunits, STRAD and MO25 (Hawley et al. 2003; Woods et al. 2003; Shaw et al. 2004). Binding of AMP causes conformational changes in AMPK that promote its activation via three independent mechanisms: (1) promotion of Thr 172 phosphorylation (Oakhill et al. 2010), (2) inhibition of Thr 172 dephosphorylation (Suter et al. 2006; Oakhill et al. 2010), and (3) allosteric activation of AMPK already phosphorylated on Thr 172 (Suter et al. 2006).

1.5.1. AMPK activation

AMPK is activated by metabolic stresses that either interfere with catabolic generation of ATP (e.g., glucose deprivation, hypoxia, ischemia, and treatment with metabolic poisons) or accelerate ATP consumption (e.g., muscle contraction), thus increasing cellular ADP: ATP and AMP: ATP ratios (Hardie, 2007). In addition to its role in the regulation of energy balance in a cell-autonomous manner, AMPK is also modulated by numerous hormones and/or cytokines that regulate energy balance at the whole body level, including leptin, adiponectin, insulin, and ghrelin (Kahn et al, 2005).

As activation of AMPK enzyme requires phosphorylation of Thr172 residue on catalytic α subunit, numerous kinases that might lead to phosphorylation of the residue have been identified. The best studied activator of AMPK is LKB1, followed by calmodulin-dependent protein kinase-β (CaMKK-β), which phosphorylates AMPK in response to increases in intracellular Ca2+ levels instead of AMP. As the master cellular energy switch, AMPK activation promotes catabolic processes while inhibiting energy-consuming anabolic metabolism. In this capacity, AMPK is known to phosphorylate/inhibit Acetyl-CoA carboxylase (ACC) at Ser79, which, in turn, relieves the inhibitory effects of ACC on fatty acid oxidation, an important ATP-producing process (Steinberg, 2009). AMPK is also known to inhibit phosphorylation of mTOR at its activating residue Ser 2448, thereby shutting down protein synthesis, an ATP-consuming process.

1.5.2. AMPK role in Cancer

Due to its role in maintaining energy balance, a dysfunction in AMPK signalling pathway may result in systemic perturbations that contribute to development of metabolic disorders. In support, there is a strong correlation between low AMPK activation state, mainly due to over-nutrition and lack of exercise, and metabolic disorders associated with insulin resistance, obesity and sedentary lifestyle (Ruderman and Prentki, 2004).

Epidemiological analyses indicate that treatment with the anti-diabetic drug metformin may reduce the cancer burden in diabetic type 2 patients (reviewed in (Billaud and Viollet, 2008; Fogarty and Hardie, 2009) have led to the notion that activation of AMPK by various pharmacological agents may find clinical applications in cancer chemoprevention and therapy. The main hypothesis behind the role of AMPK in prevention of oncogenesis lies in the down regulation of mTORC1 by phosphorylation via LKB1-AMPK pathways (Viollet et al, 2010).

AMPK impacts mTOR via phosphorylation and activation of the TSC2 which negatively regulates mTOR activity resulting in inhibition of mTOR signalling, a reduction in phosphorylation 4EBP1 and p70S6K1, and an inhibition of global protein synthesis and proliferation in a number of different cancer cell lines (Dowling et al, 2011).

1.5.3. AMPK –mediated regulation of cell cycle progression

Recent research utilizing AMPK activation by the widely used AMP-mimetic 5-aminoimidazole-4-carboxamide ribonucleoside (AICAR) has been shown to cause cell cycle arrest in hepatoma HepG2 cells (Liang et al. 2007) and mouse embryonic fibroblasts (Jones et al. 2005). AICAR induced activation of AMPK in cultured tumor cells was found to cause a G1–S-phase cell cycle arrest that involved up-regulation and/or stabilization of p53 and the cyclin-dependent kinase inhibitors $p21^{Cip1}$ and $p27^{Kip1}$ (Jones et al., 2005; Liang et al., 2007).). These effects were proposed to be the result of activation of the AMPK and subsequent phosphorylation of p53 at Ser 15 (Jones et al., 2005) and of $p27^{Kip1}$ at Thr 198 (Liang et al., 2007).

1.5.4. AMPK-mTOR regulation

In response to sensing low ATP levels within the cell, mTORC1 activity is inhibited though phosphorylation of TSC2 protein by AMPK. Phosphorylation of TSC2 leads to formation of TSC1/TSC2 complex and subsequent inhibition of Rheb GTPase. In addition to AMPK involvement in inhibition of mTORC1 complex as a response of low cellular energy levels, AMPK inhibits mTORC1 complex upon sensing increased hypoxia environment through HIF-1α dependent transcript REDD1(Easton and Houghton, 2006).

While TSC2 is clearly a central receiver of a wide variety of positive and negative inputs that regulate mTORC1, cells lacking TSC2 still partially suppress mTORC1 following AMPK

activation, suggesting that additional AMPK substrates may directly or indirectly modulate mTORC1 activity (Hahn-Windgassen et al. 2005; Gwinn et al. 2008). Recent study performed by Gwinn and colleagues discovered the critical mTOR binding partner raptor acts a direct substrate of AMPK, and demonstrated that phosphorylation of raptor by AMPK at two highly conserved serines – Ser722 and Ser792 – induces their direct binding to 14-3-3, which leads to a suppression of mTORC1 kinase activity towards its downstream substrates (Gwinn et al., 2008).

1.6 Radiation and Radiation Therapy

Human cancer therapy has been one of the most challenging tasks in medicine and today three key therapeutic modalities are utilized in cancer treatment: surgery, chemotherapy and radiotherapy.

Radiotherapy is a key therapeutic modality for the treatment of a larger number of human cancers that is utilized in the majority of non-hematological malignancies at different stages of the disease. With cancer of the lungs being one of the most challenging cancers to successfully respond to conventional treatment options, such as surgery and radiotherapy, it remains of crucial importance to understand the impacts of radiotherapy on lung cancer on both physiological and molecular levels to further improve treatment options for the patients. One of the shortfalls of radiotherapy treatments in NSCLC patients is poor overall treatment outcome, with patients displaying less than 10% survival rate five years post radiotherapy treatment. Moreover, high rates of local tumour recurrence are the main reason behind high death rates in NSCLC patients.

1.6.1. Ionizing Radiation

Radiation is usually defined as energy with the ability to travel through physical matter in the form of waves or high speed particles (Tannock and Hill, 1998). Radiation energy takes the

form of electromagnetic waves (EM) with a broad spectrum, ranging from waves emitted by nuclear power plants, nuclear weapons, clinical radiation units to essential daily objects, such as microwaves, electrical power lines, cellular phones, and light emitted from the sun. Based on their frequency and place in the electromagnetic spectrum, radiation energy is typically subdivided into two main categories: non-ionizing and ionizing radiation. Non-ionizing radiation consists of low-frequency long EM waves that fall below the ultraviolet EM spectrum and typically consist of radiation emitted from electrical power lines, AM/FM radio frequencies, television sets and microwaves.

Unlike non-ionizing radiation, short EM waves with high frequencies belong to a class of ionizing radiation, with the waves having enough energy to knock electrons off atoms or molecules. The three main types of ionizing radiation are alpha particles, beta particles, and high energy photons (gamma rays are photons of a specific energy). Most of the particulate types of radiation are directly ionizing i.e. individual particles with adequate kinetic energy can directly disrupt the atomic structure of the absorbing medium through which they pass producing chemical and biological damage to molecules (Tannock and Hill, 1998).

High energy photos such as Gamma rays are electromagnetic radiation given off by an atom as a means of releasing excess energy. They are bundles (quanta) of energy that have no charge or mass and can travel long distances through air, body tissues, and other materials. The capability of high energy photons to do damage is a function of their energy, while the distance between ionizing events is large on the scale of the nucleus of a cell. For this, conventional radiotherapy treatments in cancer patients utilize high energy photons, delivered by Linear Accelerators, or γ-rays, delivered by $Cobalt^{60}$ radiotherapy units, to treat tumours (Tannock and Hill, 1998).

Radiotherapy is commonly divided into three distinct types: external beam radiotherapy (EBRT), brachytherapy, and systemic radioisotope therapy. The type of radiation therapy employed depends on the location of the radiation source delivered to the tissue. With ERBT, the photons travel outside the body, brachytherapy uses sealed radioactive sources placed precisely in the area under treatment, while systemic radioisotopes are given by infusion or oral ingestion.

1.6.2. IR effects on cellular pathways

The primary focus in radiotherapy is to induce permanent DNA damage in tumour cells that is mediated by double strand breaks which are typically fatal. Other effects of radiation are to: alter cellular homeostasis, modify signal transduction pathways, modify redox state, and to induce apoptosis. The aim of clinical radiotherapy delivery is to enhance the killing of tumor cells while reducing the probability of normal cell damage. Induction of DNA damage and generation of reactive species are the two main pathways by which IR exposure leads to cell death.

1.6.2.1. Generation of Reactive Oxygen Species

Exposure of cells to ionizing radiation leads to rapid generation of vast amounts of free radicals that arise in the process of energy absorption and breakdown of chemical bonds in molecules. These are known to play a major role in radiation effects on biological tissues and organisms and play a key role in numerous biological processes, such as metabolism, oxidation, reduction, and pathological diseases and oncogenesis. Free radicals generated by ionizing radiation can have direct and indirect effects on the cell. Direct cellular effects of the ionizing radiation result in immediate macromolecule damage, such as DNA damage, phospholipid damage of the cellular membranes, and initiation of intracellular signalling that leads to activation of apoptotic cellular pathways (Tannock and Hill, 1998).

Indirect effects of free radicals on the cell result in absorption of radiation energy by cellular water, known as water radiolysis. Interaction of radiation with water causes ionization and excitation process producing short-lived H2O+ radical-cations and electronically-excited water molecules (H2O+), which will undergo breakdown into hydroxyl (OH•) radical and free hydrogen atoms (H•) (Tannock and Hill, 1998). The breakdown of charged water leads to chain reactions of radicals with nearby water molecules, resulting in generation of highly reactive superoxide anion (O2•). High levels of superoxide species within the cell lead to extensive damage within cell's macromolecular structure, mainly phospholipids, DNA, proteins and carbohydrates (Tannock and Hill, 1998).

1.6.2.2. Ionizing Radiation and DNA Damage Response pathways

Ionizing radiation induces numerous DNA lesions, which include base damage, single-strand breaks (SSBs) and double-strand breaks (DSBs), which are considered to be the most lethal, since frequently DSB lead to permanent chromosomal damage.

The presence of DSBs leads to a cascade of post-translational modifications of a wide variety of proteins, including phosphorylation, ubiquitylation, sumoylation, poly (ADP-ribosylation), acetylation and methylation (Huen and Chen, 2010). The early DSB response utilizes phosphorylation-dependent protein–protein interactions to coordinate DNA damage recognition and signal amplification. Following DSB formation the histone H2AX, a histone H2A variant that comprises 10-15% of total cellular H2A in higher eukaryotes, is rapidly phosphorylated on its serine residues 139 (γH2AX) (Rogakou et al., 1998) by members of the phosphatidylinositol-3-OH kinase (PI3K)-like family, such as ATM, DNA-PK and ataxia telangiectasia and Rad3 related (ATR) (Kinner et al., 2008). γH2AX formation occurs within

minutes after damage, and extends for up to 1-2 megabases from the site of the break in mammalian cells, providing a platform for subsequent DNA repair protein recruitment and amplification at DSBs (Harper and Elledge, 2007).

The phosphorylation of H2AX creates a signal recognized by many proteins of the DNA damage response, which are recruited to the sites of DSBs, forming the ionizing radiation-induced foci (IRIF, Lukas and Bartek, 2004). The biological function of IRIF is thought to shelter the broken DNA ends from decay and prevent illegitimate repair processes, to amplify the DNA damage signal and to provide a local concentration of DDR factors relevant for DNA repair and metabolism. Stabilization of DDR factor recruitment to γH2AX nucleosomes is achieved through the recruitment of a wide variety of proteins regulating ubiquitylation, sumoylation, acetylation, and methylation.

The mediator of DNA damage checkpoint 1 (MDC1) is the major protein to localize to the sites of DNA breaks in a γH2AX-dependent pathway (Riches et al., 2008; Stucki, 2009). MDC1 has a role in controlling the assembly of multiple repair factors at DNA breaks and in amplifying the DNA damage signal. MDC1 orchestrates the recruitment of IRIF-associated proteins, specifically the MRN complex (MRE11, RAD51, and NBS1) and many DNA damage repair proteins, including p53-binding protein 1 (53BP1) and BRCA1 (breast cancer 1). DDR is characterized by the synthesis of ubiquitin conjugates at the sites of damage-induced repair foci (Tanq and Greenberg, 2010).

1.6.3. Tumour Radioresistance.

Tumours from different origins respond differently to radiotherapy, mainly due toDNA stranded breaks caused by irradiation (Driscoll and Jeggo, 2006). An important protein involved

in this repair machinery is the DNA-dependent protein kinase catalytic subunit (DNA-PKcs), which has been shown to be largely affected by EGFR signalling through the PI3K/Akt pathway (Toulany et al, 2006). Stimulation of EGFR results in an increase in the nuclear content of DNA-PK subunits, thereby enhancing the DNA-PK-dependent non-homologous end-joining system, while selective inhibition of EGFR-Ras-PI3K pathway by tyrosine-kinase inhibition in combination with radiotherapy leads to an increase in residual DSBs, which is a sign of impaired DNA repair in radio-resistant K-Ras mutated cells (Toulany et al, 2005). It has also been shown that the targeting of AKT activity by small interfering RNA (siRNA) sensitises human tumour cells to IR, as Ras-activation by mutation or by receptor tyrosine-kinase activity is a frequent event in human tumours, suggesting that the PI3K/Akt-mediated repair of DNA damage might be an important mechanism of radioresistance (Kim et al, 2005) and variation in radiosensitivity. Squamous-cell carcinomas and adenocarcinomas in lung cancer are generally deemed to have intrinsic resistance to radiotherapy. Several studies have defined Ras activation as a contributor to the radioresistance of tumour cells, with the Ras signalling to the PI3K/Akt pathway increasing the survival of tumour cells that have been exposed to agents that cause DNA damage, irrespective of whether Ras activation results from mutation of K-Ras or from overexpression of EGFR (Kim et al, 2005).

DNA double-strand breaks, induced by ionizing radiation are potentially lethal cell lesions and the repair of these breaks by homologous recombination takes place during the S-phase and G2-phase of the cell cycle and is responsible for the repair of about 20% of all double-strand breaks.

In addition to intrinsic radioresistance due to molecular mutation in cancer cells, the resistance to cytotoxic effects of radiation therapy is attributed to proliferation rate of carcinoma

cells. Proliferation is affected by several factors, such as differentiation status, cell-cycle gene regulation, and micro-environmental factors, including oxygen and nutrient availability. Hypoxia delays progression of the tumour cell through the cell cycle but repopulation takes place with reoxygenation (Webster et al, 1998). Cells that retain proliferative capacity under hypoxic conditions represent an important clonogenic subpopulation of tumour cells that are responsible for treatment failure (Hoogsteen et al, 2005). A mechanism by which cells enhance their proliferation in response to ionizing radiation is by induction of EGFR phosphorylation and activation, which leads to activation of mitogenic or proliferative signalling pathways, a major route being the RAS/RAF/mitogen-activated protein kinase (MAPK) pathway (Schmidt-Ullrich et al, 1997).

Studies of PI3K and Akt have mainly focused on their role in cell survival, and they are generally considered to work in parallel with the RAS/RAF/MAPK pathway that drives cell proliferation. However, another function of PI3K/Akt in increased cell proliferation relies on amplification of signals to the cell-cycle machinery, mainly in prevention of cyclin D1 degradation by Akt, resulting in increased progression through G1-S stage of the cycle (Diehl et al, 1998). Previous *in vitro* reports have concluded that inhibition of EGFR causes a G1 arrest, which prevents repopulation during radiotherapy in various cancer cell lines (Gennaro et al, 2003).

In addition to native radioresistance and increased proliferation rate, tumour hypoxia is a third main factor contributing to resistance of cancer cells to radiotherapy (Bussink et al, 2008). Tumour hypoxia is known to promote genetic instability, driving the tumour towards a more malignant phenotype by stimulating the invasion of tumour cells and, therefore, metastasis (Harris, 2002). Mutations of key regulatory genes that are induced or promoted by hypoxia can

select tumour cells with an increased resistance to treatment, resulting in poor clinical outcome, with the PI3K/Akt signalling playing a key role in tumour adaptation to hypoxic conditions (Bussink et al, 2008). Vascular Endothelial Growth Factor (VEGF) is one of the most widely investigated hypoxia-inducible proteins. Two distinct pathways (one including HIF-1α translation and the other involving HIF-independent processes) have been recognised as regulators of VEGF expression, both of which involve PI3K and Akt (Fukumura et al, 2001; Pore et al, 2006). Recent study focusing on correlation between angiogenesis and tumour radioresistance has shown that by treatment of xenografted lung carcinomas with Nelfinavir, an HIV-protease inhibitor that inhibits Akt signalling, significantly inhibits tumour angiogenesis and activation of hypoxia driven pathways (Pore et al, 2006).

1.6.4. Standard Radiotherapy Options for NSCLC lung cancer

Approximately 40% of patients with newly diagnosed NSCLC first present with locally advanced disease (extensive disease that is confined within the chest) with the majority of tumours being inoperable. Traditionally, these patients have been treated with radiotherapy alone, resulting in a median survival of approximately 9 to 10 months and a 5-year survival rate of approximately 7% (Sause and Turrisi, 1996). Clinical trials showed that lung tumour control is more effective when local treatment with radiotherapy is combined with systemic treatment (chemotherapy) (Johnson, 2000). Radio-sensitizing agents, such as the anti-neoplastic agent cisplatin and topoisomerase-inhibiting agent etoposide are now commonly given to NSCLC patients along with radiotherapy doses ranging from 60-66 Gy in 2Gy doses over a period of six weeks (Rowell and Williams, 2004).

While conventional radiotherapy employs fractionated doses of about 60Gy for a curative treatment, many clinical studies in non-operable NSCLC have concluded that radiotherapy doses as high as 90Gy need to be used for radical therapy (Lichter and Lawrence, 1995). Another method of increasing radiotherapy dose while minimizing normal tissue toxicity is the use of multiple daily radiation fractions (Peters and Ang, 1986). The studies revealed that hyperfractionation of irradiation doses yields greater tumour control and survival outcomes in comparison to conventional radiotherapy (Johnson, 2000). Continuous hyperfractionated accelerated radiotherapy (CHART) was compared with standard daily radiotherapy (total dose, 60 Gy in 30 fractions) for the treatment of patients with inoperable NSCLC, with CHART regiment consisting 1.5-Gy fractions of irradiation given for 12 consecutive days three times per day to a total dose of 54 Gy (Johnson, 2000). However, despite multiple studies in the past two decades including some that investigated escalated doses of radiotherapy outcomes in NSCLC remain very poor both in terms of local control and survival and is limited to 15 – 20% at 5 years (Johnson, 2000).

1.6.4.1.Fractionation of RT doses

While it seems logical that high single doses of radiation therapy would inflict a more prominent damage to cancerous cells resulting in cell death, conventional radiotherapy treatments in lung cancer patients include fractionation of radiation therapy doses over the course of several weeks. Today's standards for radiotherapy fractionation developed over many years based on principals of radiation biology that determine sensitization of tumours and protection of normal tissues.

One of the bases of using fractionated radiotherapy in oncology is based on 4R principle that describes the events seen in cells undergoing radiotherapy: Repair of DNA damage, Reoxygenation, Redistribution and Repopulation.

The first principle assumes that tumour cells have intrinsic defects in DNA repair machinery in comparison to healthy non-cancerous cells and delivery of small fractionated doses of radiotherapy would contribute to chronic DNA damage within the cells. Since the repair machinery in cancerous tissues would not be able to handle the damage, cancer cells specifically would essentially undergo apoptosis.

The proliferative cells of a tumour, being unrestrained by homeostatic control, divide and proliferate as rapidly as they are able to, limited only by their own inherited characteristics and the availability of an adequate supply of nutrients. Since a tumour is not an organized tissue, it tends to outgrow its own blood supply, where areas of necrosis often develop and are frequently accompanied by hypoxic cells, which often constitute about 15% of the total viable cells. As the tumour outgrows its vascular system, rapid cell proliferation near capillaries will push other cells into regions remote from a blood supply, where there is an inadequate concentration of oxygen and other nutrients, rendering the rise of the “hypoxic” centre within growing tumour. It is noted that while single doses of IR will lead to cell death in cancer cells with adequate oxygen supplies (periphery of the tumour); hypoxic cells are more resistant to effects of ionizing radiation. Thus, fractionation of radiotherapy would result in constant damage to the oxygenated cancer cells,

leading to reoxygenation of hypoxic cells and improved cytotoxicity as the amount of RT-resistant hypoxic cells is reduced (Figure 4).

Cancer cells have varying sensitivity to radiation depending on their current phase of the cell cycle. It is generally noted that mitosis phase of cell cycle (M) renders cells to be most susceptible to DNA damaging effects produced by IR, while latent G0 and G1 phases lead to cells resistance in response to RT. Between treatments, some proportion of cells will cycle into a more sensitive phase, rendering them more susceptible to radiation damage. The remaining cells will undergo synchronized entry into the cell cycle, upon which daily doses of radiotherapy will lead to damage of these cells at the M stage of cell division.

As radiotherapy can lead to damage of surrounding healthy tissues when delivered in large doses, fractionation of RT allows the healthy tissues to repopulate, thus minimizing the side effects associated with the therapy.

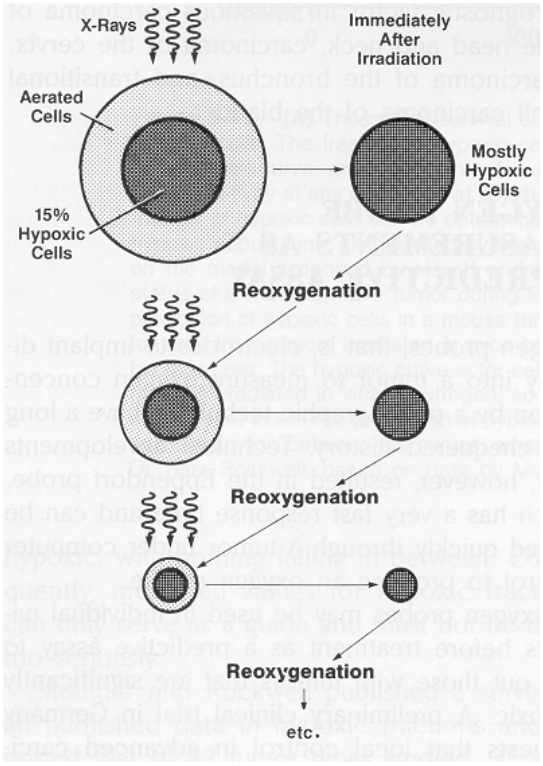

Adapted from Padhani et al, 2007.

Figure 4. The process of reoxygenation. Tumors contain a mixture of aerated and hypoxic cells. A dose of x-rays kills a greater proportion of aerated than hypoxic cells because they are more radiosensitive. Immediately after irradiation, most cells in the tumor are hypoxic. But the pre-irradiation pattern tends to return because of reoxygenation. If the radiation is given in a series of fractions separated in time sufficiently for reoxygenation to occur, the presence of hypoxic cells does not greatly influence the response of the tumor.

1.7 Metformin

Metformin belongs to a class of compounds called biguanines that were first isolated from the plant *Galegaofficinalis* (French lilac or goat's rue) known for its medicinal value (Witters, 2001). Although the glucose lowering actions of metformin were described as early as 1929 by Slotta and Tsechse, availability of metformin for human consumption did not occur until 1950s in the UK and the drug has gained worldwide interest as anti-diabetic agent in 1995 upon its approval by FDA (Witters, 2001; Kourelis and Siegel, 2011).

1.7.1. Anti-hyperglycaemic actions of metformin

Currently, metformin is prescribed to over 120 million patients worldwide as a main treatment choice for type 2 diabetes. Metformin is considered a safe therapeutic choice, as its glucose lowering actions are not accompanied by hypoglycaemia. Additionally, metformin has been reported to have insulin sensitizing effects, leading to reduction in insulin resistance and management of insulin resistant type II diabetes.

Numerous in vivo and clinical studies have confirmed that the primary action of metformin in lowering circulating glucose levels is via inhibition of gluconeogenesis and inhibition of hepatic glucose production (Hundal et al, 2000; Natali and Ferrannini, 2006). The increased inhibition of hepatic glucose production by metformin is associated with increased expression of OCT1 (organic cation transporter 1) in hepatocytes that facilitate cellular uptake of metformin into hepatic tissues (Shu et al, 2007).

1.7.1.2. Metformin Bioavailability and Pharmacokinetics

Metformin has been prescribed to T2DM patients in 500 and 850 mg tablet doses, with most patients taking from 500mg to 1700 mg of metformin daily. However, many require much higher doses of metformin to achieve glycemic control and tolerate doses as high 3.00 grams or higher. The absolute bioavailability of a metformin hydrochloride 500 mg tablet given under fasting conditions is approximately 50-60% (Martin-Castillo et al, 2010). At usual clinical doses and dosing schedules of metformin hydrochloride tablets, steady state plasma concentrations of metformin are reached within 24-48 hours and are generally around 1 µg/mL (Martin-Castillo et al, 2010). During controlled clinical trials, maximum metformin plasma levels in test subjects did not exceed 5µg/mL, even when the subjects received maximum biologically safe dose of metformin at 3500 mg/day (Martin-Castillo et al, 2010). Metformin is excreted by renal system through the body, and is usually eliminated in the urine 7 hours post initial intake.

1.7.2. Metformin and AMPK

Metformins glucose lowering effects lead to an ATP/AMP imbalance within the cells, resulting in activation of the LKB1-AMPK pathway, which in turn results in inhibition of glucose, protein and lipid synthesis, while promoting oxidation of fatty acids and uptake of glucose from the bloodstream (Hardie, 2011). Early studies investigating relationship between metformin and activation of AMPK have concluded that metformin does not directly activate LKB1 or AMPK, rather the activation of the pathway is the result of metformin-mediated inhibition of mitochondrial respiratory chain complex I which leads to increases in cellular AMP levels. Central involvement of LKB1-AMPK pathway in hypoglycemic actions of metformin

have been first reported in a study showing that animals lacking hepatic LKB1 failed to have increased hepatic glucose uptake upon metformin administration (Hardie, 2011).

1.7.3. Metformin and Cancer

In the past few years, metformin gained global attention as potential anticancer agent. The interest in metformin and its connections to oncology was first revealed in retrospective epidemiological studies of diabetic patients with cancer. An observational study conducted by Evans and colleagues on connections between diabetes and cancer revealed that cancer incidence and cancer-related mortality in diabetics receiving standard doses of metformin (1500 to 2250 mg/day in adults) was significantly lower in comparison to a placebo group (Evans et al, 2005). Furthermore, a recent retrospective analysis of 2,529 women with breast cancer reported higher pathologic complete response rates to neoadjuvant systemic therapy in diabetic patients receiving metformin (24%) compared to diabetic patients not receiving metformin (8%) and non-diabetic patients not receiving metformin (16%) (Jiralespong et al, 2009).

Numerous studies investigating anti-oncogenic actions of metformin have concluded that metformin effectively inhibits the proliferation of a range of cancer cell lines, including breast, glioma, renal, prostate, colon, ovarian and lung carcinomas (Zakikhani et al, 2006; Dowling et al, 2007; Sahra et al, 2008; Buzzai et al, 2008; Isakovic et al, 2007). Inhibitory effects of metformin on cancer cell proliferation were associated with AMPK activation, reduced mammalian target of rapamycin (mTOR) signalling and protein synthesis, as well as a variety of other responses including decreased epidermal growth factor receptor (EGFR), Src, and mitogen-activated protein kinase (MAPK) activation, decreased expression of cyclins, and increased expression of $p27^{kip1}$ (Cantrell et al, 2010; Isakovic et al, 2007; Liu et al, 2009).

In addition to in vitro cellular studies, anti-cancer properties of metformin have been validated in animal studies utilizing tumour xenografts from various carcinomas of epithelial origins. An early study investigating metformin effects on development of breast carcinomas have concluded that metformin treatment significantly inhibited tumour burden and development of mammary carcinomas in HER2/neu transgenic mice (Anisimov, 2005). A study performed by Zakhikani and colleagues concluded that treatment of breast cancer cells with metformin lead to significant downregulation in protein translation rate within the cell, which was paralleled by activation of AMPK and subsequent inhibition of mTOR activity (Zakhikani et al, 2006). Metformin has been shown to significantly inhibit growth of lung, prostate and colon tumours in vivo, mainly through modulation of cell cycle and activation of LKB1-AMPK axis (Sahra et al, 2008; Buzzai et al; 2007; Tomimoto et al, 2009).

1.7.3.1. Molecular Effects of Metformin

The main mechanism of metformins regulatory actions on growth and development of cancer cells is attributed to activation of LKB1/AMPK pathway following metformin administration. It has been established that activation of the AMPK pathway leads to significant inhibition of mTOR activity, halting cellular growth, protein synthesis and proliferation, while simultaneously regulating cell cycle progression and DNA damage response molecular effectors such as Cyclin D1, $p21^{cip1}$, $p27^{kip1}$, Akt and p53 (Sahra et al, 2008; Buzzai et al; 2007; Tomimoto et al, 2009; Sahra et al, 2010) (Figure 4).

It has been also suggested that metformin exhibits anti-proliferative effects in AMPK-independent fashion by decreasing levels of free circulating insulin within the system. Hyperinsulenima is directly correlated to increased circulation of IGF-1 hormone, which has been

established as a powerful tumor- promoting factor. Lowering of the IGF-1 levels by modification in dietary lifestyle, caloric restriction and decreased insulin levels have been positively correlated to decreased incidences of cancer in rodent models (Kalaany, 2009). Schneider and colleagues showed that the prevention of pancreatic cancers in hamsters treated with metformin and fed with a high-fat diet is correlated with a marked decrease in insulinemia (Schneider et al, 2001). In contrast, metformin treatment did not affect insulinemia in PTEN +/− and HER-2/neu animals, suggesting an insulin-independent antitumoral action of the drug (Huang et al, 2008; Anisimov et al, 2005; Tomimoto et al, 2008).

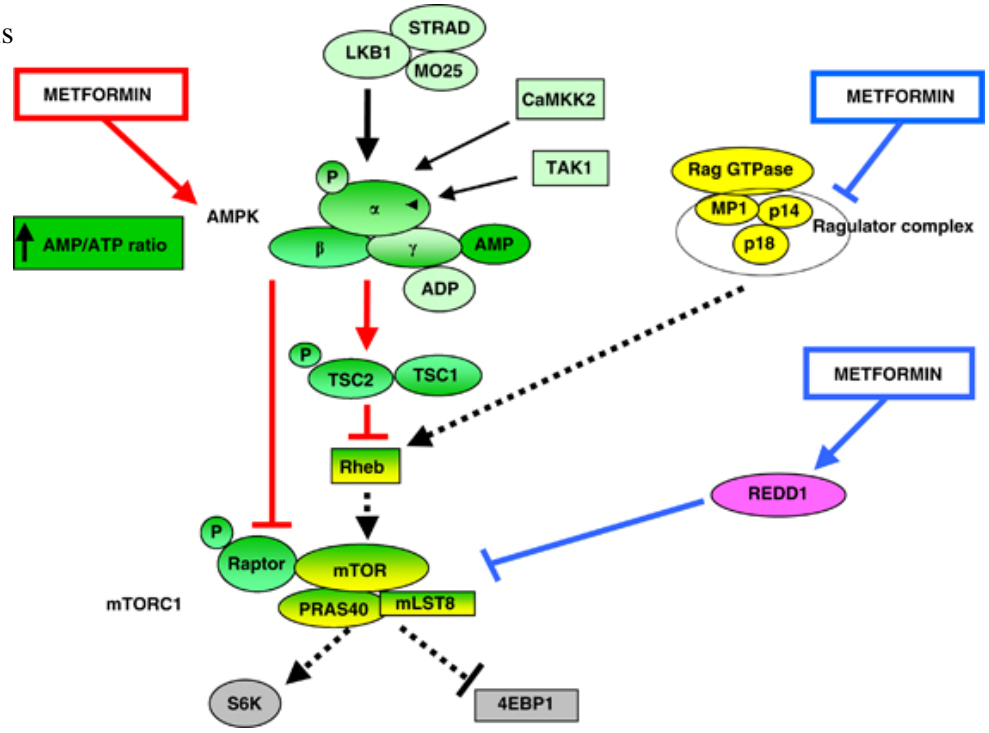

Adapted from Shackelford and Shaw, 2009.

Figure 5. Metformin suppression of mTORC1 signalling occurs through AMPK-dependent (red lines) and AMPK-independent (blue lines) mechanisms. The AMPK-dependent mechanism may in turn be sustained by direct (green) or indirect (light green) AMPK activation. The direct activation or allosteric activation is governed by AMP binding, whereas the indirect activation is achieved through Thr172 phosphorylation (P in green circle) by LKB1 trimetric complex, calmodulin-dependent kinase kinase 2 (CaMKK2) or TGF beta-activated kinase-1 (TAK1), and the protective effect of ADP, which makes Thr172 dephosphorylation-insensitive. Both types of AMPK activation result in the suppression of mTORC1 signalling mediated by TSC1/TSC2/Rheb/raptor/mTOR axis.

1.7.4. Metformin as an Enhancer of Standard Cancer Therapies

1.7.4.1. Metformin Enhances Chemotherapy Responses

Chemotherapy remains one of main therapeutic modalities for treatment of highly progressive and non-localized cancer. Even though chemotherapeutic regimens often suppress tumor growth, cancer patients show high variability in their responses and commonly develop resistance to these drugs and recurrence of the tumor. This phenomenon can be explained in part by the novel cancer stem cell (CSC) hypothesis, which suggests that tumors contain a small number of tumor-forming, self-renewing CSCs within a population of non-tumor-forming cancer cells (Ailles and Weissman, 2007; Polyak and Weinberg, 2009). Unlike most cells within the tumor, CSCs are resistant to chemotherapy, and after treatment, they can regenerate all the cell types in the tumor through their stem cell–like behaviour.

It has been suggested that treatments with selective inhibition towards CSCs should function together with chemotherapeutic drugs to delay relapse. Recent observations concluded that metformin selectively kill CSCs and act together with doxorubicin to reduce tumor growth and prolong remission (Hirsch et al, 2009; Iliopoulos et al, 2010). Moreover, studies conducted by the same group have concluded that metformin significantly enhances chemotherapeutic responses of breast, prostate and lung xenografts to treatment with chemotherapeutic agent doxorubicin, and combination of both treatments leads to increases in remission time (over 65 days) in comparison to either treatment alone (Iliopoulos et al, 2011).

Another study performed by Rocha and colleagues in 2011 concluded that metformin enhances chemotherapy responses of paclitaxel in A549 human NSCLC and MCF7 breast

carcinoma xenografts (Rocha et al, 2011). The enhanced anti-tumour action of of combined paclitaxel and metformin treatment was associated with greater activation of AMPK pathway and lower mTOR activity than was seen in untreated animals or mice undergoing treatment with either agent alone (Rocha et al, 2011).

1.7.4.2. Metformin and Radiotherapy

Similar to chemotherapy, radiation therapy inhibits growth and proliferation of cancer cells by inducing genotoxic stress and apoptosis through lethal DNA damage. Very few studies have investigated the effects of combining metformin with clinical doses of radiotherapy on growth and development of cancer cells or tumours in animal models.

One study investigating the effects of metformin, radiotherapy, heat treatment or combination of either on viability of CSC have concluded that metformin treatment for a 48 hour period at doses of 5mM has significantly inhibited the amount of CSC in MCF-7 breast carcinoma cells (3.4% vs. 1.2 %) and has selectively inhibited the markers of the stem cells of MIAPaCa-2 pancreatic cancer cells expressing CD44+/CD24+ (Park et al, 2011). Combination of metformin and radiation therapy treatments produced a significantly greater tumour growth inhibition in MIAPaCa-2 xenografts when compared to individual therapies (Park et al, 2011).

A study with prostate cancer cell lines have concluded that monotherapy with IR (1-8Gy) or metformin caused significant dose-dependent reduction in colony formation rates in PrCa cell lines, while ($p<0.001$) combination treatment further significantly reduced colony formation rates ($p<0.03$) (Klotz et al, 2011).

A common concern with the majority of published pre-clinical studies of metformin in cancer to date remains that that most studies suggested requirements of milli-Molar (mM) doses

of metformin to achieve significant anti-proliferative effects. Certainly, this has been the weakness of all preclinical studies with the drug that aim to examine the ability of metformin to induce cancer cell radiosensitization. Furthermore, there has been little focus of pre-clinical studies on lung cancer.

CHAPTER 2

2.1 Materials

Cell culture materials: RPMI 1640 and DMEM media, fetal bovine serum (FBS), phosphate buffered saline (PBS), trypsin-EDTA enzyme and antibiotic-antimycotic solution with penicillin and streptomycin were purchased from Invitrogen Canada (Burlington, ON).

Culture flasks, dishes and plates: BD Falcon tissue culture materials were purchased from VWR International (Mississauga, ON).

Antibodies: Antibodies against AMPKα, P-AMPKα(Thr172), P-ACC (Ser139), ATM, P-ATM(S1981), γH2Ax (Ser139) P-Chk2 (Thr68) , p53, P-p53(Ser15), Akt, P-Akt(Ser473), P-Akt(Thr308), p21waf1/cip1, mTOR, P-mTOR(S2448), Bax, PUMA, Cleaved Caspace 3, and β-actin were purchased from Cell Signalling Technology (Denver, Massachusetts, USA). CD31 antibody was purchased from Abcam (Cambridge, Massachusetts, USA). Horseradish peroxidase (HRP) - conjugated IgG secondary anti-rabbit and anti-mouse antibodies were supplied by New England Biolabs (Mississauga, ON, Canada).

2.2 Cell Culture and Treatments

Cell Culture: Human lung cancer cell lines A549 (LKB1-negative, p53 positive), H1299 (LKB1 positive, p53 negative), SK-MES (LKB1 positive, p53 negative), human prostate adenocarcinoma PC3 (LKB1 positive, p53 negative), and human breast adenocarcinoma cell lines MCF7 (LKB1 positive, p53 positive), and MDA-MB231 (LKB1 positive, p53 negative) were purchased from ATCC (Philadelphia, PA, USA). A549 and H1299 cells were cultured and maintained in RPMI 1640 media containing 5mM glucose, 10% (v/v) FBS and 1% (v/v) antibiotic-antimitotic solution

(100 U/ml penicillin, 100 µg/ml streptomycin, and 250 ng/ml amphotericin B), in an atmosphere of 5% CO2 at 37°C. SK-MES, MCF7 and MDA-MB231 cell lines were maintained in DMEM media supplemented with 10% FBS and 1% A/A. Cells were trypsinized upon reaching 80% confluency state by washing the cell layer with sterile 1XPBS solution followed by addition of 1mL of 0.2% EDTA-trypsin solution. After addition of trypsin enzyme, cells were placed in the incubator for a five minute period allowing the cells to detach from the flask. 10 mL of fresh media was added to the flask and 9mL of media solution containing cells and diluted trypsin was removed and discarded into biohazardous waste. Fresh media was added to the remaining cell fraction in the flask and cells were placed into the incubator to allow for subsequent growth and proliferation.

2.3 In *vitro* experimental techniques

2.3.1 Cell Viability Assay

Cells were seeded at a density of $1X10^3$cells/well in 96-well plates containing 200µl of complete medium in triplicate. Cells were allowed to adhere to the plate and replicate overnight prior to indicated treatments with Metformin (MET) or Rapamycin. Once appropriate doses of either pharmaceutical were added, cells were allowed to incubate for 24 hours prior to subsequent radiation treatment. After IR exposure, plates were left to incubate for additional 48 hours. At the end of treatment time point, cells were washed with PBS, fixed with formalin for 30 minutes and stained with Crystal Violet dye for 15 minutes. Cell viability was quantified with BioTek Plate reader spectrophotometry software at 570nm.

2.3.2 Cell Cycle Analysis

A549 cells were seeded at $1x10^6$ cells/mL in 10 cm culture dishes. After 24 hour incubation, cells were treated with indicated doses of metformin and were left to further incubate overnight. The following day, cells were exposed to 8Gy dose of IR and were allowed to incubate over 48 hours. After incubation period, cells were washed in PBS, trypsinized, centrifuged at 1500 RPM for 5 minutes and cell pellets were submerged in 1mL of ice-cold 95% ethanol and stored at -20°C for a 24 hour period. Ethanol-fixed cell pellets were subsequently centrifuged at 1500 RPM for 5 minutes and resuspended in 1mL of PI staining solution (10mL of 1X PBS, 100µL of Triton X-100 and 50µg/mL PI). Cell distribution was analyzed with FACS-calibur flow cytometry and the data was analyzed using FACS-calibur flow cytometry software.

2.3.3 Immunoblotting analysis

2.3.3.1. Preparation of Whole Cell Lysates

Approximately $1x10^3$ cells were plated in 6 well plates in complete medium and were allowed to proliferate for 2-3 days. Cells were treated with specified doses of MET, rapamycin, and/or Ionizing radiation for specific time points according to experimental guidelines. After treatment completion and upon specific time lapse, cells were washed twice with ice-cold sterile 1X PBS. Approximately 250µL of 1X lysis buffer was added to each well in a plate (lysis buffer: 50mM Tris (pH 7.4), 150mM NaCl, 5mM MgCl2, 2mM EDTA, 5mM NaF, 1mM Na3VO4, 5mM Na2P2O4, glycerol, 1% NP40, 0.5% Na deoxycholate, 0.1% SDS, 20mg/ml aprotinin, 4 mg/ml leupeptin, 1mM PMSF)). Cells were allowed to lyse for 15-30 minutes after which they were scraped from the wells via sterile plastic cell scraper. Lysates were collected into individual 1000µL sterile eppendorf tubes, vortexed and centrifuged at 13000 rpm for 5 minutes. The

supernatant of each lysate was collected and placed in fresh sterile eppendorf tubes while the platelet was discarded. The lysates were stored in -20°C for short- term storage or were placed in -80°C freezer for prolonged use.

2.3.3.2. Protein Quantitation

Protein concentration in cell lysates was determined via Bio- Rad protein determination assay (Bio-Rad Laboratories, Mississauga, ON, Canada). Lysates were diluted in 90µL of sterile distilled water at 1: 10 ratio (90µL ddH2O: 10µL lysate) in 96-well Falcon plates. 10 µL of diluted sample was withdrawn and placed into separate well in triplicates. Approximately 250µL of diluted Bio-Rad protein reagent (diluted 1:4 in ddH2O as per manufacturer's instructions) was added to each of the sample wells. The samples were read using a Bio-Tek instruments EL340 micro plate biokinetics reader at 570 nm absorbance. Data obtained from reading was plotted in Microsoft Excel against standard BSA sample curve provided by the manufacturer. Total protein concentration was calculated in each sample and immunoblotting samples with equal concentrations were prepared.

2.3.3.3. Immunoblotting Analysis

Sample buffer containing 0.2% β- mercaptoethanol and sodium dodecyl sulphate (SDS) was added to collected lysates and the mixture was vortexed to achieve homogeneity. The samples were further denatures by placing lysates on the hot plate at 95°C for five minutes. After boiling, samples were immediately resolved on SDS-PAGE gel or stored at -20°C until further use.

For immunoblotting analysis, equal amounts of protein (20µg) were loaded onto acrylamide gel (8-12%) and were separated by SDS-polyacrylamide gel electrophoresis at 100V for 90 minutes. Proteins were transferred from gels onto PVDF membranes by electrophoresis. After transfer

completion, membranes were blocked for non-specific antibody and protein binding in 5% dry milk-TBST solution at 4°C overnight (5% (w/v) dry skim milk powder in 1X TBS solution, 0.1% ween-20). After blocking period, membrane were washed in 1X TBST solution for approximately 40 minutes and incubated in primary antibody (dilution fraction and diluent components specified as per manufacturer's instructions) for approximately two hour period at room temperature with gentle agitation. The membranes were subsequently washed for 40 minutes using 0/1% Tween-20 in 1X TBS-T solution and incubated with HRP-conjugated anti-rabbit or anti-mouse secondary antibodies (1: 10 000 dilution) in 0.1% tween-20, 5% (w/v) dry milk in TBS-T for 2 hours at room temperature with gentle agitation. Antibody-protein complexes were detected using ECL detection reagent and protein bands were visualized using Bioflex scientific imaging films. Obtained protein bands were later subjected to Densitometry analysis.

2.3.3.4. Densitometry Analysis

All marker band densities were first normalized for loading against the density of anti-actin immunoblots. In tissue culture experiments lysates from the control and treated cells were run on the same gel. For tumour lysate analysis immunoblots for each marker were run simultaneously and were exposed to the same antibody solutions. Normalized average density values of bands belonging to the 6 control tumours were used as the master-control value against which all individual tumour band densities were normalized. Data are shown as Mean ± SEM of normalized values in each treatment group.

2.4 In *vivo* experimental techniques

2.4.1. Development of Animal xenograft model:

Forty four-week old Balb/c nude mice were obtained from Charles River (Mississauga, Ontario, Canada). Animals had ad libitum access to food and water and were maintained in sterile environment with 12 hour light and dark cycles. At five weeks of age, twenty four animals were grafted with $1x10^6$/0.5mL PBS A549 human lung adenocarcinoma cells and sixteen animals were injected with $1x10^6$/0.5mL PBS H1299 human lung adenocarcinoma cells by subcutaneous injection into the right flank. Once the tumour volume reached 100 mm^3, animals were equally divided into four treatment groups: untreated (control), Metformin alone (MET), ionizing radiation (IR) treatment or combined treatment (MET+IR) (n=6 per group in A549 cohort and n=4 per group in H1299 cohort). Metformin treatment was delivered daily via drinking water at the dose of 300 mg/kg body weight. Tumour volume was measured every five days and estimated from calliper measurements, with the volume calculated at (V=length*width*height*0.5236). Treatment termination was initiated either after sixty day period, or when tumour volume reached 1000mm^3.

2.4.2 Animal Radiation

The IR treatment was carried out using a clinical radiation therapy unit. Tumour xenografts were subjected to 10Gy IR while animals were subjected with isofluorane gaseous anaesthesia housed inside a protective Plexiglas tube equipped with high efficiency particulate air (HEPA) filters.

2.4.3 Tissue Extraction

At the end of the treatment course or when the animal has approached the endpoint, mice were euthanized with carbon dioxide gas according to McMaster Animal Research Ethics Board Instructions, with tumour tissues extracted and immediately snap frozen in liquid nitrogen for immunoblotting experiments or submerged in 10% formalin solution for 24 hours following paraffin embedding for subsequent immunohistochemical analysis.

2.4.4 Immunoblotting

Overall, 20µg of total protein extracts from xenografts tissues or from cell lysates were subjected to SDS-PAGE and resolved on 8-12% SDS gels and transferred onto PVDF membrane at 100V for two hours. Membranes were incubated with primary antibodies in 5% Bovine Serum Albumin (BSA) solution at 4°C overnight followed by 1 hour incubation with appropriate hydrogen peroxidise-conjugated secondary antibody. Band intensity was visualized using highly sensitive ECL reagent and protein density was quantified by optical densitometry using Image J software (See sections 2.3.4.2. - 2.3.4.4.)

2.4.5. Immunohistochemistry on paraffin embedded tissue.

IHC analysis was performed on tumours extracted post-treatment and immediately fixed with formalin. Paraffin embedded tissues were cut into four µm thick sections followed by mounting partially charged IHC glass slides. Prior to immunohistochemistry analysis, glass slides with tissues of interest were put into oven and heated at 60^{o}C overnight. The following day, the slides were deparaffinised and rehydrated by multiple washes in xylene and ethanol. Antigen retrieval was performed with Citrate buffer (10mM, pH 7.6) with standard pressure cooker for 35 min at sub-boiling temperature. Slides were then blocked against endogenous peroxidase activity by

incubation with 3% hydrogen peroxide solution for 15 minutes, rinsed with sterile ddH2O and Tris-buffered saline (TBS), and then blocked with 3% normal goat serum diluted in TBS at room temperature for 1 hour. Following blocking with normal goat serum, tissue were incubated with primary antibodies for p-AMPK (T172) (1:200 dilution), anti-CD 31(1:100 dilution) and anti-cleaved caspace 3 (1:800 dilution) at 4°C overnight. The following day slides were rinsed with TBS for three 10 minute consecutive washes and incubated with secondary biotinylated anti-rabbit immunoglobulin antibody (Sigma-Aldrich) for 30 minutes at room temperature. Slides were then subjected to treatment with Vectastain Elite ABC kit for 20 minutes to allow conjugation of avidin-peroxidase to the biotinylated secondary antibody followed by visualization of peroxidase- activated antibody by slide incubation with Nova RED substrate kit. Slides were counterstained with haematoxylin solution (1:2 dilutions) for visualization of the nuclei, followed by dehydration with a series of ethanol and xylene washes. Signals of antibody localization in plasma membrane, cytoplasm, and the nucleus were evaluated by a trained pathologist.

2.4.6. Statistical Analysis

Paired t-test and Two-way ANOVA was performed to analyze the results from proliferation and immunoblotting experiments using Graph Pad Prism software (GraphPad Software Inc., California, USA). Results are presented as mean ± SEM. Statistical significance was determined at $p<0.05$.

CHAPTER 3

Our laboratory has previously implicated AMPK as part of an ATM-p53 signalling axis that responds to IR to regulate the cell cycle. Those initial observations suggested that AMPK is not only a sensor of metabolic stress but also a sensor a genomic stress. We observed then that inhibition of AMPK inhibited radiation induction of p53 and $p21^{cip1}$ (Sanli et al, 2010). Radiation regulation of AMPK was independent of LKB1 but dependent of ATM activity. Further, we observed (Sanli et al, 2010) that AMPK, i) facilitated the well described G2-M checkpoint that is activated in radiated cells and facilitates DNA repair in radiated tissues and that ii) mediates radiation-induced cytotoxicity in lung cancer cells.

Those observations were made utilizing biochemical inhibitors and molecular knock down studies to address the role of AMPK in molecular pathway. However, given the novelty and significance of above mentioned studies, we needed to verify those observations using genetic approaches that would allow us to establish reliably the role of AMPK in mediation of signalling events, regulation of cell cycle and survival.

In these studies I utilized genetically engineered mouse embryonic fibroblasts (MEFs) that lack expression of AMPK a-subunit (both 1 and 2) ($AMPK\alpha^{-/-}$) and investigated whether absence of AMPK catalytic subunit and lack of its enzymatic function would affect the ATM pathway at the basal level and in response to 8Gy IR.

The specific objectives of the work included in this chapter were to:

i) Verify the role of AMPK in IR responses using genetic models lacking AMPK expression

ii) Assess the chronic effects of IR on the expression of AMPK, it upstream regulators and downstream effectors in xenografted human lung tumours.

Chapter 3

Results

3.1 Ionizing radiation leads to activation of AMPK pathway and cell cycle regulators in mouse embryonic fibroblast cells (MEFs)

Since earlier studies pursued by our laboratory have found that upon exposure to Ionizing Radiation (IR), human lung cancer cells exhibit increased expression and activity of the AMPK enzyme. Moreover, inhibition of AMPK by specific molecular inhibitor Compound C significantly decreased up regulation of molecular pathways associated with DNA damage response and cell cycle checkpoints.

In order to further investigate the effects AMPK status has on IR molecular responses, I have utilized cell culture experiments using normal wild type (WT) MEFs and knock out mutants lacking catalytic α subunit of the AMPK enzyme (AMPKα$^{-/-}$ -MEFs). Cells were seeded in six well plates, allowed to incubate overnight and later subjected to either 0 Gy or 8 Gy of IR. Cells were lysed 1 hour post IR treatment and status of the DNA damage molecular effectors was investigated via immunoblotting using anti-AMPKα, -P-AMPKα (Thr172), -P-ACC (Ser139), -p53 (total), - p21^{cip1}and- actin antibodies (Figure 6.1 A).

We have observed that upon radiation with 8Gy, WT MEFs exhibited increases in expression and activity of AMPK enzyme marked by P-AMPK (Thr172) and P-ACC levels respectively in comparison to their control counterparts (0 Gy). As expected, there were no detectable bands for enzyme expression or activity for either 0 Gy or 8 Gy treated AMPKα$^{-/-}$ -

MEF cells. Interestingly, AMPKα$^{-/-}$-MEFs showed higher basal levels of total p53 and p21^{cip1} protein levels in comparison to WT counterparts (Figure 6.1 A, B). While IR treatment lead to acute increases in p53 and p21^{cip1} protein levels in WT MEFs, these events were inhibited in AMPKα$^{-/-}$-MEFs (Figure 6.1 A, B).

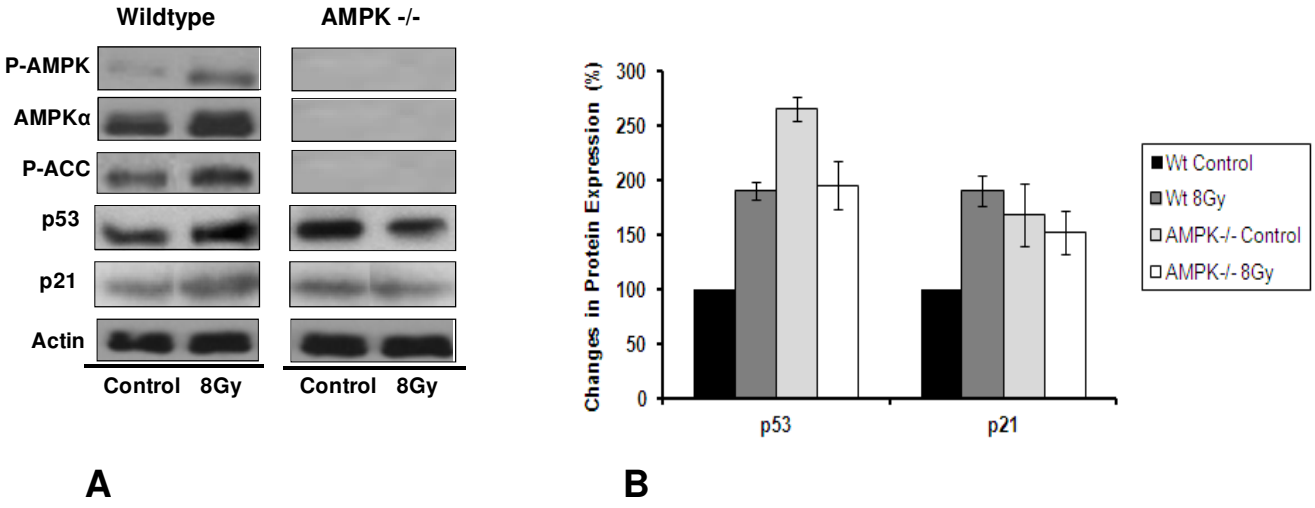

Figure 6.1 Involvement of AMPK on cell cycle regulators. (A) Wildtype (WT.) or AMPKα$^{-/-}$ MEFs (AMPK$^{-/-}$) were lysed in lysis buffer and subjected to western blotting with antibodies against the AMPK and p53-p21 pathway**. (B)** The densitometry of untreated or IR-treated MEF cells in (a) were quantitated and presented as Mean ± SEM of three independent experiments.

3.2 AMPK is required for propagation of DNA damage response pathway upon IR treatment in MEF cells.

Our lab has previously reported that AMPK activation upon IR exposure occurs in ATM-dependent manner (Sanli et al, 2010). For that, we examined in AMPKα$^{-/-}$ MEFs the ATM signalling pathway, including ATM and its downstream targets Chk2 and histone H2Ax (γH2Ax), representing ATM activity. Expression of the ATM molecular pathway was analyzed with

immunoblotting of MEF lysates as described in Chapter 3.1 using anti-ATM (Total), -P-Chk2 (Thr68), -γH2Ax (S139), and –actin antibodies (Figure 6.2).

Surprisingly, AMPKα$^{-/-}$-MEFs showed significantly increased total ATM protein levels as well as γH2Ax compared to WT cells (Figure 6.2a). Although, IR alone enhanced acutely the levels of ATM, phosphorylated Chk2, and γH2AX in WT-MEFs, these events were inhibited in AMPKα$^{-/-}$-MEFs (Figure 6.2A). Results from three independent experiments were quantitated and are summarized in Figure 6.2B.

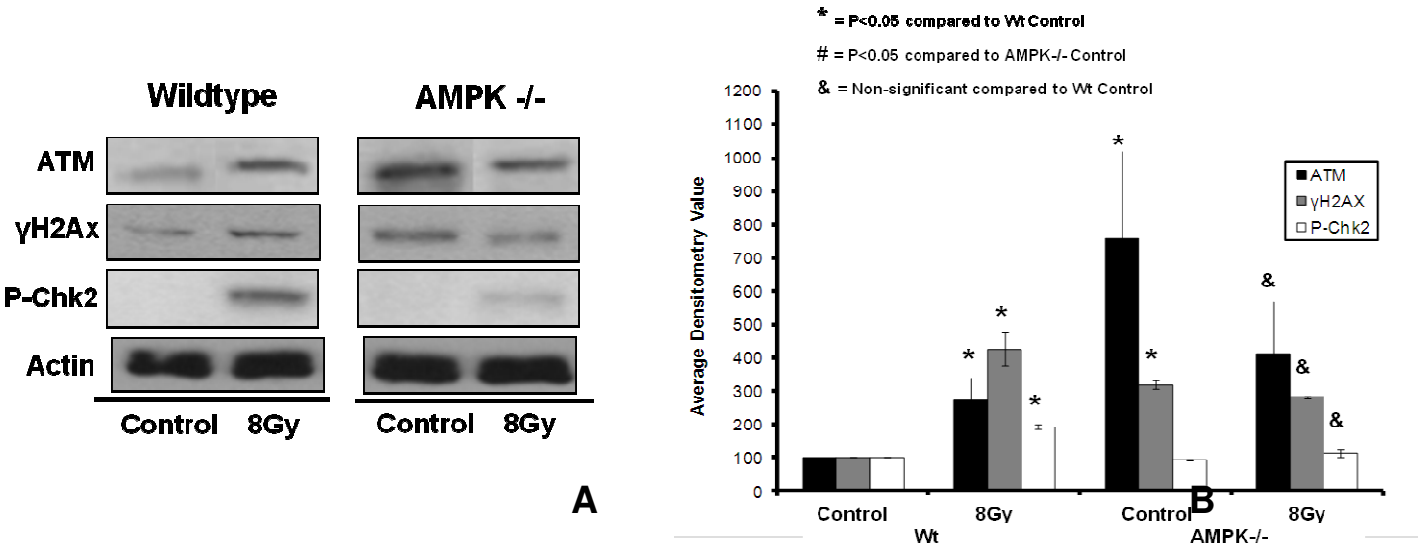

Figure 6.2 AMPK involvement in Akt-mTOR pathway in response to IR. (A) Wild-type (WT) or AMPKα -/-MEFs were treated with 0Gy or 8Gy dose of Ionizing Radiation and one hour later were lysed in lysis buffer and subjected to western blotting with antibodies against the Akt-mTOR. **(B)** The densitometry of untreated or IR-treated MEF cells were quantitated and presented as the Mean ± SEM of three independent experiments.

3.3 The role of AMPK status in IR modulation of Akt-mTOR pathway in fibroblast cells

Previous reports cell have suggested that acute IR leads to up regulation of pro-survival Akt-mTOR pathways in addition to increased expression of AMPK and DDR responses. In this part of the study, I focused on investigating potential effects of AMPK status on induction of pro-survival signals in acutely irradiated cells.

WT- and AMPK$\alpha^{-/-}$-MEFs were subjected to IR treatment and lysed as described in section 3.1, with the cell lysates probed with anti-Akt, -P-Akt (T308), -P-Akt(S473), -mTOR, -P-70s6k (S371), -P-4EBP1, and -actin antibodies. We have observed that unradiated AMPK$\alpha^{-/-}$-MEFs had increased total protein levels of Akt , mTOR, phosphorylated Akt on Ser473 residue, but not on Thr308 site in comparison to their WT counterparts. Increased mTOR levels in AMPK$\alpha^{-/-}$-MEFs were paralleled with significantly elevated phosphorylation of $p70^{S6k}$ and 4EBP1, indicating increased activity of mTOR kinase in the absence of functional AMPK (Figure 6.3 A). Upon acute exposure to IR (8 Gy), phosphorylation levels of Akt (T308), $p70^{S6k}$ and 4EBP1 were detected WT MEFs, however, the activation of these biomarkers was not apparent in 0Gy or 8Gy AMPK$\alpha^{-/-}$-MEFs (Figure 6.3 A, B).

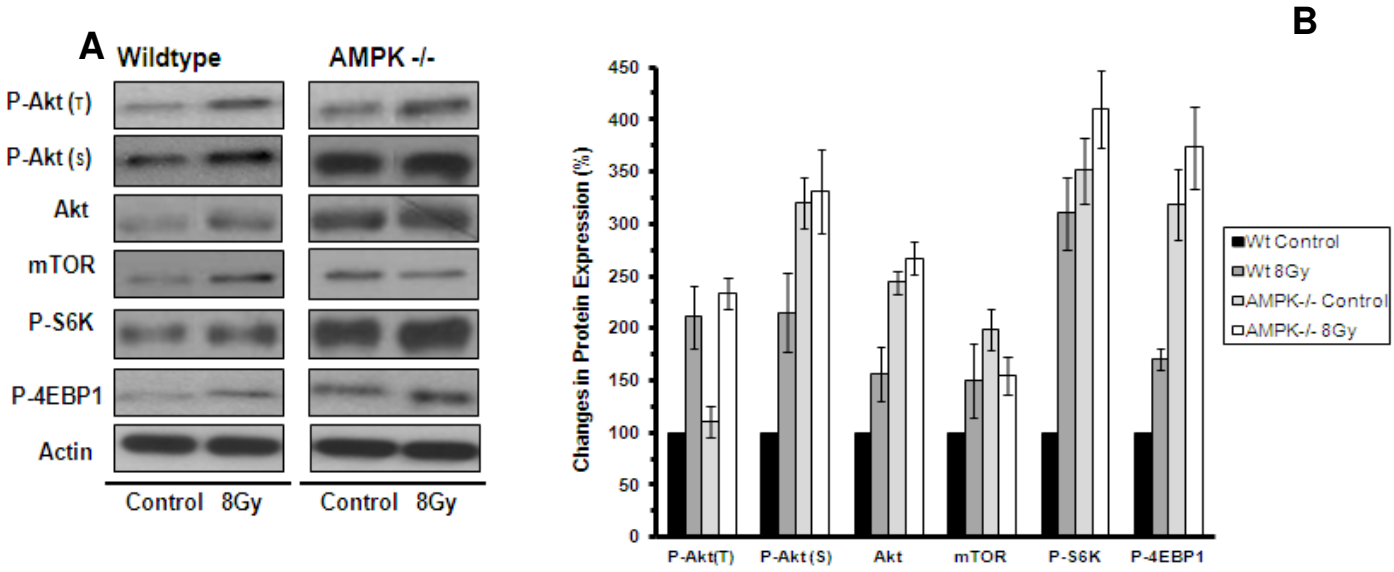

Figure 6.3 AMPK involvement in Akt-mTOR pathway in response to IR. (A) Wild-type (WT) or AMPKα $^{-/-}$MEFs were treated with 0Gy or 8Gy dose of Ionizing Radiation and one hour later were lysed in lysis buffer and subjected to western blotting with antibodies against the Akt-mTOR. **(B)** The densitometry of untreated or IR-treated MEF cells were quantitated and presented as the Mean ± SEM of three independent experiments.

3.4. AMPK status and IR effects on cell cycle in MEF cells

Since reports suggested that p53 functions downstream of AMPK, we hypothesized that absence of the enzyme will result in altered expression of cell cycle regulators p53 and $p21^{cip1}$ after radiation treatment.

Interestingly, we observed that lack of AMPK catalytic activity in AMPK$\alpha^{-/-}$-MEFs was associated with basal increases in cell cycle regulating proteins (checkpoint mediators) marked by p53 and $p21^{cip1}$ levels in comparison to WT-MEFs (Figure 6.4 B). Upon exposure to 8Gy IR, WT-MEFs exhibited an increase of their levels of p53 and $p21^{cip1}$ biomarkers, while AMPK$\alpha^{-/-}$-MEFs failed to respond to IR and showed if anything a trend for reduced levels of p53 and $p21^{cip1}$ after IR (Figure 6.4 B). The results of three independent experiments were quantitated as shown in Figure 6.4 B.

We have previously implicated AMPK in the IR-induced G2-M checkpoint in lung cancer cells using AMPK knockdown with specific anti-AMPKα1/2 subunit siRNAs (Sanli et al, 2010). To verify these results in cells lacking AMPK, we analyzed cell cycle distribution in WT and AMPK$\alpha^{-/-}$-MEFs before or 48 h after IR of 8 Gy (Figure 6.4 A, B). WT-MEFs demonstrated a shift in cells from G1/S to G2/M in response to IR (G1/S: 82% and G2/M: 18% for untreated vs. G1/S: 62% and G2/M: 38% for 8 Gy treated cells) (Figure 6.4 A, B). Conversely, AMPK$\alpha^{-/-}$-MEFs cells did not exhibit a detectable change in cell cycle distribution in response to IR (G1/S: 77% and G2/M: 23% for untreated, vs. G1/S: 78% and G2/M: 22% for 8 Gy (Figure 6.4 A, B). These findings are consistent with our earlier work and the results of Figure 5.2 indicating lack of induction of p53 and $p21^{cip1}$ in AMPK$\alpha^{-/-}$-MEFs after IR.

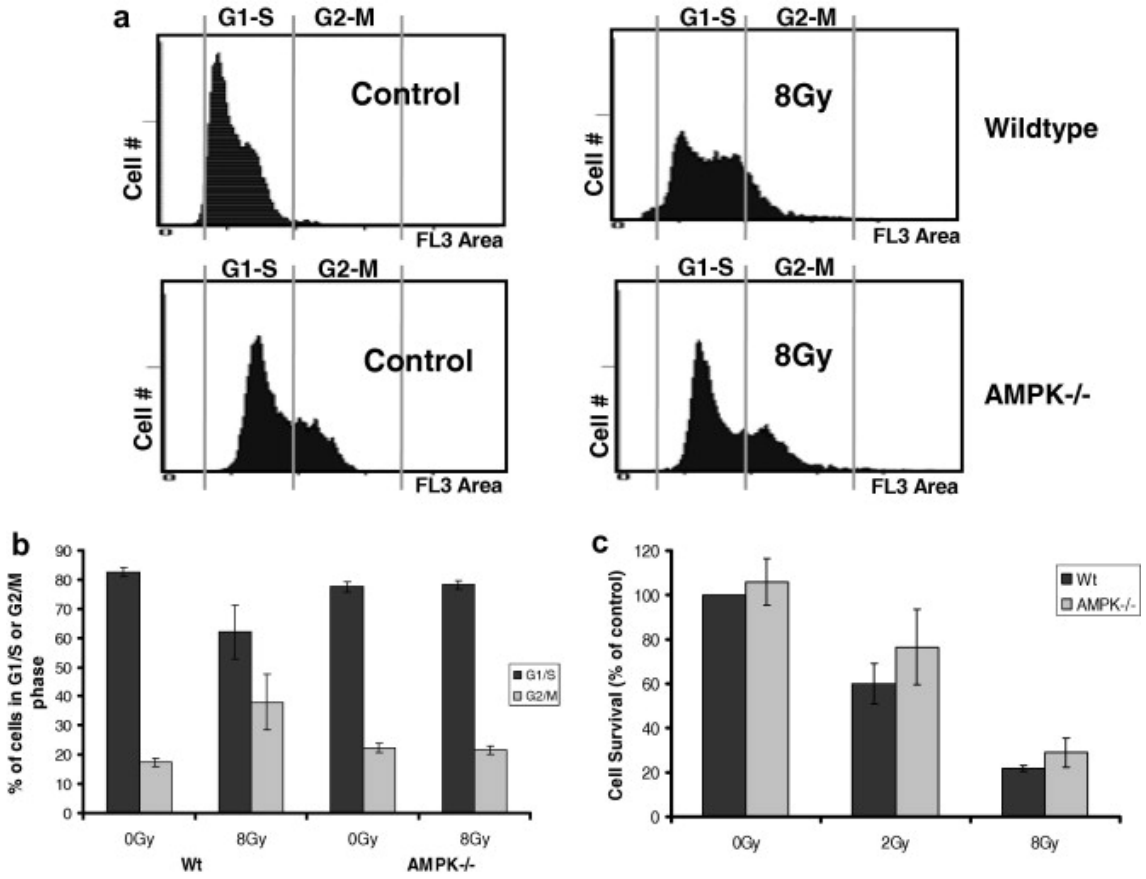

Figure 6.4 Cell cycle regulations in the absence of AMPK. (A) Wildtype (WT) or AMPKa $^{-/-}$-MEFs (AMPK-/-) were treated with or without a dose of 8 Gy IR and fixed in ethanol 48 h later. These cells were then stained with propidium iodide and subjected to cell cycle analysis. **(B)** The results from the experiments in (A) were quantitated and presented as Mean ± SEM from three independent experiments.

Chapter 3

Results

Part 2: Long-Term Effects of Ionizing Radiation Treatment on Lung Cancer Xenografts

3.5 Ionizing Radiation significantly inhibits lung cancer tumour growth.

In order to investigate the long term effect of exposure to radiation on growth and development of human lung cancer tumours, we have utilized an animal model in order to better understand physiological impacts of IR on lung cancer growth. We have obtained male Balb/c nude mice at five weeks of age from Charles Rivers (Mississauga, ON, Canada). The animals were maintained and grafted with A549 or H1299 human lung adenocarcinoma cells as described in Methods (see section 2.4.1). The animals were equally divided into two treatment groups: Control (received no treatment) (CON) and IR group that received a single 10Gy dose of ionizing radiation when tumour volume has reached 100 mm^3. Tumour growth was observed for a 60 day period and the tumour volume was measured by callipers every five days.

Within 15 days after IR treatment, xenografts began to show differences in growth kinetics for both A549 and H1299 treatment groups, and the growth differences between treatment groups became statistically significant by day 25 (Figure 7). At the end of the 60 day treatment period, irradiated tumours were on average 67 ± 3.4 % (A549) and 70 ± 4.2 % (H1299) smaller than their control (non-irradiated) counterparts respectively.

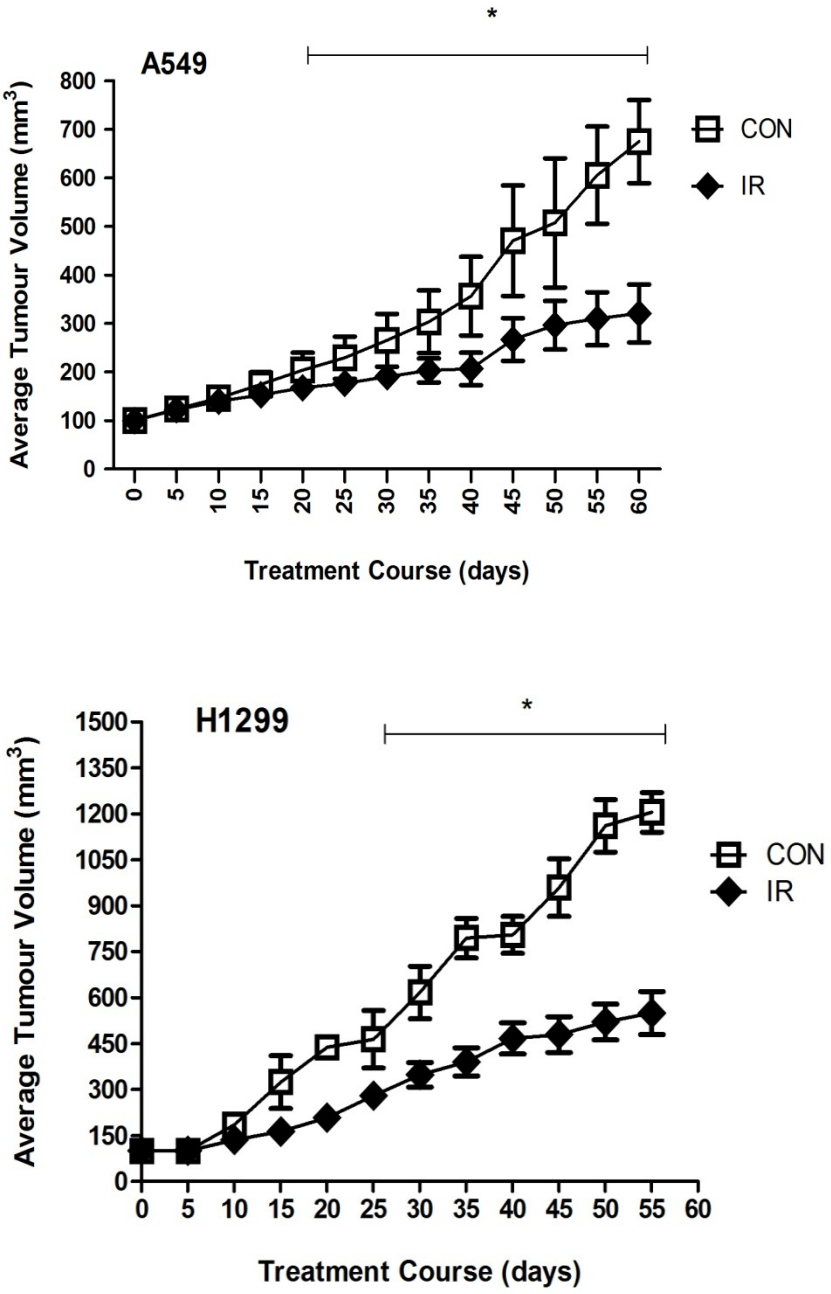

Figure 7. IR treatment down regulates tumour growth kinetics in A549 and H1299 human lung cancer xenografts. Balb/c nude male mice were grafted with A549 or H1299 human lung adenocarcinoma cells. When tumour reached the volume of 100 mm³, animals were equally divided into untreated group (Control) or subjected to a treatment with a single fraction of ionizing radiation therapy at the dose of 10Gy. Tumour volume was monitored every 5 days for a period of 8 weeks. Representative graphs of average tumour volume over treatment course are shown; data is presented as MEAN ± SEM. *$p<0.05$ compared with control tumour volume.

3.6 Effects of long-term IR treatment on AMPK in lung cancer tumours

We wanted to investigate whether marked increases in AMPK enzyme expression and activity could be sustained in tumour tissues weeks after radiation exposure. Molecular pathways of interest were investigated via immunoblotting of tumour lystates against - AMPKα, P-AMPK (Thr172), -P-ACC, and -actin antibodies.

Basal levels of total AMPK α-subunit increased in irradiated xenografts along with activation of the enzyme marked by phosphorylation on Thr172 residue (Figure 7.1 A, C). Additionally, P-ACC levels were also significantly higher in tumours collected from irradiated xenografts compared to control (Figure 7.1 a, c), indicating increased activity of AMPK enzyme.

To examine whether increased levels of P-AMPK (Thr172) signals are indeed attributed to cancer cells, rather than to the surrounding tumor microenvironment, we have performed immunohistochemistry analysis of xenografts using anti-P-AMPKα (Thr172) antibody (Figure 7.1 B). In those experiments we also observed significant increases in P-AMPK levels in irradiated tumour cells compared to controls that distributed across cytoplasm and nuclei of tumor cells of A549 origin but mainly in cytoplasm of H1299 tumour cells.

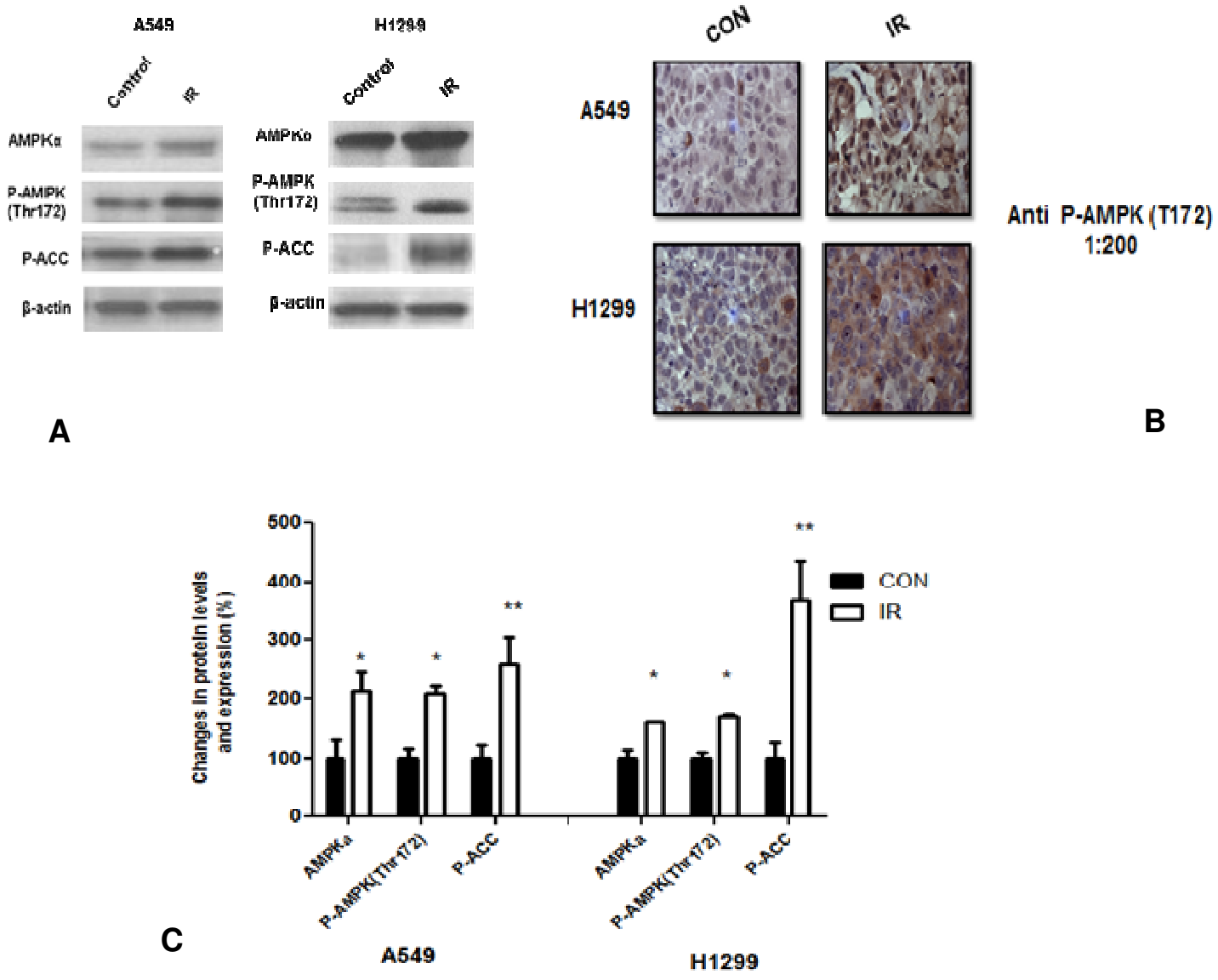

Figure 7.1 Ionizing Radiation (IR) upregulates AMPK expression and activity in A549 and H1299 human lung tumours. **(A)** Control and IR-treated tumours were subjected to immunoblotting analysis using AMPK-α, p-AMPK (Thr172), and p-ACC antibodies (Ser139) (1:1000). Anti-actin was used as a loading control. Representative immunoblots from at least 3 independent experiments are shown. **(B)** Tumours were fixed in formalin, followed by immunohistochemistry analysis using a specific p-AMPK (Thr172) antibody (1:200 dilution). **(C)** Immunoblot densitometric values are shown as percent change in protein expression relative to the control group; data is presented as MEAN ± SEM, where *p<0.05; **p<0.001.

3.7 Long-term IR treatment leads to ATM pathway activation.

Since it is well known that acute exposures of cells to IR leads to up regulation of the DNA damage response pathways, including the ATM-γH2Ax axis, we wanted to investigate if the same notion holds true in tumour tissues eight weeks post single radiation dose. In order to investigate the molecular pathways, tumours collected from A549 and H1299 cohorts were lysed and subjected to immunoblotting for anti-ATM, -γH2AX(S139), -P-Chk2 (Thr68), and – actin antibodies.

We have observed that damage response biomarkers were significantly elevated in irradiated tumours from both lung cancer cohorts in comparison to the tissues that were left untreated (Figure 7.2 A). In both A549 and H1299 xenografts we detected increased levels of phosphorylated H2AX (γH2AX) in the irradiated tumours compared to untreated control tumours that were significantly higher in H1299 xenografts in comparison to tumour tissues collected from the A549 cohort (Figure 7.2 A, B).

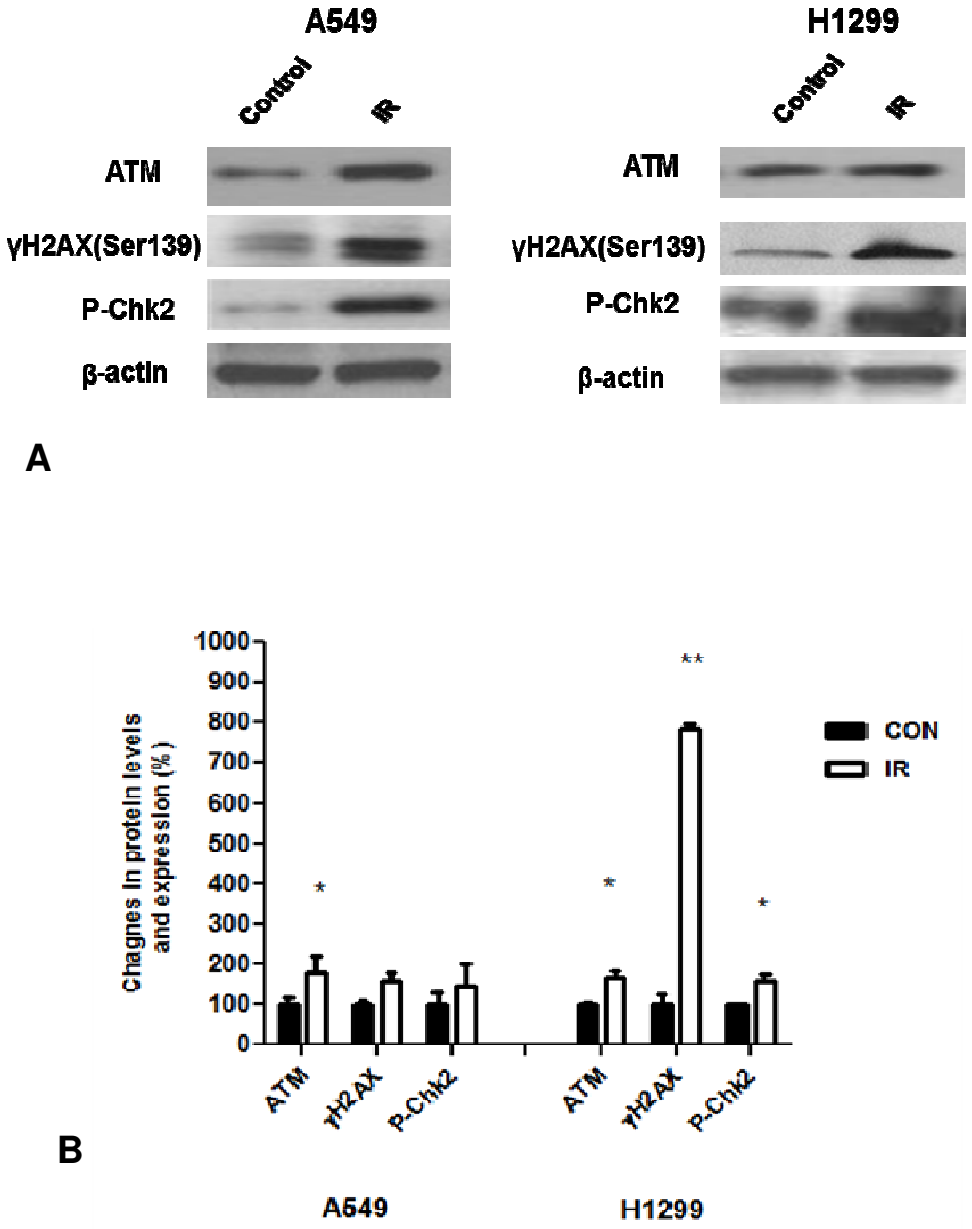

Figure 7.2 Ionizing Radiation (IR) upregulates ATM expression and activity in A549 and H1299 human lung tumours. (A) Control and IR-treated tumours were subjected to immunoblotting analysis using ATM, γH2AX (S139), and P-Chk2 (Thr68) antibodies (1:1000). Anti-actin was used as a loading control. Representative immunoblots from at least 3 independent experiments are shown**. (B)** Immunoblot densitometric values are shown as percent change in protein expression relative to the control group; data is presented as MEAN ± SEM, where *p<0.05; **p<0.001

3.8 IR regulation of cell cycle checkpoints in lung cancer tumours

To examine whether chronic effects of IR treatment on cell cycle checkpoint regulators in whole tumour tissues are comparable to the results obtained in the in vitro experiments, we have performed immunoblotting analysis of tumour lysates collected from A549 and H1299 cohort animals. Control and IR-treated xenografts were probed with anti-p53, -P-p53 (Ser15), -$p27^{kip1}$, -$p21^{cip1}$, and – actin antibodies.

A single fraction of IR exposure sustained a significant increase of $p27^{kip1}$ and $p21^{cip1}$ levels in irradiated A549 and H1299 tumours compared to CON tissues (Figure 7.3 A, B) . Total and phosphorylated (P-) p53 levels were analyzed specifically in A549 tumours only as H1299 tumours lack p53 expression (Figure 7.3 A). Interestingly, we detected highly significant increase in total and phosphorylated (Ser15: 5.5-fold increase) p53 levels in A549 tumours collected from IR group when compared to A549 CON tissues (Figure 7.3 B).

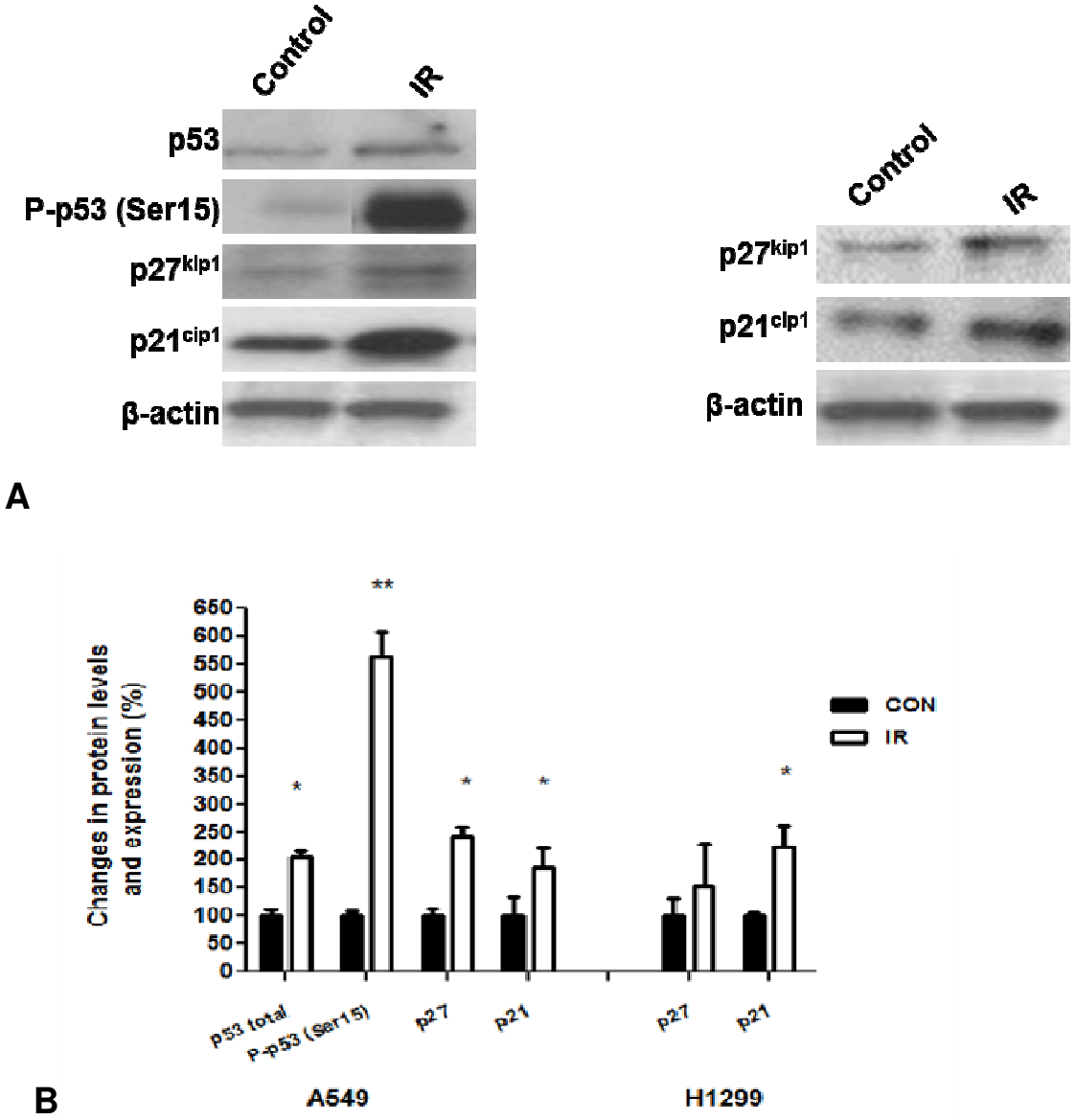

Figure 7.3 Ionizing radiation (IR) activates cell-cycle regulatory proteins in lung cancer tumours. **(A)** Tumour tissues collected from A549 and H1299 injected animals were subjected to immunoblotting analysis using p53, p-p53 (Ser15), p27kip, and p21waf/cip antibodies. Anti-actin immunoblotting was used as a loading control. Representative immunoblots from at least 3 independent experiments are shown. **(B)** Immunoblot densitometric values are shown as percent change in protein expression relative to the control group; data is presented as MEAN ± SEM, where *p<0.05; **p<0.001.

3.9 Long-term IR effects on modulation of Akt-mTOR pathway in lung cancer tumours

Immunoblotting analysis of A549 and H1299 tumours collected from CON and IR tumours was performed to analyze the status of Akt-mTOR pro survival pathway eight weeks post IR exposure. Figure 6.4 illustrates immunoblotting experiments of A549 and H1299 tumours lysates probed with anti-Akt, -P-Akt (S473 and T308), -mTOR, -P-mTOR (S2448), -P-4EBP1, and –actin antibodies.

We did not detect significant differences in the total Akt levels between control and irradiated tumours in either A549 or H1299 tissues (Figure 7.4 A). However, we observed that IR caused a sustained reduction in the levels of P-AktS473 in both A549 and H1299 xenografts that reached significance in A549 but not in H1299 tumours. A trend for reduced P-AktT308 levels was also detected in irradiated tumours of both types but that was not statistically significant in either of them (30.0 ± 6.4 % and 55.0 ± 10.9 % vs. 15.0 ± 4.3 % and 42.0 ± 2.3 % decrease for T308 and S473 phosphorylation in A549 and H1299, respectively) (Figure 7.4 A, B).

Consistently, both IR treated tumour types showed reduced P-mTOR (Ser2448) levels without a significant change in total-mTOR levels. Irradiated xenografts of the two lung cancer types showed reduced levels of phosphorylation of 4EBP1 (P-4EBP1) indicating reduced mTOR activity (reduction by 81.0 ± 4.75 % and 47.0 ± 3.20 % in A549 and H1299 xenografts, respectively) (Figure 7.4 A, B).

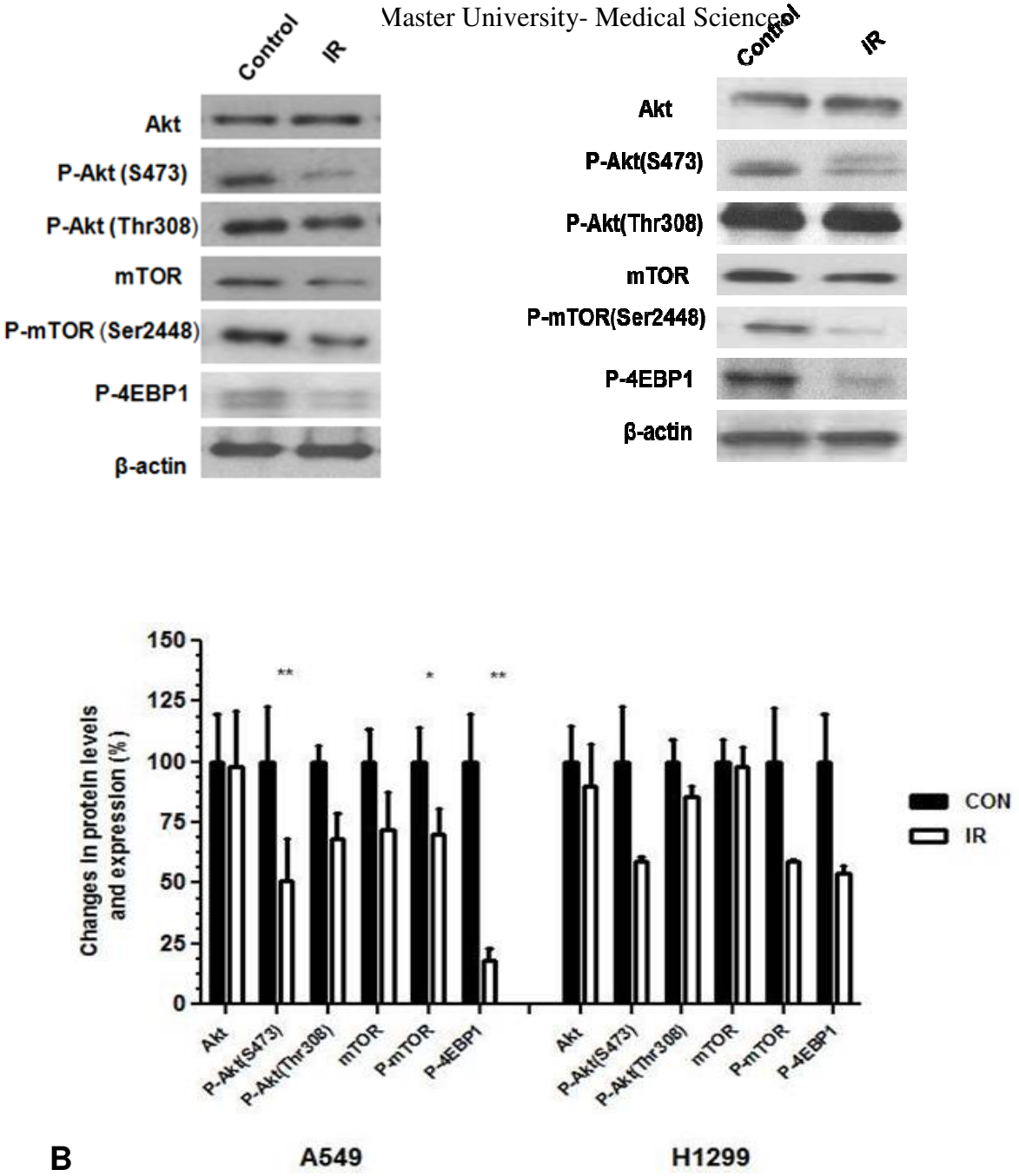

Figure 7.4 Ionizing Radiation (IR) inhibits Akt-mTOR pro-survival pathway in A549 and H1299 lung adenocarcinoma xenografts.(A) Lysates from Control and IR treated tumours extracted from A549 and H1299 animal cohorts were subjected to immunoblot analysis using Akt, p-AKT (S473), p-Akt (Thr308), mTOR, p-mTOR (Ser2448) and p-4EBP1 antibodies. Representative immunoblots from at least 3 independent experiments are shown. **(B)** Immunoblot densitometric values are shown as percent change in protein expression relative to the control group; data is presented as MEAN ± SEM, where *p<0.05; **p<0.001.

Chapter 3 Discussion

Modulation of AMPK expression and activity by IR

Previous studies conducted in our laboratory have concluded that AMPK has potential role not only as a regulator of cell metabolism, but can also play a pivotal role in cellular responses to genotoxic stress (Sanli et al, 2010). In order to further elucidate AMPK involvement in responses to acute radiation exposures, we have utilized –MEFs, which closely resemble transformed cancer cells of epithelial origins due to high replicative potential. More importantly, the model has utilized genetically engineered cells to lack expression of AMPK catalytic α subunits.

We compared molecular responses to 8Gy doses of IR in genotypically normal MEFs (WT) and knock-out MEFS lacking catalytic subunits of AMPK enzyme (AMPK$\alpha^{-/-}$-MEFs). Interestingly, we observed a marked up-regulation in basal ATM protein levels in the absence of AMPK (as seen in AMPK$\alpha^{-/-}$-MEFs) which was paralleled by stimulation of its activity seen as increased γH2Ax as detected by immunoblotting analysis (Figure 6.1 A, C). Increased activity and expression of DNA damage response proteins without presence of genotoxic stress stimulator suggests that AMPK may have an important role regulating / fine-tuning the response of cells to DNA damage. AMPK may be stabilize – fine-tune the basal activity of DDR pathway. Up-regulation of the activity a genomic stress pathway in untreated cells may have significant implication of DNA replications in those cells and potentially in genomic stability. In response to 8Gy IR, WT-MEFs showed the well-established stimulation in the ATM/γH2Ax/Chk2 cascade, while AMPK$\alpha^{-/-}$-MEFs showed decreased activity of this pathway upon IR treatment, decreased induction of γH2Ax and inhibited Chk2 phosphorylation (Figure 6.1 A, C). This compromised

response of ATM to IR appears to have implications in signal transduction to downstream effectors of ATM such as p53 and Akt-mTOR, discussed below. Our observation suggests that AMPK may exert control over basal ATM activity and support the normal responsiveness and propagation of ATM signalling after IR.

AMPK status affects regulation of Akt-mTOR pathways.

As acute genotoxic stress caused by IR leads to marked increases in Akt signalling pathways and AMPK has been implicated to have a role in down regulation Akt activity, we wanted to investigate whether native absence of AMPK enzyme leads to increased Akt-mTOR activity in cells not exposed to genotoxic agents. We have observed enhanced phosphorylation levels of mTOR and 4-EBP1 in untreated AMPK$\alpha^{-/-}$-MEFs (Figure 6.2 A, C), which is attributed to the absence of inhibitory effects of AMPK on mTOR in those cells. Here, we have detected significantly higher levels of total Akt and mTOR and enhanced S473-Akt phosphorylation in AMPK$\alpha^{-/-}$-MEFs indicating an overall stimulation of Akt-mTOR signalling pathway in cells lacking AMPK. Interestingly, marked increases in Akt phosphorylation were observed only on Ser 473 residue, but not on Thr 308, indicating increased activity of PDK2, but not PDK1 kinases. Overall, we have observed that cells lacking functional AMPK enzyme exhibited enhanced phosphorylation of Akt on S473 residue, indicating an overall overstimulation of Akt-mTOR pathway in AMPK$\alpha^{-/-}$-MEFs. This, in part, can be related to the proposed function of ATM acting as PDK2. As we observed increased phosphorylation of Akt on Ser473 but not on Thr308 residues along with increases in total ATM levels in AMPK$\alpha^{-/-}$-MEFs, it is reasonable to conclude that enhanced ATM activity may indeed regulate Akt through phosphorylation on Ser473 residue.

Further, we observed that AMPK influences also the expression and activity of Akt and mTOR, indeed the significant up-regulation of S473 phosphorylation suggest potential that may be related to lack of tonic mTOR inhibition in cells lacking AMPK. The responses of the two key targets of mTOR and regulators of gene translation 4-EBP1 and p70S6k were consistent with the overall behaviour of the Akt-mTOR pathway and levels of Akt-S473 phosphorylation. Phosphorylation of 4-EBP1 and p70S6k was significantly increased in untreated AMPK$\alpha^{-/-}$-MEFs in the absence of IR exposure. Interestingly, we did not observe acute up regulations of mTOR activity in cells lacking AMPK upon IR treatment, which was seen in WT MEFs (Figure 6.2 A, B). These results are indicative of possible over-stimulation of Akt-mTOR pathway in AMPK$\alpha^{-/-}$-MEFs. The implication of these observations are significant as they indicate that lack of AMPK permits activation of radio-resistance and survival pathways that are known to drive resistance to cytotoxic therapy of tumours.

Regulation of the p53-p21^{cip1} pathway, cell cycle and survival

Since we previously observed that AMPK mediates the IR-induced expression of p53 and p21^{cip1} (Sanli et al, 2010), we hypothesized that AMPK$\alpha^{-/-}$-MEFs cells would show defective levels of these molecules. However, the expression of p53 and p21^{cip1} were increased in AMPK$\alpha^{-/-}$-MEFs compared to WT-MEFs, although the latter was not statistically significant (Figure 6.3 A, B). Since AMPK and p53 positively regulate each other under metabolic stress, it is possible that loss of AMPK in the MEF model initiates feedback loops of expression and activation of p53 as a means to control cycle progression. The induction of p53 expression may be the result of enhanced ATM expression and activity that may regulate p53 in an AMPK-independent manner. Interestingly, we did not observe enhanced p53 and p21^{cip1} levels after IR in AMPK$\alpha^{-/-}$-MEFs in comparison to up regulation of the markers in WT MEFs by IR (Figure 6.3 A, B). This is

consistent with our observations in cancer cells that AMPK acts as transducer of IR signals to regulate expression of p53 and $p21^{cip1}$.

Ionizing Radiation significantly inhibits lung cancer tumour growth

Since we observed the effects of acute IR exposure on regulation of AMPK, p53-p21 axis and Akt-mTOR pathways *in vitro*, we wanted to investigate whether long-term radiation treatment in whole lung tumours would lead to similar effects observed in the above mentioned studies.

We have utilized animal models of two distinct human lung cancer types: adenocarcinoma A549 (K-Ras (G12S) oncogenic mutant and truncated LKB1-null and wild-type p53) and H1299 (p53-null, wild-type K-Ras and LKB1). The main goal of this study was to analyze how genotypically distinct tumours would respond to treatment with radiotherapy at the molecular level . We analyzed the effects of a single fraction of therapeutic IR (10 Gy) on the steady state levels of expression and activity of AMPK and Akt pathway members eight weeks after treatment induction.

Treatment of human lung xenografts with a single fraction of IR (10 Gy) caused an expected significant inhibition of tumour growth kinetics (Figure 7). We have noted that H1299 xenografts seemed to respond more favourably to the treatment with IR, which agrees with the notion of increased radioresistance in NSCLC with K-Ras mutation that is present in A549 tumours.

AMPK regulation by chronic IR treatment.

Our study was the first to report modulation of AMPK enzyme expression and activity by Ionizing Radiation in whole lung cancer tumours. Irradiated tumours had significantly higher

levels of total and phosphorylated AMPK as well as P-ACC suggesting maintained enhanced expression and activity of the enzyme. Since we and others have shown that AMPK is a transducer of ATM signals sustained activation of AMPK would be an expected finding in the presence of ATM activation.

However, our results also showed increased AMPKα protein levels, suggesting that IR drives AMPKα gene expression. Although these findings should be eventually verified by mRNA expression assays in whole tumour xenografts, other members of our group demonstrated that IR indeed stimulates AMPK subunit expression not only in the translational (protein synthesis) but also in the transcriptional level by inducing mRNA expression of these genes. In addition, tt is important to note that we have shown that up regulation of AMPK enzyme occurred in LKB1 or p53 independent manner as seen from immunoblotting and immunohistochemistry results of both A549 and H1299 xenografts (Figure 7.2 A-C).

Regulation of cell cycle regulation markers by IR in LC xenografts

We observed that irradiated tumours maintain significantly increased levels of total and phosphorylated p53 and of CDK inhibitors $p21^{cip1}$ and $p27^{kip1}$ (Figure 7.2 A, B). We also detected in irradiated tumours highly increased level of p53-Ser15 phosphorylation a post translational modification believed to contribute to a greater stability of this protein. These results support the notion that IR activates the p53/CDKI signalling pathways in tumours in a sustained fashion probably through increased expression, phosphorylation and stabilization of p53 and increased levels of CDKIs $p27^{kip1}$ and $p21^{cip1.}$

These results support the earlier in vitro findings, in which we showed that induction of p53 and $p21^{cip1}$ in response to IR is dependent on AMPK and that AMPK activity is required for the mediation of IR-induced G2-M checkpoint and IR cytotoxicity (Figure 7.3). AMPK may

indeed mediate the inhibitory effects of IR on xenograft growth through regulation of p53 and CDKIs. Similar to our earlier observation on the acute response of $p21^{cip1}$ to IR in A549 and H1299 cell cultures (Sanli et al, 2010), the induction of this CDKI in irradiated xenografts seems to occur in p53 independent manner as similar results were obtained from immunoblotting of H1299 xenografts which lack p53 expression (Figure 7.3 A,B).

Long-term IR effects on modulation of Akt-mTOR pathway in lung cancer tumours

Despite the fact that IR treatment leads to acute activation of Akt-mTOR pathways and increased protein translation, we observed significantly reduced levels of Akt-S473 phosphorylation in both types of lung cancer xenografts and a trend for reduced AktT308 phosphorylation. Consistently, mTOR phosphorylation was partially reduced and so was the activity of this key enzyme indicated by lower 4EBP1 phosphorylation that was more significant in A549 tumours (Figure 7.4 A, B). We have observed similar trends in down-regulation of the pathway in both A549 and H1299 tumour, indicating that these are likely universal responses of human epithelial tumours to IR that are independent of K-Ras mutation status and LKB1 or p53 function.

It is reasonable to assume that reduction in mTOR activity in xenografts is attributed to the enhanced AMPK activity. However, increased activity of AMPK enzyme is not expected to attribute to significant decreases in phosphorylation of Akt on both Thr308 and Ser473 residues. IR is known to mediate rapid activation of Akt pathways, and it has been suggested that ATM can function as a PDK2 kinase leading to Ser473 phosphorylation on Akt, which was observed in above mentioned in-vitro studies with MEFs. Despite the detection of increased ATM expression and activity in radiated xenografts, we observed significant reductions in Akt phosphorylation on

both Ser473 and Thr308 residues, indicating marked decreases in the activities of both PDK1 and PDK2. In addition to reduced Akt phosphorylation, we have also observed suppressed activity of mTOR kinase marked by decreases in 4EBP1 phosphorylation levels. This reduction of mTOR activity can be contributed to long-term activation of AMPK, however, the exact mechanisms of regulation of Akt phosphorylation still remain to be elucidated.

It is possible that in irradiated tumours conditions develop, long after delivery of IR, the combined effects of sustained increased expression of AMPK-p53-$p21^{cip1}$/$p27^{kip1}$ pathway, that is shown to lead to inhibition of cell cycling, and inhibition of Akt-mTOR-4EBP1 pathway, known to lead to gene transcription and translation, may be capable of mediating an effective anti-proliferative action in those tumours, which may be adequate to mediate the cytotoxic action of IR. Our observations with regards to long-term activation of ATM in irradiated tumours weeks after delivery of IR treatment is a novel finding within the field, as ATM is proposed to be a common regulator of both AMPK-p53$p21^{cip1}$ and Akt-mTOR-4EBP1 pathways. However, future studies are needed to investigate the exact mechanisms of sustained ATM activation on irradiated tissues.

Overall, this part of our studies indicated that IRR can enhance activity and expression of AMPK. Furthermore, using MEFs that lack functional AMPK has helped evaluate its role in regulating pathways that modulate cell cycle, survival, and genomic stability at the basal state and in response to IR.

Chapter 4

Investigation of Metformin as a radiation sensitizer in NSCLC

Metformin (MET) has recently emerged as an effective anti-cancer agent with the ability to inhibit proliferation of numerous human cancer cell lines of epithelial origins both *in vitro* and in tumour xenograft models. These cytostatic properties of MET were proposed to occur in AMPK-dependent and independent manners, mainly through inactivation of Akt- mTOR pro-survival pathway and up regulation of cell-cycle checkpoint proteins along the p53-$p21^{cip1}$ pathway. Numerous studies have concluded that MET leads to indirect activation of AMPK, mainly by increasing AMP to ATP ratios within the cell and this activation can occur in both LKB1-dependent and LKB1-independent manners. Most of the studies addressing actions of MET alone or in combination of well-known cytotoxic agents such as chemotherapeutic drugs utilized milli-Molar doses of MET (1mM-100mM), which are not achievable in the circulation of human patients.

After the initiation of this project, few studies have explored the effects of MET in combination with radiation (Park et al, 2011). However, these studies have reported enhanced sensitivity of human cancer cells to ionizing radiation in combination with MET have utilized only mM doses of the pharmaceutical agent. Moreover, there have been no studies conducted to date with a specific focus of a combined treatment of MET and IR on human lung cancer cell lines.

In order to access how clinically relevant doses of MET impact growth of human cancer cell lines, we performed proliferation experiments on various human cancer cell lines of epithelial origin, specifically focusing on lung, breast and prostate cancer, for which radiotherapy is

employed as a therapeutic modality. While MET treatment led to sustained inhibition of cancer cell line growth, I have specifically observed that, amongst epithelial cancer cell, NSCLC cells exhibit higher sensitivity in micromollar doses of MET in comparison to prostate or breast carcinoma cells. With this increased sensitivity of specific subtype of lung cancer to MET treatment, I continued my investigation with a specific focus to examine whether clinically relevant doses of MET can inhibit NSCLC proliferation and sensitize them to radiation.

The studies performed on IR responses in MEFs and whole lung cancer xenografts (described in Chapter 3) helped to better understand the short and long term molecular effects of radiation on murine fibroblast and human lung cancerous cells. Since MET is known to modulate the activity of the molecular pathways that are also affected by IR, I decided to investigate whether combined treatment of MET with radiation could augment the molecular anti-tumour effects of radiation and enhance radiation cytotoxicity.

Overall, this part of my work had the following specific objectives:

i. **Examine the time course of the molecular effects of MET in cancer cells**
ii. **Compare MET sensitivity amongst epithelial cancer cell lines**
iii. **Investigate whether low micromollar doses of MET have anti-proliferative effects in NSCLC**
iv. **Examine whether those doses of metformin can sensitize cells to radiation**
v. **Examine potential mechanisms of action of MET: effects of signalling pathways, cell cycle**
vi. **Examine the effects of MET and IR on intact xenograft NSCLC tumour model , i) tumour growth kinetics, ii) Molecular signals and ii) angiogenesis and apoptosis**

Chapter 4

Results

4.1. Molecular Responses of A549 lung cancer Cells to MET

First, I investigated the time-course of the effects of MET on molecular signalling pathways of cancer cells. I treated A549 cells with a low dose MET (5μM) and collected cell lysates after 1 hour to 72 hours post MET treatment. Lysates were subjected to immunoblotting using anti- P-AMPK (T172), -P-Akt (S473), -P-p70s6k1, and – actin antibodies.

We have observed that activation of AMPK enzyme marked by Thr172 phosphorylation site exhibited highest expression at 72 hour and while protein expression was also increased in a time dependent manner. Interestingly, increases in AMPK activation due to prolonged MET treatments were paralleled by time- dependent inhibition of Akt kinase phosphorylation on Ser473 site along with decreases in expression of p70s6k1 protein, indicating decreased activity of the pathway (Figure 8.1 A).

As we have observed that MET resulted in similar modulation of the same pathway to that of IR treatment in LC cells, we also wanted to investigate whether DNA damage response molecular effectors would exhibit similar pattern of expression as was seen in long-term IR treatment. For that, we have performed immunoblotting analysis on lysates that were treated with MET in abovementioned manner and probed proteins with anti-ATM (total), -γH2AX (S139), and -actin antibodies. Interestingly, we have observed that both markers exhibited increases in expression in a time –dependent manner relevant to MET treatment (Figure 8.1 B).

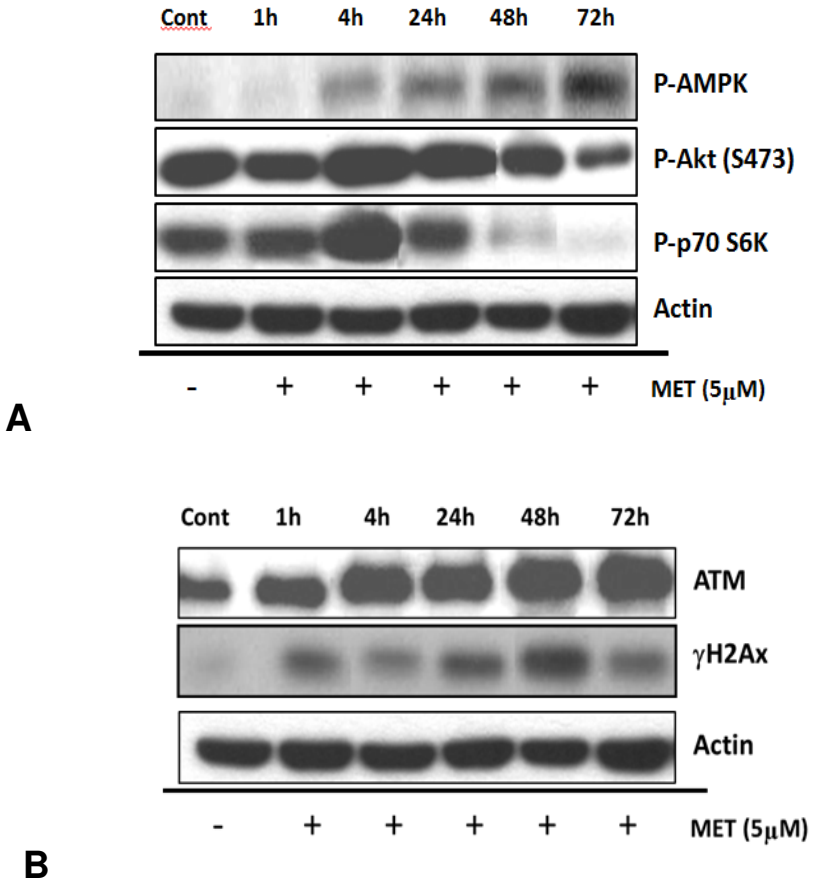

Figure 8.1 Chronic modulation of ATM- AMPK and Akt-mTOR pathways by Metformin (MET). **(A)** A549 cells were treated with MET (0 or 5µmol) for a period of 1h-72h. Cells were lysed and the lysates were probed for P-AMPK (T172), P-Akt (S473), P-p70S6K and actin antibodies. Representative immunoblots of at least three independent experiments are shown. **(B)** A549 cells were treated with MET (0 or 5µmol) for a period of 1h-72h. Cells were lysed and the lysates were probed for ATM, γH2AX (S139) and actin antibodies. Representative immunoblots of at least three independent experiments are shown

4.2 Metformin (MET) effects on human cancer growth and development

Numerous reports suggested that the anti-diabetic drug metformin may be an effective cytostatic agent aiding in growth reduction of epithelial human cancer cells.

Unfortunately, most of the studies investigating these effects have utilized high millimollar (mM) concentrations of MET, a dose range which is not achievable in the serum plasma of human patients. In order to investigate how pharmacologically tolerable doses of MET might impact growth of various human cancer cell line models, we have performed proliferation experiments on various human cancer cell lines of epithelial origin, where cells were seeded in 96 well plates in triplicate. After overnight incubation, cells were treated with a dose range of MET (0μM, 5μM, 25μM, 100μM. 500μM, 1mM or 5mM doses) and were allowed to further proliferate for 48-72 hours, depending on the proliferation rate specific to each cell line.

Interestingly, we observed that human lung cancer cell lines are more sensitive to the effects of MET regardless of subtype of cancer or specific mutation status when compared to epithelial prostate or breast carcinoma cell lines (Figure 8.2). MET treatment at 5μM significantly inhibited growth of A549 cells ($p<0.05$), with even more prominent inhibition in SK-MES1 and H1299 cell lines respectively ($p<0.001$). Conversely, reduction in cell growth did not reach significant levels in MDA-MB231 breast carcinoma cells until treatment with 25μmol of MET, while PC3 prostate carcinoma or MCF7 breast carcinoma cells exhibited significant reduction in proliferation rate at 100μM MET. Inhibition of cell growth within all cell lines occurred in a dose-dependent manner, and highest percentage of inhibition was achieved at largest 5mM dose of MET exposure.

MET at 5µM inhibited proliferation rates in A549, SK-MES1 and H1299 lung cancer cell lines were reduced to 89.8±4.2%, 74.9±5.1% and 78.0±3.4%, respectively, while PC3, MDA-MB231 and MCF7 cells had growth reduction at 98.5±0.9%, 95.6±0.4%, and 97.5±1.2% respectively (Figure 8.2).

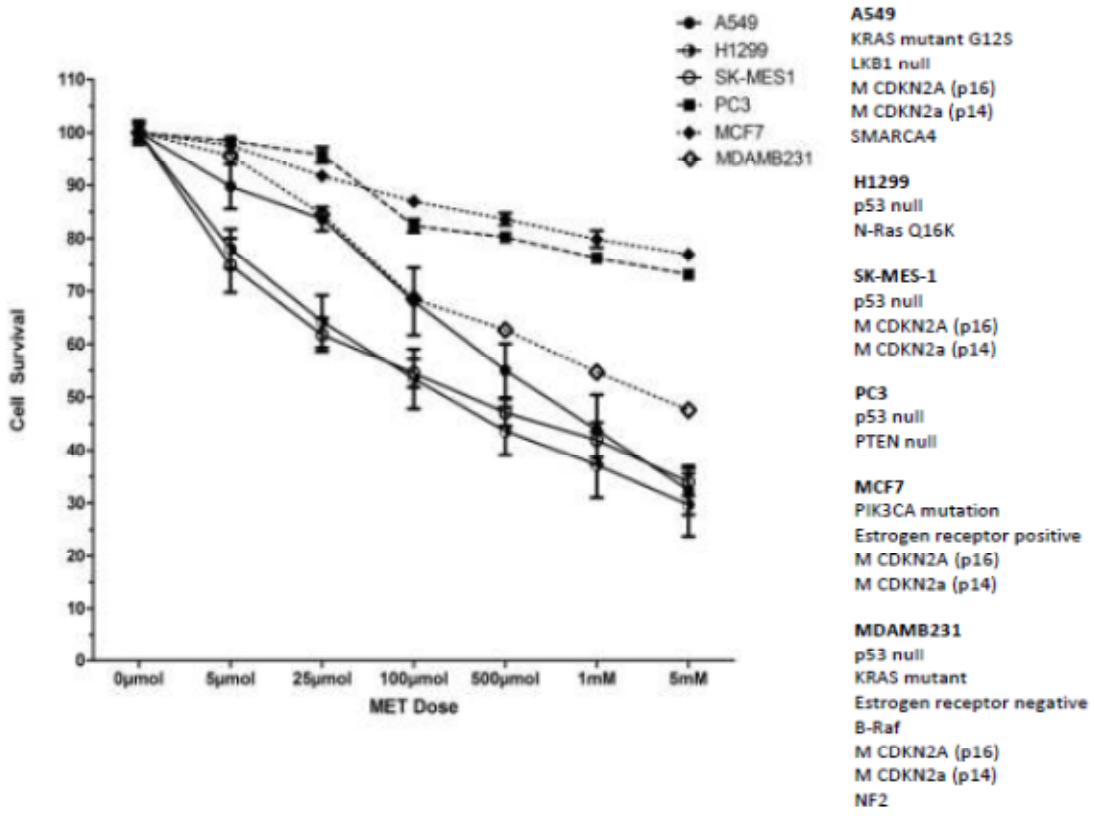

Figure 8.2 MET inhibits proliferation of human cancer cells in a dose dependent manner. A549, H1299 and SK-MES1, PC3, MCF7 and MDA-MB231 human cancer cells were treated with increasing MET doses (0µmol-5mM) for 48 hours and were later fixed with ethanol. DNA content, as a marker of proliferation, was determined with crystal violet staining. Results of three independent experiments are shown as Mean ±SEM.

4.3 Metformin sensitizes human lung cancer cells to Ionizing Radiation (IR)

Early preliminary work from our laboratory observed that low dose MET (5μM) can enhance radiation responses in NSCLC cells (Sanli et al 2010). Thus, we wanted to expand the investigation of MET actions coupled with Ionizing Radiation by analyzing dose-response of the effects of MET alone and in combination with in IR (2 or 8 Gy) on proliferation rates of A549, H1299 and SK-MES cells (Figure 8.3 A). Similar to earlier work (Sanli, et al, 2010), we observed that MET alone at doses as low as 5μM reduced significantly proliferation in all cancer cell lines (11±4.2%, 22±3.74% and 26±5.12% inhibition for A549, H1299 and SK-MES1 cells, respectively). Increasing MET concentration produced dose-dependent inhibition of proliferation that reached values of about 70% with 5mM MET. Importantly, MET also showed a fairly constant dose-dependent inhibition of proliferation when combined with both conventional (2Gy) and large radiation doses (8Gy) and reduced proliferation to 20% or less when combined with 2Gy and 10% or less when combined with 8Gy IR (Figure 8.3 A).

Since MET is a proposed to be an effective inhibitor of mTOR we compared the anti-proliferative effects of MET to those of the widely used mTOR inhibitor Rapamycin. We performed cell proliferation experiments in which A549 lung adenocarcinoma cells were treatment with a dose range of either MET (0-5mM) or Rapamycin (5nM-500nM), and subsequently exposed to 0Gy, 2Gy or 8Gy of IR dose. We observed that cells treated with low doses of MET at 5 - 100μM exhibited reduced proliferation levels comparable to those achieved by widely used concentrations of rapamycin (5 - 25nM) (Figure 8.3 B). Although rapamycin inhibited proliferation of untreated cells to a greater extent in comparison to MET, irradiated cells (2Gy and 8Gy) showed similar effects in proliferation

reduction across both MET (5 – 100μM) and rapamycin (5nM-25nM) treatment groups. Overall, both pharmaceutical agents exhibited parallel dose-dependent inhibition of proliferation in both untreated and irradiated cells (Figure 8.3 B).

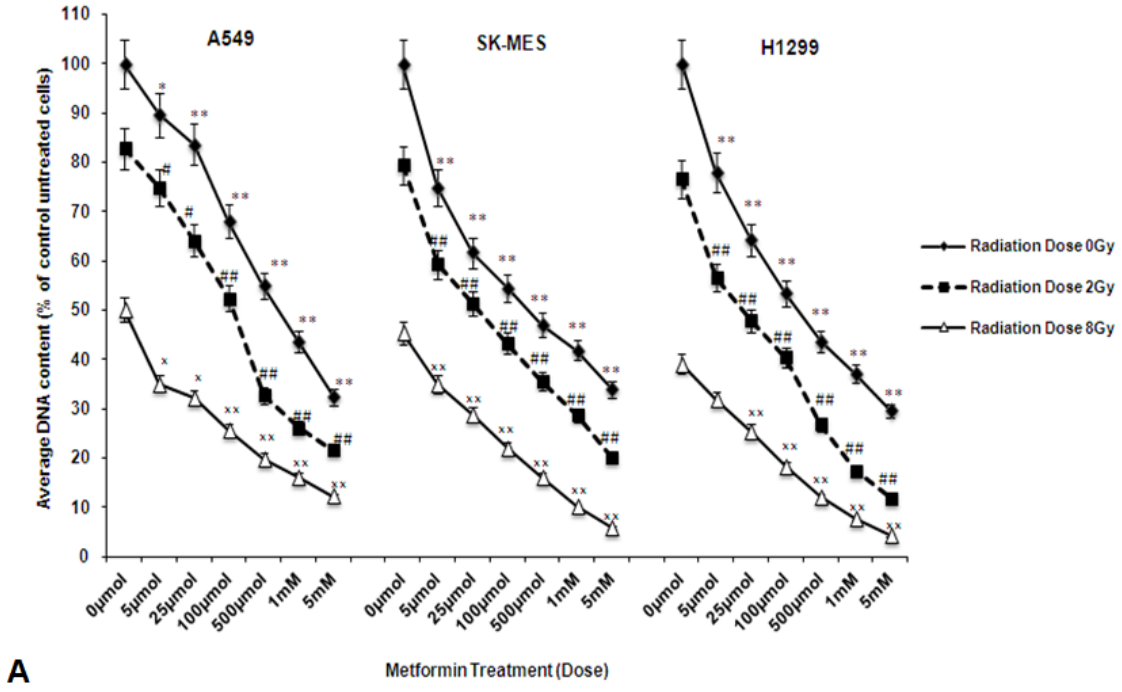

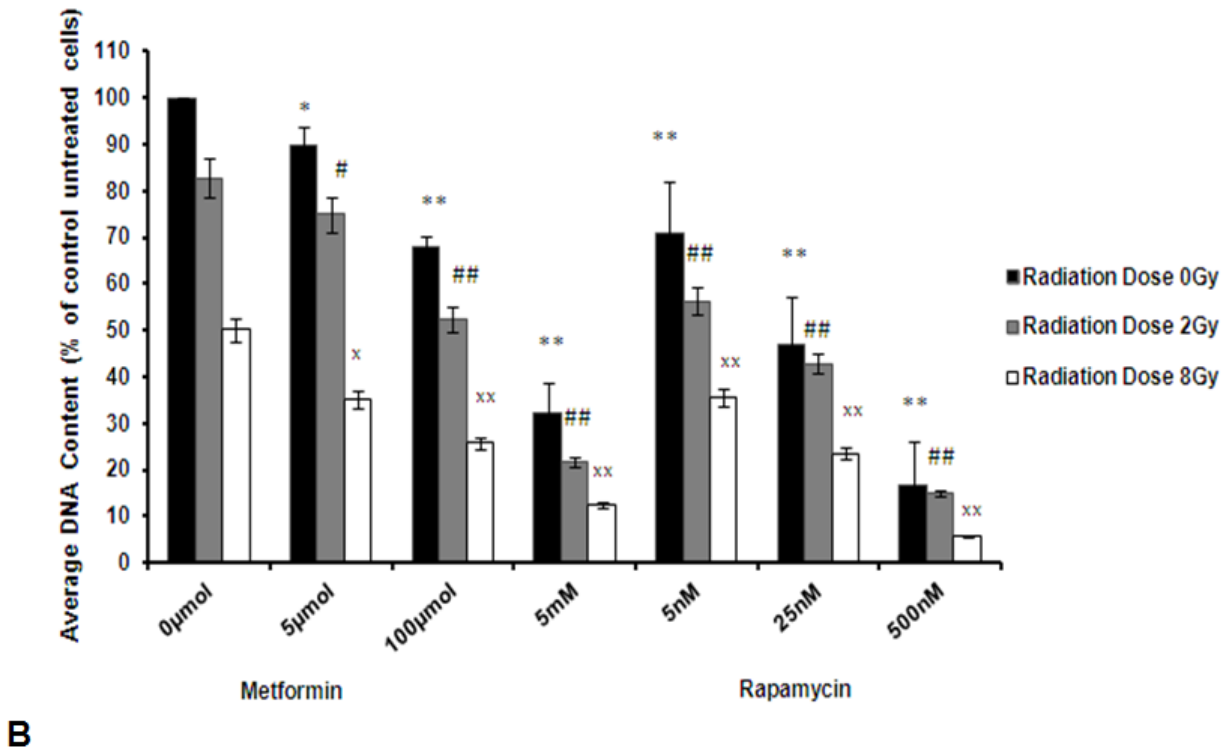

Figure 8.3. Effects of MET and IR on proliferation, clonogenic survival and molecular signals in human lung cancer (LC) cells. (A). A549, SK-MES1 and H1299 human LC cells were treated with increasing MET doses (5μmol-5mM) for 24 hours before treatment with 0, 2 or 8 Gy IR. Cells were fixed 48h later with methanol. DNA content, as a marker of proliferation, was determined with crystal violet staining. Results of three independent experiments are shown as Mean±SE. Statistically significant differences compared to corresponding control cells (not treated with MET) within the 0Gy 2Gy and 8Gy IR treatment groups are shown(*: P< 0.05, **: P<0.01). **(B)** Comparison of MET and Rapamycin effects in combination with IR on A549 human LC cell proliferation. Cells were treated with either 5μM, 100μM or 5mM MET or 5nM, 25nM, and 500nM Rapamycin for a 24 hours followed by treatment with either 0Gy, 2Gy or 8Gy of IR and incubation for an additional 48 hours. Cell fixation and proliferation rate was determined as outlined in A. Results of 3-4 independent experiments are shown. Data is represented as Mean±SE. Statistically significant differences of MET or rapamycin treatments from no-drug treatment control in the same radiation dose group are shown: *:P<0.05, **: P<0.001 for 0Gy group; #: P<0.05, ##:P<0.001 for 2Gy group; x:P<0.05, xx: P<0.001 for 8Gy treatment group.

4.4 Modulation of AMPK-p53 and Akt-mTOR pathways by MET in IR treated A549 cells

To explore the activation state of the AMPK pathway in the time-course of our proliferation experiments we analyzed in A549 cells the effects of MET and IR on AMPK and its downstream targets 24h after IR and 48h following treatment with MET. IR led to sustained stimulation of AMPK phosphorylation on Thr172 residue (P-T172-AMPK) and activity, marked by phosphorylation of its direct target AcetylCoA Carboxylase (ACC), in response to 8Gy IR (Figure 8.6 A, B). Consistently, IR induced significant increases in total p53 and $p21^{cip1}$ levels and enhanced p53-Ser15 phosphorylation in a dose-dependent manner. Conversely, we did not observe significant alterations in total and phosphorylated (T308 and S473) Akt levels or the total levels of mTOR, 24h after IR, but we detected inhibition of 4EBP-1 phosphorylation levels, after 8Gy IR (by 34.3±14.3%) indicating reduced mTOR activity (Figure8.6 A-C).

Exposure of cells to 5 or 100 micro-molar (μM) MET for 48h and treatment with 0 or 8 Gy of IR 24 hours post MET treatment initiation induced AMPKα-T172 phosphorylation in a dose dependent manner. No further significant induction of AMPK phosphorylation was detected after IR in those cells but IR enhanced further ACC phosphorylation significantly indicating enhanced AMPK activity. MET pre-treatment potentiated the IR-mediated induction of total and phosphorylated levels of p53 but did not induce further $p21^{cip1}$ expression. Apart from a trend for increased T308-Akt phosphorylation in cells treated with 8Gy IR and 100μM MET, the two agents did not induce sustained modulation of Akt and mTOR levels 24 and 48 hours after treatments. However, we observed consistent and significant inhibition of 4EPB1 phosphorylation in cells treated with either 8Gy IR or 100 μM MET alone and highly significant further inhibition of 4EBP1 phosphorylation in cells treated with MET+IR 5μM/8Gy: 38.3±8.7%; 100μM/8Gy:46.5±10.8% compared to control.

Since 8Gy IR inhibited 4EBP1 phosphorylation only modestly (by 34.4±4.3%), our results suggest a potential for MET and IR to mediate a synergistic inhibition mTOR activity (Figure 8.6 A-C).

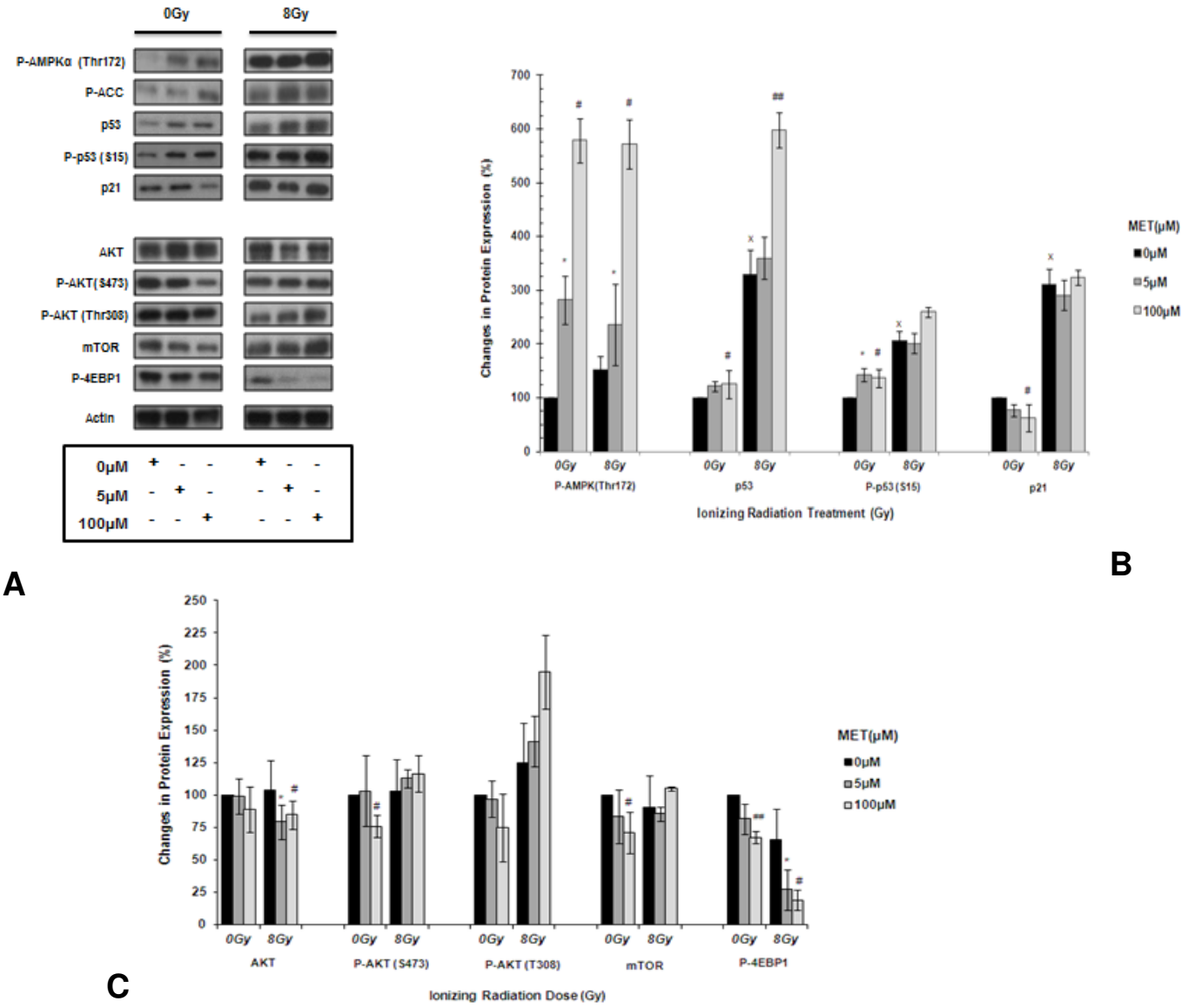

Figure 8.4 MET and IR mediate sustained modulation of molecular tumour growth and suppression pathways. A549 cells were treated with MET (0, 5 or 100μmol) for 48 hours, IR (0 or 8Gy) for 24 hours or combined MET+IR treatments. The cells were washed and lysed. Lysates were analyzed with immunoblotting using indicated antibodies. **(A)**Representative immunoblots are shown. Mean ± SEM densitometric quantification values from 3 independent immunoblotting experiments are shown for markers of the AMPK-p53-p21cip1 **(B),** the Akt-mTOR-4EBP1 **(C)** pathways.

4.5 MET and IR have distinctive effects on cell cycle distribution in human NSCLC cell lines.

We analyzed the effects of IR and MET on the cell cycle distribution of NSCLC cells. A549 cells were treated with 5μM or 100μM MET, IR (8Gy) or combined treatment (Figure 8.5 A). Untreated A549 cells distributed mainly at the G1 phase (G1: 86.3%, S phase: 10.5%, G2-M: 3.5%) (Figure 8.5 B). MET 5μM resulted in a shift of cells into S phase (G1:76.5%, S: 19.7%, G2-M: 3.8%) and MET 100μM showed similar effects (G1:77.4%, S: 16.7% and a minor increase of cells in G2-M phase: 5.83%). IR (8Gy) induced the expected G2-M checkpoint arrest G2-M: 28.9% vs. 3.5% in controls, (G1: 50.8% and S phase: 20.2%) (Figure 8.5 A). However, combination treatment of MET (5 and 100μM) and IR resulted into G1 shift and reduction of S and G2-M phases compared to cells treated with IR alone (G1 phase: 50.8% for IR vs. 65.8% for 5μM MET/8Gy and 66.9% for 100μM MET/8Gy and S phase: IR: 20.2% vs. 12.2% for 5μM MET/8Gy and 14.7% for 100μM MET/8Gy) (Figure 8.5 A, B).

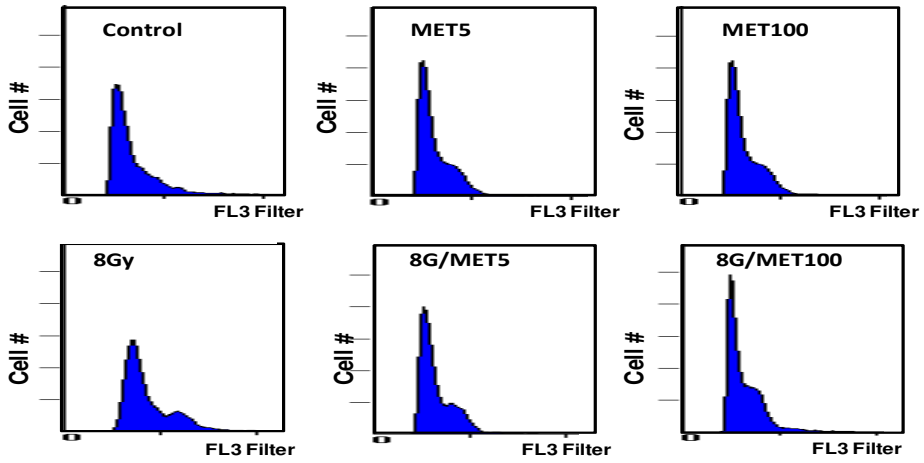

A

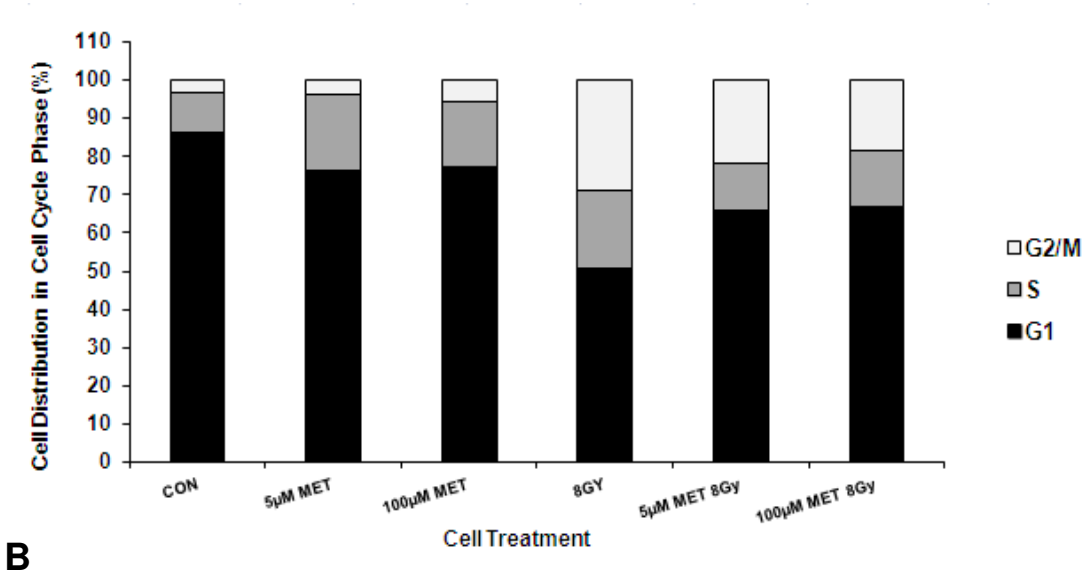

Figure 8.5 Modulation of A549 LC cell cycle by **chronic MET and IR treatments. (A)** Cells were treated with 0, 5, 100 µmol for 24 hours and subjected to 0Gy or 8Gy IR for 48 hour period. Cell cycle was evaluated as stated in Materials. Data of three independent experiments are shown as Mean ± SEM. **(B)** Quantitation of cell cycle distribution shown in (a).

4.6 MET and IR treatments result in additive growth inhibition of human lung cancer tumours

Since in vitro investigations on combined actions of MET and IR on growth of human lung cancer cells have concluded an additive effect on growth reduction in comparison to either agent alone, we wanted to investigate whether combination of both treatments would lead to growth reduction in whole lung cancer tumours.

For this, we have developed an animal model as described in Methods (section 2.4). Overall, forty four week old male Balb/c immunocompromised nude mice were grafted with either A549 or H1299 human lung cancer cells by subcutaneous injection. When tumours have reached 100 mm^3 in volume, animals were equally subdivided into four treatment groups: CON animals (received no treatment), MET animals (received daily MET at 300mg/kg dose via drinking water), IR (received single 10Gy dose) or MET and IR (received single IR treatment in addition to daily MET delivery). A549 animal cohort compromised six animals per treatment group, while H1299 cohort was arranged at four animals per treatment.

Throughout a sixty day growth period, tumour growth kinetics showed similar pattern of response amongst the treatment conditions in both A549 and H1299 xenografts, with highest inhibition of tumour growth occurring in MET+IR treatment group for both cohorts. Within fifteen days of treatment, animals from either A549 or H1299 cohorts undergoing MET+IR treatment exhibited significantly reduced growth in comparison to their CON counterparts, while single MET and IR treatments achieved statistically significant differences in tumour growth past day 25. At the end of the treatment period, final tumour volumes reached by A549 cohort were Control: 679.5±50.6mm^3, MET: 470.53±35.2mm^3, IR: 342.9±21.8mm^3 and MET+IR: 257.9±15.2 mm^3, while H1299 tumours reached the volumes of 1122.39±39.17 mm^3,

646.02±40.42 mm³, 428.02±18.89 mm³, and 300.25±24.25 mm³ for CON, MET, IR and MET+IR treatments respectively (Figure 8.6).

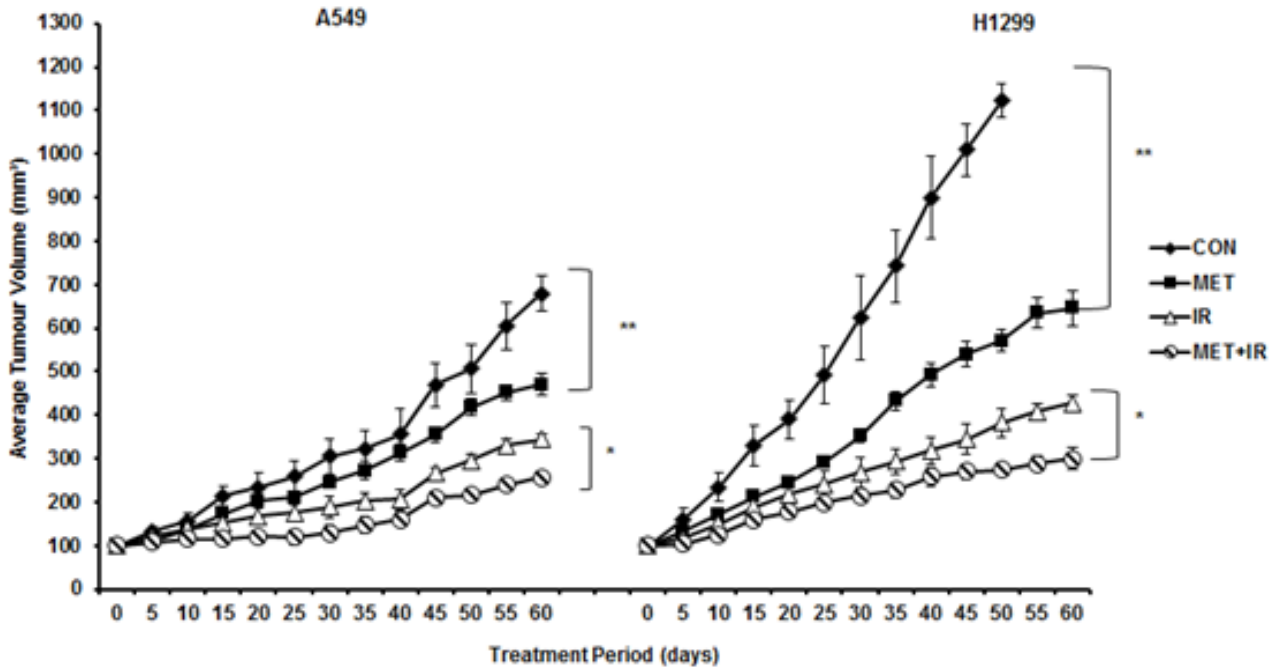

Figure 8.6 Inhibition of A549 and H1299 tumour growth by MET and IR. Twenty four and sixteen male Balb/c nude mice were grafted with 1x106 A549 or H1299 cells into the right flank respectively. Treatment with MET, IR or combination was initiated once tumour volume reached 100mm³. Tumour volume was measured every five days for a period of 8 weeks as described in Methods. Average (Mean ± SEM) tumour volume data of six animals (A549) or four animals (H1299) per treatment group are shown. Statistically significant differences ($P \leq 0.01$) of average tumour volumes between the Control and treated groups as shown (**: $P \leq 0.01$ of MET vs. Control, *: $P \leq 0.01$ of IR vs. MET+IR).

4.7 Long-term Regulation of AMPK expression and activity by MET and IR

We investigated whether the combined MET and IR treatments regulated the expression and activity of AMPK enzyme in intact tumours, as was previously supported by both in vitro and in vivo works on the actions of individual MET and IR treatments on AMPK expression.

For that, we have lysed A549 whole tumours and performed immunoblotting analysis on tissue lysates against -AMPKα, -P-AMPK (T172), -P-ACC, and -actin antibodies (Figure 8.7 A). Tumours excised 8 weeks after a single dose of IR (10Gy), continuous treatment with MET or combined treatment showed sustained enhancement of total AMPKα, P-Thr172-AMPKα and phospho-(P)-Acetyl-CoA Carboxylase (P-ACC) levels, indicating definitive enhancement of AMPK activity. Representative immunoblots and quantification results for all markers are shown in Figure 8.7A, B. IR and MET increased significantly and independently basal levels of AMPK α-subunits but combined treatment enhanced that by over two-fold. More significant increases of the activated form of the enzyme (P-Thr172- AMPKα) were achieved by MET and IR (3-fold and 4-fold increase compared to untreated (CON) tumours) and 5-fold by MET+IR (Figure 8.7 A, B). P-ACC levels were 2-fold higher in irradiated tumours compared to controls, while MET+IR treatment resulted in 4-fold increase in the expression of this marker AMPK enzymatic activity (Figure 8.7 A, B).

To confirm the immunoblotting results and examine the tumour gross cellular and subcellular distribution of AMPK activation we performed immunohistochemical analysis against P-(Thr172)-AMPKα in paraffin embedded A549 tumours. The experiment confirmed the distribution of activated AMPK (P-T172-AMPKα) in the cytoplasm and nucleus of tumour cells and reproduced the results obtained by immunoblotting (Figure 8.7 a, c) with MET and IR

tumours showing increased levels of activated AMPK and the combined treatment demonstrating a further increase above that achieved by the MET or IR alone.

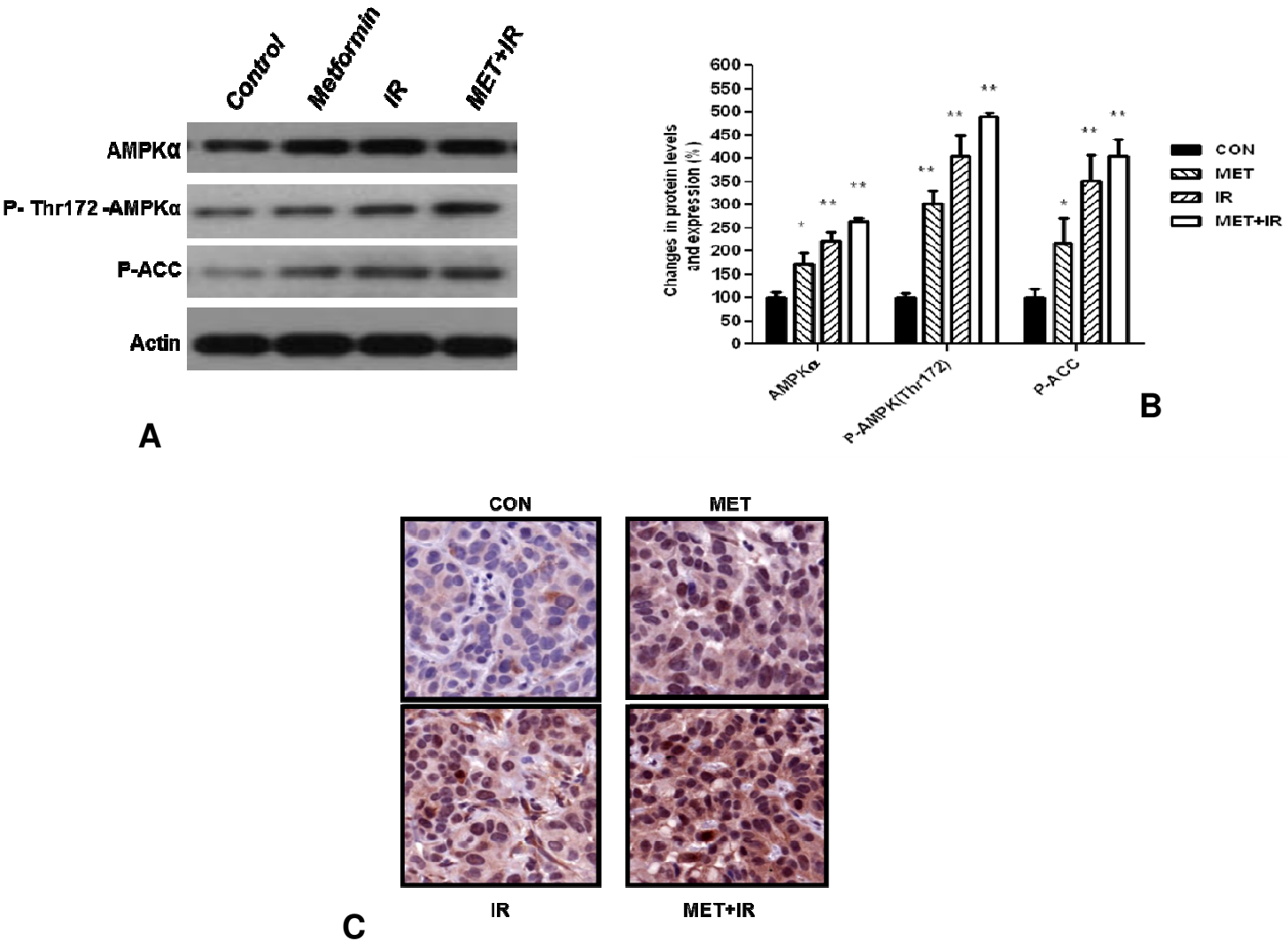

Figure 8.7 MET and IR lead to long-term activation of AMPK in A549 tumours. Tumours collected from Control (CON), MET, IR and MET+IR treatment groups were subjected to lysis and immunoblotting with anti-AMPKα, -P-AMPKα(Thr172), -P-ACC, and -actin antibodies. **(a)** Representative immunoblots are shown. **(b)**Densitometry analysis was carried out as described in Methods. Data are shown as Mean±SEM of the normalized values in each treatment group (n=6 in each group). **(c)**Immunohistochemical analysis of A549 tumours from four different treatment groups using an anti-P-AMPKα (Thr172) antibody. Representative images from three independent experiments are shown

4.8 Long-Term MET and IR treatments enhance expression of DDR biomarkers

Our work with tissue culture models (Section 4.4) described above showed that not only IR but also MET alone modulated the expression and activity of members of the DDR pathway including ATM, p53 and Chk2. In addition, our human NSCLC xenograft work (Section 3.5) demonstrated a long term up-regulation of those pathways in radiated tumours that was sustained many weeks after a single fraction of radiation. For that examined those pathways in tumours treated with MET with or without radiation.

In A549 tumour lysates we analyzed with immunoblotting the levels of ATM, γH2AX, -P-Chk2, -p53 (total), -P-p53 (Ser15), - $p21^{cip1}$, and – actin antibodies (Figure 8.8 A). Apart from an enhancement of ATM protein levels and its activity, evident by increased γH2AX levels and a trend for increased Chk2 phosphorylation (not statistically significant). We also observed a robust enhancement of ATM levels and activity (γH2AX levels) by MET treatment alone. Furthermore, we detected further enhancement of the IR-induced levels of ATM expression and activity in tumours treated with MET and IR.

Tumours lysates were also probed with anti-p53, P-p53 (S15) and $p21^{cip1}$ antibodies. The single IR treatment produced chronic significant increase, of 2-fold or higher, in total and S15-phosphorylated p53 and in $p21^{cip1}$ levels (Figure 8.8 A, B). Similar to *in vitro* observations (Section 4.4) MET enhanced total and S15-phosphorylated p53 and $p21^{cip1}$ levels but the combined MET+IR treatments produced significant synergistic enhancement of those markers that approached additivity for $p21^{cip1}$ expression (Figure 8.8 A, B).

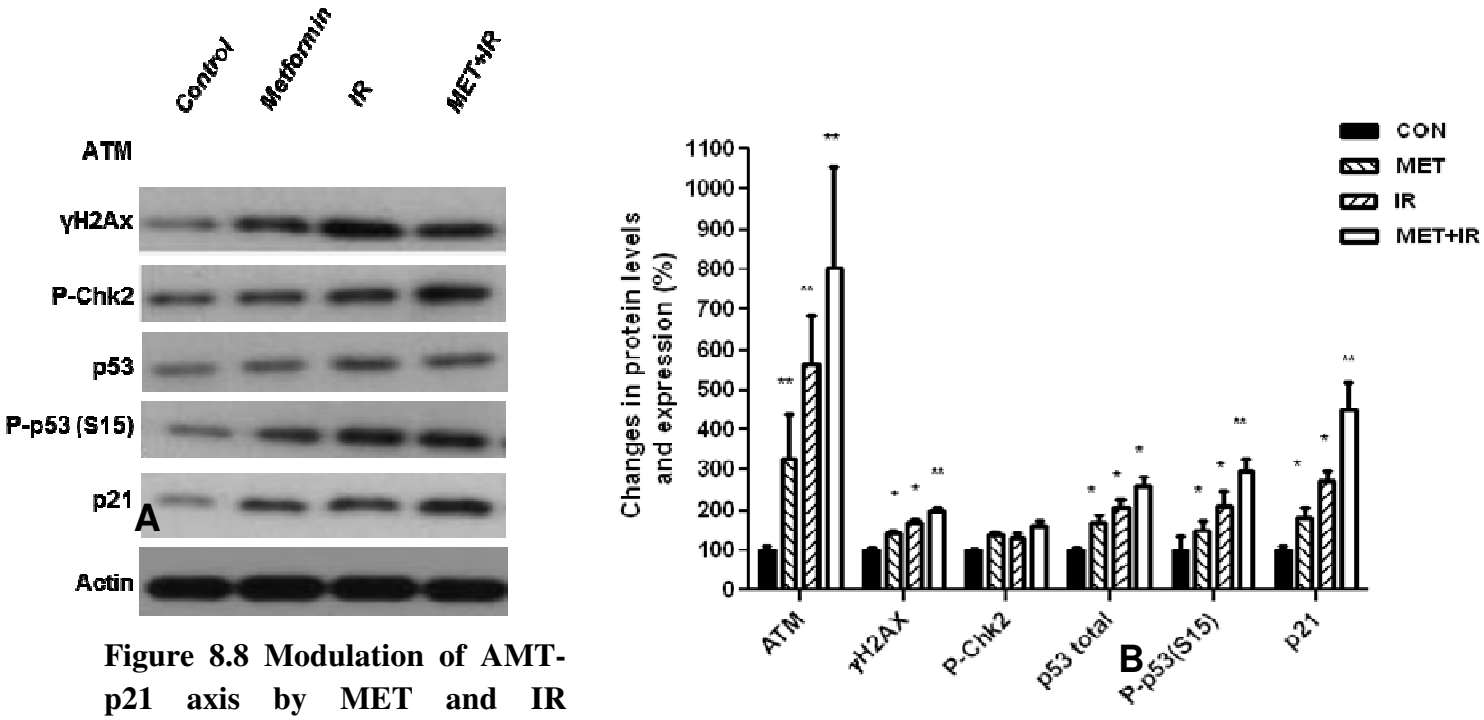

Figure 8.8 Modulation of AMT-p21 axis by MET and IR treatments in lung cancer tumours. **(A)** Immunoblotting analysis of lysates from Control, MET-, IR- and MET+IR-treated tumours with anti-ATM, -γH2AX, -P-Chk2, -p53, -P-p53(S15), -p21cip and -actin antibodies. **(B)**Densitometry analysis of immunoblotting experiments (n=6 in each group). Data are presented as Mean±SEM of normalized densitometry values.

4.9 Modulation of Akt-mTOR pathway by long-term MET and IR treatments

We did not detect significant differences in the total AKT levels between individual MET or IR treatments and untreated tumours, however, combined treatment of MET and IR induced an average 30% decrease in the expression of AKT protein, which did not reach statistical significance (Figure 8.9 A, B). Tumours treated with MET alone showed a potent reduction of Akt phosphorylation on both T308 and S473 residues (Figure 8.9 A, B).

There was no detectable consistent modulation of total or phosphorylated mTOR levels by either MET or IR treatment, however, both treatments led to significant inhibition of mTOR activity indicated by reduced 4EBP1 phosphorylation (MET: 26.8±4.8%; IR: 29.5±5.2%) while combined treatment resulted in a highly significant 51.5±8.3% reduction in P-4EBP1 (Figure 8.3 A, B) consistent with cell culture results (Figure 8.9 A, B).

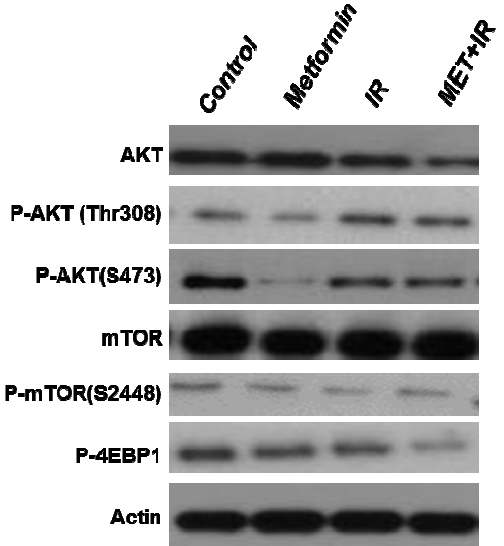

A

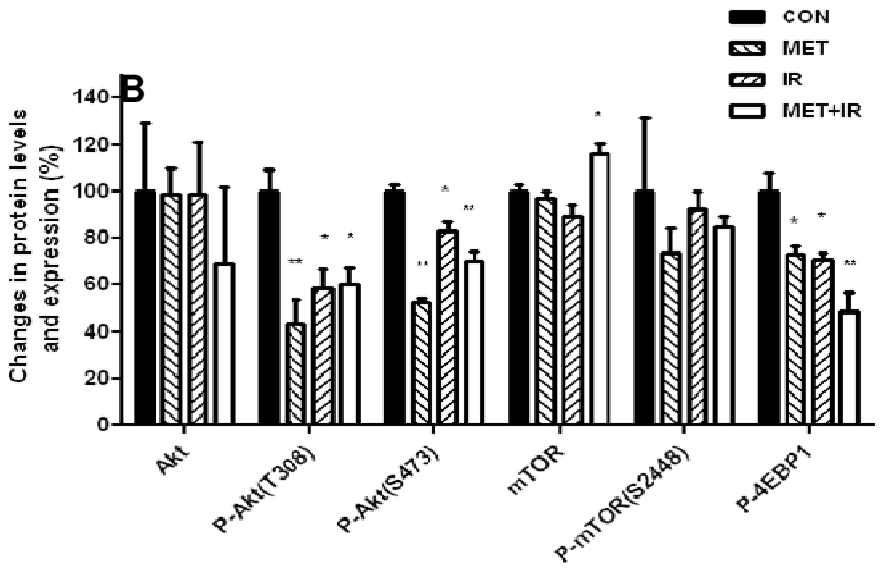

Figure 8.9 Chronic MET and IR exposure synergistically inhibits Akt activity in A549 xenografts. (A) Representative immunoblots from Control, MET, IR and MET+IR treatment groups were analyzed with anti-total-AKT, -P-AKT (S473), -P-AKT (Thr308), -total-mTOR, -P-mTOR(S2448), -P-4E-BP1 and -actin antibodies. **(B)** Results (Mean±SEM) from three independent experiments are shown (n=6 in each group). *: P≤ 0.05, **: P≤ 0.001 statistically significant difference between treatment groups and Control for each marker

4.10 Modulation of tumour vasculature by MET and IR treatments

We examined in tumour lysates the expression of the endothelial angiogenesis marker CD31 using immunoblotting (Figure 8.10 a). Irradiated tumours (IR) showed significant

reduction in CD31 expression (29.3±3.9%). However, tumours of animals treated with MET and MET+IR showed a higher reduction in CD31 levels of 51±4.1% and 47±4.9 %, respectively, compared to CON tissues (Figure 8.10 A, B). To confirm the results obtained from immunoblotting analysis on A549 tumour lysates, we performed immunohistochemistry with an anti-CD31 antibody and observed a significant reduction in the density of microvessels in tumours treated with MET, IR or the combined treatment (Figure 8.10 C).

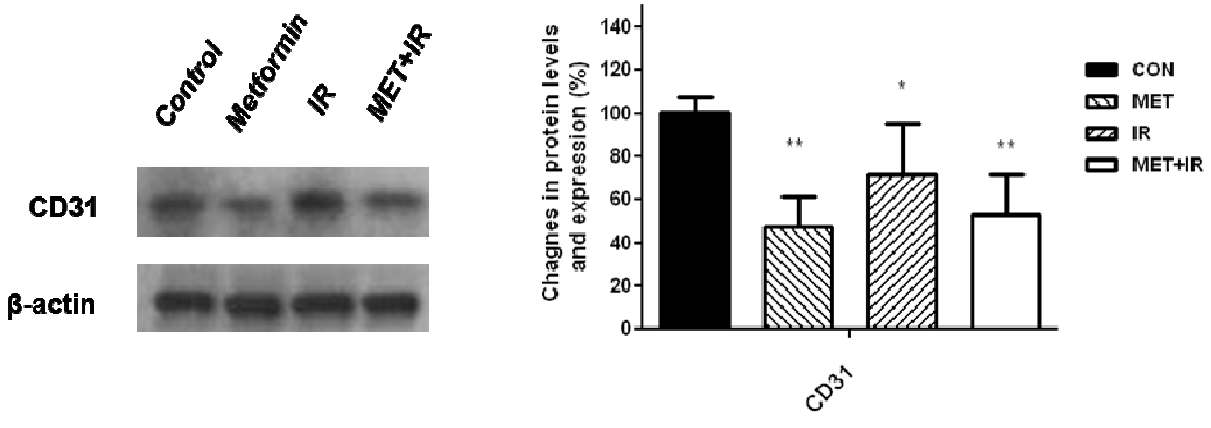

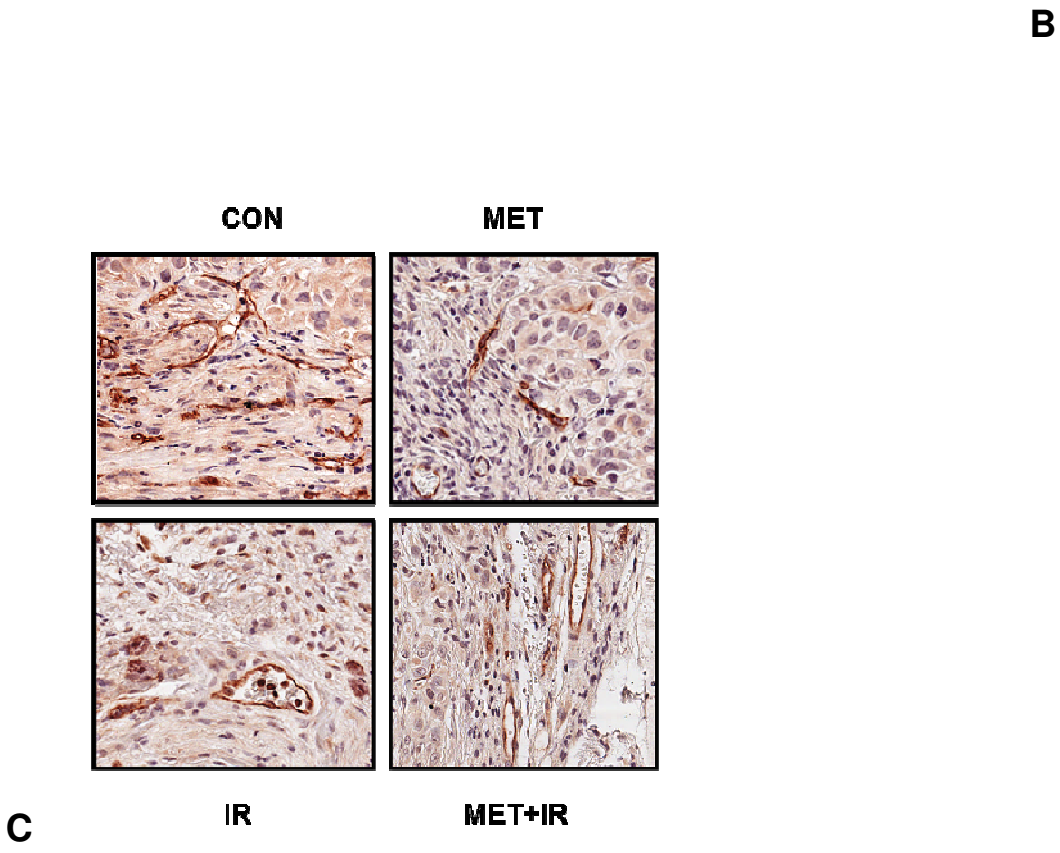

Figure 8.10 MET and IR treatments inhibit angiogenesis in tumours. (A) Lysates from Control, MET-, IR- and MET+IR-treated tumours we analyzed with immunoblotting using anti-CD31 and -actin antibodies. Representative immunoblots are shown. **(B)** Densitometry analysis of immunoblotting results from lysates of tumours in all experimental groups (n=6 in each group). Data are Mean ± SEM of normalized densitometry values (*: P≤ 0.05, **: P≤ 0.001 statistically significant difference between treatment groups and Control for each marker). **(C)** Representative images of anti-CD31 immunohistochemisty analysis of A549 Control (CON), MET-, IR- and MET+IR-treated tumours.

4.11 Regulation of pro-apoptotic markers

To explore the mechanism of inhibition of tumour growth and cell death in response to MET and IR treatments, we analyzed three separate markers of apoptosis (Bax, PUMA, and Cleaved Caspace 3) in whole A549 tumours using immunoblotting or immunohistochemistry

analysis (Figure 8.11 A-C). In tumour lysates, individual MET and IR treatments increased BAX and PUMA but this was statistically significant only for irradiated tumours. MET worked synergistically with IR to further enhance the induction of both markers in comparison to individual treatments or untreated tissues (Figure 8.11 A, B).

To further verify the activation of the apoptotic pathway, we examined the levels of Cleaved Caspace 3 (CC3) in paraffin embedded A549 tumours via immunohistochemical analysis. In comparison to CON tumours, MET and IR significantly increased the expression of the marker, however, the highest activation was seen in tumours that underwent combined treatment of MET and IR (Figure 8.11 C).

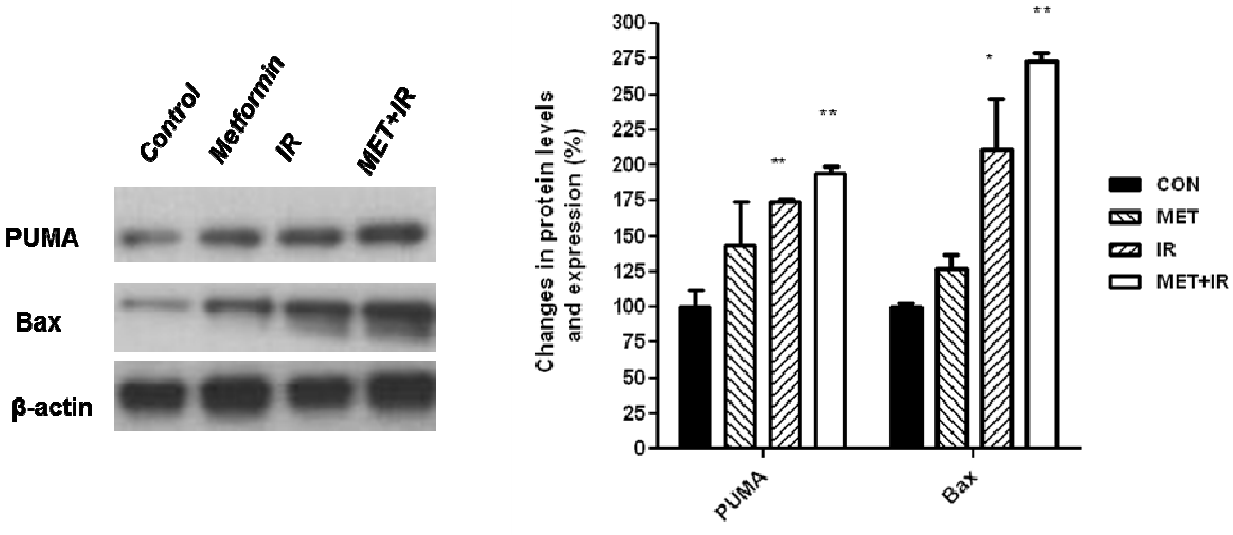

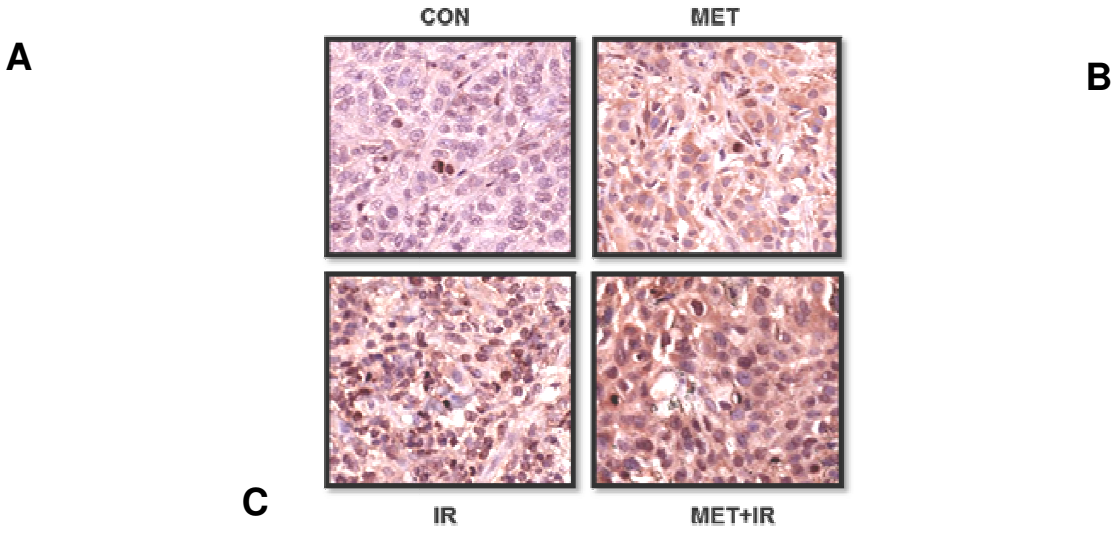

Figure 8.11 Modulation of pro-apoptotic pathways by MET and IR treatments in A549 lung cancer xenografts. (a) Immunoblotting analysis of Control, MET-, IR- and MET+IR-treated A549 tumours with anti-Puma, -Bax, and -actin antibodies. Representative immunoblots of three independent experiments is shown**. (b)** Densitometry analysis of immunoblotting results in all treatment conditions (n=6 in each group). Mean±SEM of normalized densitometry values are shown (*: P≤ 0.05, **: P≤ 0.001 statistically significant difference between treatment groups and Control for each marker). **(c)** Representative images of immunohistochemistry analysis of Control (CON), MET-, IR- and MET+IR-treated tumours with an anti-Cleaved Caspace 3 (CC3) antibody

Chapter 4

Discussion

Metformin (MET) has been extensively studied for its properties to inhibit cancer cell proliferation and slow tumour growth in numerous animal models utilizing human cancer xenografts of breast, lung and prostate origins. However, the potential of MET as an anti-cancer

agent specifically in NSCLC tumours was not investigated systematically. Moreover, most of the in vitro studies utilizing MET as a therapeutic alone or in combination with cytotoxic therapies used milli-mollar (mM) concentrations of the drug, which are not achievable in the clinical setting. Our laboratory was the first to show reduced growth of NSCLC cells with MET treatment at doses as low as 5μM, which represents an average blood serum dose in human patients treated with daily oral doses of the drug (Sanli et al, 2010). For this reason, we wanted to further investigate the anti-proliferative potential of small MET doses on NSCLC and elucidate whether these doses can enhance sensitivity of lung cancer cells and whole lung cancer tumours to radiotherapy.

Molecular Responses of A549 lung cancer Cells to MET

We have initiated this study by observing molecular responses of A549 NSCLC cells treated with 5 μM MET doses for a period ranging from 4 hours to 72 hours. The immunoblotting experiments of the lysates have confirmed that AMPK activation upon MET treatment occurs in a time-dependent manner and the activation of the enzyme marked by Thr172 phosphorylation of the catalytic α subunit is most prominent at the 72 hour treatment mark. We have also observed time-dependent decreases in phosphorylation of both Akt kinase on Ser473 residue and p70s6k1 protein, which is a downstream target of mTOR. The decrease in phosphorylation of both proteins can be explained by consistent activation of AMPK, which is known to negatively regulate the Akt-mTOR pathway. The results obtained from the time-course MET treatment in A549 cells is consistent with various in vitro studies which concluded that MET treatment of human cancer cells (prostate and breast carcinomas) inhibits activation of Akt-mTOR pathway in a dose- and time-dependent manner. However, unlike other studies, it is a novel finding to report AMPK

activation and Akt-mTOR pathway inhibition with prolonged treatment of MET at clinically relevant doses.

MET inhibits human cancer cell growth

I investigated whether anti-proliferative actions of MET are cell-line and tumour site and mutational genotype specific or occur in a non-selective manner. We observed that MET supresses growth of various human cancer cell lines of epithelial origin in a dose-dependent manner, however, NSCLC cell lines (A549, H1299 and SK-MES1) showed a higher sensitivity towards MET doses at clinically relevant levels (5-25μM) in comparison to human prostate carcinomas (PC3) or breast carcinoma cell lines (MCF7 and MDA-MB231). While growth suppression of breast and prostate carcinoma cell lines by MET has been reported previously, this study is the first to compare actions of MET raging from clinical relevant doses at 5μM to mM doses utilized in in-vitro studies (1-5mM). Moreover, this study is the first of its kind to compare MET action across several genotypically and morphologically distinct cell lines simultaneously. The findings of NSCLC having higher sensitivity towards MET treatment in comparison to cells of breast or prostate carcinomas might prove to be a useful tool for further pre-clinical and clinical studies utilizing the drug as an anti-cancer treatment, however, future studies elucidating the reason behind MET impact on particular types of cancer lines vs. others are needed.

MET enhances sensitivity of human lung cancer cells to Ionizing Radiation (IR)

We showed that MET causes dose-dependent inhibition of proliferation of a number of tissue culture models of NSCLC. We used lines that represent common histologies and mutation genotypes of NSCLC (A549 adenocarcinoma: LKB1-deficient (nonsense mutation of codon 37

leading to stop codon), K-Ras G12S activating mutant, p53-wild type (WT); H1299 adenocarcinoma: LKB1-WT, p53-deficient (*TP53* partial deletion) and SK-MES squamous cell carcinoma: LKB1-WT, p53-deficient (exon 8 mutation). The efficacy of the drug to inhibit proliferation and clonogenic survival in all models of NSCLC used indicates increased potential for clinical development of MET in most NSCLCs. We observed that MET alone at smallest doses of 5μM significantly inhibited cell proliferation across all cell lines, and the inhibition was further enhanced in a dose-dependent manner. These results indicate the efficacy of MET as cytostatic agent in NSCLC occurs independently of the mutations present within the cancer cell lines.

For relevance to clinical radiotherapy, we utilized standard radiation doses of 2-10Gy delivered to cells by clinical linear accelerators. Beyond the expected IR cytotoxicity in LC cells, we observed that both low and higher doses of MET augmented, in a synergistic fashion, the anti-proliferative effects of both lower (2Gy) and greater (8Gy) IR fractions. Proliferation rates of three distinct NSCLC cell lines occurred in a dose dependent manner with regards to both MET and IR treatments. This report is the first study to demonstrate radio-sensitizing effects of MET at clinically achievable μM doses of the drug in human lung cancer cell lines.

As MET is known to modulate mTOR activity we compared it to the macrocyclic lactone mTOR inhibitor rapamycin (Sirolimus), which has been utilized as an enhancer for both radiotherapy and chemotherapy in cancer patients. In clinical pharmacokinetic studies 2–3mg oral rapamycin led to C max plasma levels of 5–29nM with limited toxic side effects, however, higher doses led to severe toxicity in human patients, including mucositis, thrombocytopenia, diarrhea and hyperglycaemia (Jimeno et al, 2008). As MET treatment is known to be well tolerated by both diabetic and non-diabetic patients with minimal side effects, we wanted to

investigate whether cytostatic effects of MET in combination with IR would be comparable to those of rapamycin and IR. Through proliferation experiments of A549 NSCLC cells, we have observed that inhibition of proliferation rates in cells treated with 5μM-5mM MET and 2Gy or 8Gy IR were comparable to cells treated with 5nM-500nM of rapamycin in addition to 2Gy or 8Gy IR. These results indicate that MET has the potential to be utilized as an enhancement treatment to IR in lung cancer patients without causing severe side effects associated with rapamycin.

Modulation of AMPK-p53 and Akt-mTOR pathways by MET in IR treated A549 cells

Our experiments showed that MET offered additive anti-proliferative action to that of IR and was able to modulate signalling pathways that are affected by IR even further than what IR could achieve. Earlier studies in our laboratory reported robust activation of AMPK upon acute IR exposure (1 hour) (Sanli et al, 2010), and earlier in this project we showed, using AMPK$\alpha^{-/-}$ MEFs, that AMPK is required to stabilize the activity of the Akt-mTOR and DNA-damage-response (DDR) response pathway of ATM-γH2AX/Chk2 to maintain radiation responsiveness (Chapter 3). Consistently, in the in-vitro studies of this chapter we observed phosphorylation and activation of AMPK 24h after IR (Figure 8.4; Figure 8.5). In this time MET (5-100μM) induced a robust activation of AMPK. For consistency with proliferation experiments, signalling events were evaluated here 48h after MET and 24h after IR treatments. IR did not increase significantly AMPK activity in MET-treated cells at 24h after IR further than MET treatment alone (Figure 8.4, Figure 8.5) and MET did not enhance $p21^{cip1}$ expression beyond levels achieved by IR. However, we detected sustained enhancement of total and phosphorylated p53 levels and additive inhibition of mTOR activity with combined MET and IR treatment, as inhibition of 4EBP1 phosphorylation (Figure 8.5). The combined acute and chronic input of IR and MET into the

AMPK-p53/p21^{cip1} and Akt/mTOR axes could account for the anti-proliferative benefits of combining MET with IR

MET and IR have distinctive effects on cell cycle distribution in human NSCLC cell lines

Research reports suggest that treatment of cells with MET is expected to inhibit protein synthesis and growth of cellular biomass and to induce G1/S check point arrest. We observed an increase of cells at S phase with MET treatment in A549 cells treated with either 5μM or 100 μM MET, indicating an expected G1-S transition arrest within the cell cycle. Cells treated with IR alone underwent expected G2-M arrest in the cell cycle, while combination treatment of MET and IR led to arrest in G1-S phase, similarly to MET treatment alone. This can be attributed to a more effective modulation of p53/p21^{cip1} and mTOR by MET leading to a G1-S stage shift in the cycle.

MET and IR treatments result in additive growth inhibition of human lung cancer tumours

As we observed enhanced inhibition in proliferation rates of NSCLC treated with both MET and IR, we wanted to investigate whether combination of treatments would lead to same effect and supress growth of whole lung cancer tumours in the animal model. By using two distinct types of human NSCLC cell lines, A549 and H1299, we have observed that individual MET and IR treatments do result in a significant delay in tumour growth at three weeks post treatment initiation. However, combination of daily MET doses with a single fraction of IR produces an additive effect on tumour growth suppression, with a significant delay reached only two weeks post treatment initiation. The findings presented here are novel and can prove to be significant for future development of pre and clinical studies on combination of MET and IR in human patients with NSCLC.

Molecular effects of MET and IR treatments on lung cancer tumours

In tumours, a single fraction of IR or continued treatment with MET led to sustained expression and activation of ATM-AMPK-p53/p21^{cip1} and inhibition of Akt-mTOR pathways with significant enhancement of those effects by the combined treatment (Figure 8.7, Figure 8.10). In relation to IR action, recently, we reported chronic up-regulation of the ATM-AMPK-p53/p21^{cip1} and downregulation of Akt-mTOR-4EBP1 pathways also in H1299 xenografts (Chapter 3). This indicates that these are universal responses of epithelial tumours to radiotherapy.

Observation of enhanced levels of phosphorylated (active) AMPKα subunits in response to MET not only in whole tumour lysates but in tumour cell cytoplasm and the nucleus using immunohistochemistry (Figure 8.7) suggests a direct action of the drug at the tumour cell level rather than indirect effects in the liver or circulating insulin, that were suggested earlier(38). Intriguingly, we observed that not only IR but also MET causes a sustained enhancement of ATM expression and activity (Figure 8.8). Although, this may be related to tumour hypoxia, since MET also reduced tumour vascular supply (discussed below), these results are consistent with other reports of ATM activation by MET and a developing notion that MET may mediate in tissues a pseudo-DDR to protect against oncogenesis.

Reports on the effects of MET on tumour microvasculature remain controversial. AMPK regulates endothelial cell migration participating in angiogenesis. MET was suggested to normalize tumour vasculature in breast cancer and inhibit angiogenesis in ovarian cancer xenografts. Here we show that MET and IR reduced microvascular density and expression of the endothelial marker CD31 (Figure 8.10). MET mediated these modifications in microvasculature more potently than IR and it enhanced the effects of IR.

The significant induction of expression and phosphorylation of p53 we detected with MET both *in vitro* and *in vivo* suggested that apoptotic cell death may indeed be activated. Enhanced expression of Bax and Puma by IR and MET indicate that the intrinsic, mitochondria-dependent, pathway of apoptosis is activated by both agents and it is stimulated further by the combined treatment. Increased cleavage/activation of caspace 3 by MET and IR and the combined treatment, a key step of the common apoptotic pathway, indicates a commitment of lung tumour cells to apoptotic death (Figure 8.11).

CHAPTER 5

SUMMARY AND CONCLUSIONS

Despite the fact that radiotherapy is one of the main therapeutic modalities for treatment of lung cancer, it has limited efficacy and poor local tumour control rates which lead to poor overall survival. In order to improve the efficacy of radiotherapy, it is important to understand fully the molecular and physiological effects mechanisms of IR actions on lung cancer cells in both *in-vitro* and *in-vivo* models of the disease. (In the past few years, the work of our laboratory focused on elucidating the role the metabolic sensor and tumours suppressor AMPK in radiation responses of epithelial tumour cells. With extensive work in genetically modified MEFs and pre-clinical tissue culture and xenograft models lung cancer we have produce convincing evidence that IR activates a DDR ATM-AMPK-p53/p21^{cip1} pathway and inhibits the growth radioresistance pathway of Akt-mTOR. This work consistent the first part of M.Sc. thesis research. It is described in Chapter 3 and it has been now published in two separate manuscripts (Sanli et al, 2012, Storozhuk et al, 2012). The knowledge gained from this work indicated that targeting the ATM-AMPK/Akt-mTOR pathways by combining novel therapeutics with IR may be an effective way to sensitize further lung cancer tumours to radiation. In the second part of my thesis research, we examined the systematically in in-vitro and in-vivo models of lung cancer and other epithelial cancer cells the role of antidiabetic drug Metformin (MET) to enhance IR responses. We observed that clinically achievable doses of MET work synergistically with radiotherapy to induce a favorable molecular response and increase the cytotoxicity of radiotherapy in lung cancer cells and tumours. This suggested a strong potential for MET to serve as a clinically useful adjunct to radiotherapy for the treatment of NSCLC patients.

We observed that AMPK is involved in stabilizing in normal cells the baseline expression and activity of the DDR ATM-Chk2/p53-$p21^{cip1}$ pathway, while defective or lack of AMPK activity led to enhancement of tumour growth and radio-resistance pathways. AMPK is required for the normal propagation of IR-stimulated signals along the ATM /p53/$p21^{cip1}$ – Akt – mTOR pathways and lack of AMPK leads to abnormal cell cycle checkpoint response to radiation.

Our results were further supported *in vivo*, where we explored the long-term regulation by IR of two key tumour suppression or growth pathways that are targets of promising therapeutics. Despite established acute activation of both the AMPK and Akt-mTOR pathways by IR, irradiated tumours showed a sustained expression and activation of the AMPK-p53/$p21^{cip1}$/$p27^{kip1}$ but inhibition of the activity of the Akt-mTOR-4EBP1 pathway. This was associated with increased expression and sustained activity of the upstream regulator of the two pathways ATM that may be associated with the development of hypoxia in irradiated tumours or with potential genomic instability. These molecular responses of irradiated tumours do not appear to be dependent on typical oncogenic molecular defects detected in lung cancer involving K-Ras, LKB1 or p53 status. The findings of this study provide a basis to understand better the chronic regulation of these key pathways by IR alone. These findings present novel observations of long-term molecular IR regulation in lung cancer cells and whole tumours (Chapter 3).

The work described Chapter 3 demonstrating that IR mediates a favorable chronic modulation of the ATM-AMPK/Akt-mTOR pathways suggested that if we could enhance further those effects of radiation with additional well tolerated therapeutics could increase further the therapeutic ratio of radiotherapy. This notion led to our studies with MET described in Chapter 4. Our studies suggested that MET enhances IR-induced activation of AMPK and clonogenic death (Sanli et al, 2010). MET is proposed as a promising investigational therapeutic in a number of

cancer sites but it has not been examined systematically in lung cancer in combination with radiotherapy (Dowling et al, 2007). Further, investigators remain concerned that most in-vitro studies demonstrate anti-tumour activity at milli-Molar (mM) concentrations of MET which are not clinically achievable (Dowling et al. 2012). The purpose the second part of the study was to: i) investigate the anti-proliferative effects of MET in tissue culture models of LC and to examine its ability to modulate signalling pathways and the cell cycle at clinically achievable micro-Molar (μM) concentrations and ii) to examine whether MET can sensitize human NSCLC cells and tumours to IR (Chapter 4)**.**

We demonstrated that clinically achievable μM doses of MET, can activate molecular pathways of tumour suppression and inhibit pathways of survival and proliferation in NSCLC cells. MET treatment inhibited proliferation and sensitized NSCLC cells and tumours to radiation. Our results support the notion that the DDR – metabolic stress –growth regulation pathways of ATM-AMPK-p53-$p21^{cip1}$/Akt-mTOR-4EBP1 are points of convergence of IR and MET signals that may mediate the anti-tumour action of the two agents through modulation of cell cycle, induction of apoptosis and inhibition of angiogenesis. Figure 9 illustrates our current model of the chronic MET action in tumours. MET has the potential to improve the therapeutic ratio of radiotherapy in NSCLC. The results presented here provide a preclinical basis to consider investigation of MET in combination with radiotherapy in early phase clinical trials of patients with NSCLC.

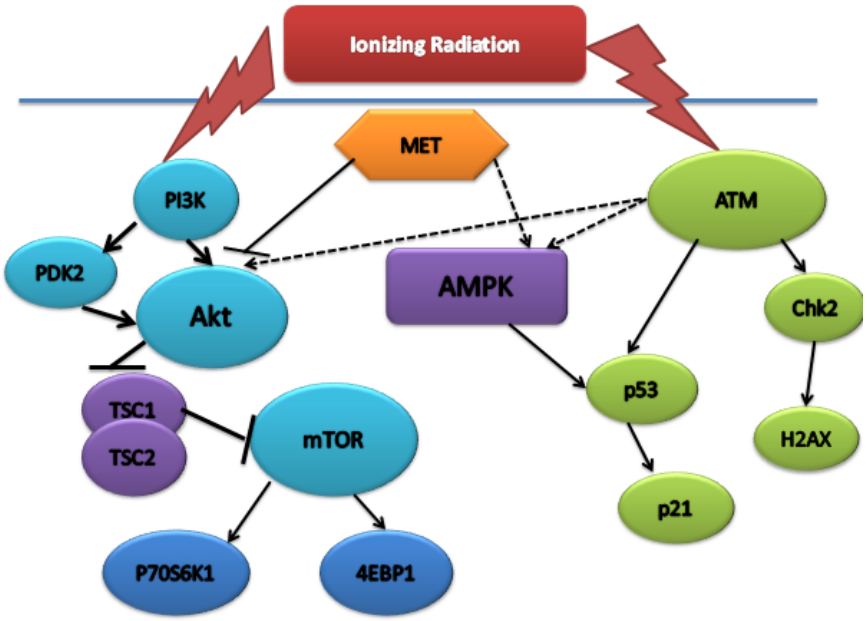

Figure 9. Model of the chronic effects of metformin and radiotherapy in NSCLC tumours. Acutely, ionizing radiation (IR) activates the DNA damage response (DDR) pathway including ATM and leads to activation of both AMPK- and Akt-dependent signal transduction. However, in tumours IR or chronic metformin therapy lead to sustained enhancement of expression and activity of ATM that is associated with stimulation of the AMPK-p53-p21^{cip1} but inhibition of Akt-mTOR-4EBP1pathwaysand this is enhanced further by combined metformin + IR treatment. This favourable modulation of the signalling pathways is suggested to inhibit gene expression and cancer cell survival and is likely responsible for the arrest of the cell cycle, induction of apoptosis and inhibition of cell proliferation, angiogenesis and tumour growth we observed

REFERENCES

Ailles, L., Weissman, IL. (2007). "Cancer stem cells in solid tumours." Current opinion in biotechnology 18(5): 460-466.

Alessi, D., Sakamoto, K,, Bayascas, JR. (2006). "LKB1-dependent signaling pathways." Annual review of biochemistry 75: 137-163.

Anisimov, V., Berstein, LM., Egormin, PA., Piskunova, TS., Popovich, IG., Zabezhinski, MA., Kovalenko, IG., Poroshina, TE., Semenchenko, AV., Provinciali, M, Re, F., Franceschi, C. (2005). "Effect of metformin on life span and on the development of spontaneous mammary tumors in HER-2/neu transgenic mice." Experimental gerontology 40(8-9): 685-693.

Ben Sahra, I., Laurent, K., Loubat, A., Giorgetti-Peraldi, S., Colosetti, P., Auberger, P., Tanti, JF., Le Marchand-Brustel, Y., Bost, F. (2008). "The antidiabetic drug metformin exerts an antitumoral effect in vitro and in vivo through a decrease of cyclin D1 level." Oncogene 27(25): 3576-3586.

Ben Sahra, I., Laurent, K., Giuliano, S., Larbret, F., Ponzio, G., Gounon, P., Le Marchand-Brustel, Y., Giorgetti-Peraldi, S., Cormont, M., Bertolotto, C., Deckert, M., Auberger, P., Tanti, JF., Bost, F. (2010). "Targeting cancer cell metabolism: the combination of metformin and 2-deoxyglucose induces p53-dependent apoptosis in prostate cancer cells." Cancer Research 70(6): 2465-2475.

Billaud, M., Viollet, B. (2008). "Close encounters of a novel kind: a multi-targeted cancer drug meets a metabolic sensor." Cancer biology and therapy 10(1): 77-88.

Böhlig, L., Rother, K. (2010). "One function--multiple mechanisms: the manifold activities of p53 as a transcriptional repressor." Journal of biomedicine and biotechnology 2011: 1-15.

Brazil, D., Yang, ZZ., Hemmings, BA. (2004). "Advances in protein kinase B signalling: AKTion on multiple fronts." Trends in Biochemical sciences 29(5): 233-242.

Buchagen, D. L. (1991). "Molecular Mechanisms in Lung Pathogenesis." Biochemica et Biophysica Acta 1072: 159-176.

Bussink, J., van der Kogel, AJ., Kaanders, JH (2008). "Activation of the PI3-K/AKT pathway and implications for radioresistance mechanisms in head and neck cancer." The Lancet oncology 9(3): 288-296.

Buzzai, M., Jones, RG., Amaravadi, RK., Lum, JJ., DeBerardinis, RJ., Zhao, F., Viollet, B., Thompson, CB. (2008). "Systemic treatment with the antidiabetic drug metformin selectively impairs p53-deficient tumor cell growth." Cancer Research 67(14): 6745-6752.

Cantrell, L., Zhou, C., Mendivil, A., Malloy, KM., Gehrig, PA., Bae-Jump, VL.. (2010). "Metformin is a potent inhibitor of endometrial cancer cell proliferation--implications for a novel treatment strategy." Gynecologic oncology 116(1): 92-98.

Chang, F., Lee, JT., Navolanic, PM., Steelman, LS., Shelton, JG., Blalock, WL, Franklin, RA., McCubrey, JA (2003). "Involvement of PI3K/Akt pathway in cell cycle progression, apoptosis, and neoplastic transformation: a target for cancer chemotherapy." Leukimia 17(3): 590-603.

Chen, B., Li, W. (2010). "Current status of Akt in non-small cell lung cancer." Chinese Journal of Lung Cancer 13(11): 1059-1065.

Cowden Dahl KD, Zeineldin, R., Hudson, LG. (2007). "PEA3 is necessary for optimal epidermal growth factor receptor-stimulated matrix metalloproteinase expression and invasion of ovarian tumor cells." Molecular Cancer Research 5(5): 413-421.

Derheimer, F., Kastan, MB. (2010). "Multiple roles of ATM in monitoring and maintaining DNA integrity." FEBS letters 584(17): 3675-3681.

Diehl, J., Cheng, M., Roussel, MF., Sherr, CJ. (1998). "Glycogen synthase kinase-3beta regulates cyclin D1 proteolysis and subcellular localization." Genes and development 12(22): 3499-3511.

Dowling, R., Zakikhani, M., Fantus, IG., Pollak, M., Sonenberg, N. (2007). "Metformin inhibits mammalian target of rapamycin-dependent translation initiation in breast cancer cells." Cancer Research 67(22): 10804-10812.

Easton, J., Houghton, PJ. (2006). "mTOR and Cancer Therapy." Oncogene 25(48): 6436-6446.

Evans, J., Donnelly, LA., Emslie-Smith, AM., Alessi, DR., Morris, AD. (2005). "Metformin and reduced risk of cancer in diabetic patients." BMJ 330(7503): 1304-1305.

Fan, D., Ma, C., Zhang, H. (2009). "The molecular mechanisms that underlie the tumor suppressor function of LKB1." Acta biochimica et biophysica 41(2): 97-107.

Flynn, R., Zou, L. (2011). "ATR: a master conductor of cellular responses to DNA replication stress." Trends in Biochemical sciences 36(3): 133-140.

Fogarty , S., Hardie DG. (2009). "C-terminal phosphorylation of LKB1 is not required for regulation of AMP-activated protein kinase, BRSK1, BRSK2, or cell cycle arrest." The Journal of biological chemistry 284(1): 77-84.

Fukumura, D., Xu, L., Chen, Y., Gohongi, T., Seed, B., Jain, RK (2001). "Hypoxia and acidosis independently up-regulate vascular endothelial growth factor transcription in brain tumors in vivo." Cancer Research 61(16): 6020-6024.

Gennaro, G., Ménard, C., Michaud, SE., Rivard, A. (2003). "Age-dependent impairment of reendothelialization after arterial injury: role of vascular endothelial growth factor." Circulation 107(2): 230-233.

Graves, E., Maity, A., Le, QT. (2010). "The tumor microenvironment in non-small-cell lung cancer." Seminars in Radiation Oncology 20(3): 156-163.

Gregory J. Riely, J., Marks, and William Pao and (2009). "KRAS Mutations in Non–Small Cell Lung Cancer " Proceedings of the American Thoracic Society 6(2): 201-205.

Gwinn, D., Shackelford, DB., Egan, DF., Mihaylova, MM., Mery, A., Vasquez, DS., Turk, BE., Shaw, RJ. (2008). "AMPK phosphorylation of raptor mediates a metabolic checkpoint." Molecular Cell 30(2): 214-226.

Hahn-Windgassen, A., Nogueira, V., Chen, CC., Skeen, JE., Sonenberg, N., Hay, N. (2005). "Akt activates the mammalian target of rapamycin by regulating cellular ATP level and AMPK activity." The Journal of biological chemistry 280(37): 32081-32089.

Hardie, D. (2007). "AMP-activated/SNF1 protein kinases: conserved guardians of cellular energy." Nature reviews. Molecular cell biology 8(10): 774-785.

Hardie, D. (2011). "Sensing of energy and nutrients by AMP-activated protein kinase." The American journal of clinical nutrition 93(4): 891s-889s896.

Harper, J., Elledge, SJ. (2007). "The DNA damage response: ten years after." Molecular Cell 28(5): 739-745.

Hawley, S., Davison, M., Woods, A., Davies, SP., Beri, RK., Carling, D., Hardie, DG. (1996). "Characterization of the AMP-activated protein kinase kinase from rat liver and identification of

threonine 172 as the major site at which it phosphorylates AMP-activated protein kinase." The Journal of biological chemistry 271(44): 27879-27887.

Hawley, S., Boudeau, J., Reid, JL., Mustard, KJ., Udd, L., Mäkelä, TP., Alessi, DR., Hardie, DG. (2003). "Complexes between the LKB1 tumor suppressor, STRAD alpha/beta and MO25 alpha/beta are upstream kinases in the AMP-activated protein kinase cascade." Journal of biology 2(4): 1-16.

Hirsch, H., Iliopoulos, D., Tsichlis, PN., Struhl, K. (2009). "Metformin selectively targets cancer stem cells, and acts together with chemotherapy to block tumor growth and prolong remission." Cancer Research 69(19): 7507-7511.

Hoogsteen, I., Peeters, WJ., Marres, HA., Rijken, PF., van den Hoogen, FJ., van der Koge,l AJ., Kaanders, JH. (2005). "Erythropoietin receptor is not a surrogate marker for tumor hypoxia and does not correlate with survival in head and neck squamous cell carcinomas." Radiotherapy and oncology 76(2): 213-218.

Huang, S., Houghton, PJ. (2001). "Mechanisms of resistance to rapamycins." Drug Resistance Updates 4(6): 378-391.

Huang, X., Wullschleger, S., Shpiro, N., McGuire, VA., Sakamoto, K., Woods, YL., McBurnie, W., Fleming, S., Alessi, DR. (2008). "Important role of the LKB1-AMPK pathway in suppressing tumorigenesis in PTEN-deficient mice." The Biochemical journal 412(2): 211-221.

Huen, M., Chen, J. (2010). "ATM creates a veil of transcriptional silence." Cell 141(6): 924-926.

Hundal, R., Krssak, M, Dufour, S, Laurent, D, Lebon, V, Chandramouli, V, Inzucchi, SE, Schumann, WC, Petersen, KF, Landau, BR, Shulman, GI. (2000). "Mechanism by which metformin reduces glucose production in type 2 diabetes." Diabetes 49(12): 2063-2069.

Iliopoulos, D., Lindahl-Allen, M., Polytarchou, C., Hirsch, HA., Tsichlis, PN., Struhl, K. (2010). "Loss of miR-200 inhibition of Suz12 leads to polycomb-mediated repression required for the formation and maintenance of cancer stem cells." Molecular Cell 39(5): 761-772.

Iliopoulos, D., Hirsch, HA., Struhl, K. (2011). "Metformin decreases the dose of chemotherapy for prolonging tumor remission in mouse xenografts involving multiple cancer cell types." Cancer Research 71(9): 3196-3201.

Isakovic, A., Harhaji, L., Stevanovic, D., Markovic, Z., Sumarac-Dumanovic, M., Starcevic, V., Micic, D., Trajkovic, V. (2007). "Dual antiglioma action of metformin: cell cycle arrest and mitochondria-dependent apoptosis." Cellular and molecular life sciences 64(10): 1290-1302.

Jiralerspong, S., Palla, SL., Giordano, SH., Meric-Bernstam, F., Liedtke, C., Barnett, CM., Hsu, L., Hung, MC., Hortobagyi, GN., Gonzalez-Angulo, AM. (2009). "Metformin and pathologic complete responses to neoadjuvant chemotherapy in diabetic patients with breast cancer." Journal of clinical oncology 27(20): 3297-3302.

Johnson, D. (2000). "Locally Advanced, Unresectable Non-Small Cell Lung Cancer. New Treatment Strategies." CHEST 117(4): 1235-1265.

Jones, R., Plas, DR., Kubek, S., Buzzai, M., Mu, J., Xu, Y., Birnbaum, MJ., Thompson, CB. (2005). "AMP-activated protein kinase induces a p53-dependent metabolic checkpoint." Molecular Cell 18(3): 283-293.

Kahn, B., Alquier, T., Carling, D., Hardie, DG. (2005). "AMP-activated protein kinase: ancient energy gauge provides clues to modern understanding of metabolism." Cell Metabolism 1(1): 15-25.

Kalaany, N., Sabatini, DM. (2009). "Tumours with PI3K activation are resistant to dietary restriction." Nature 458(7239): 725-731.

Kinner, A., Wu, W., Staudt, C., Iliakis, G. (2008). "Gamma-H2AX in recognition and signaling of DNA double-strand breaks in the context of chromatin." Nucleic Acids Research 36(17): 5678-5694.

Kolch, W. (2002). “Ras/Raf signalling and emerging pharmacotherapeutic targets”. Expert Opinion Pharmacotherapeutic 3(6): 709-718

Kourelis, T., Siegel, RD. (2011). "Metformin and cancer: new applications for an old drug." Medical oncology 29(2): 1314-1327.

Kuo, M., Chuang, SE., Lin, MT., Yang, SY. (2001). "The involvement of PI 3-K/Akt-dependent up-regulation of Mcl-1 in the prevention of apoptosis of Hep3B cells by interleukin-6." Oncogene 20(6): 677-685.

Klotz, N., Vandersluis, R. Besla, N. Fleshner, M. N. Pollak, V. Venkateswaran, A. J. Colquhoun (2011). Utilizing metformin as a radiosensitizing agent in the treatment of prostate cancer. 2011 Genitourinary Cancers Symposium Orlando World Center Marriott in Orlando, Florida

Leverrier, Y., Thomas, J., Mathieu, AL., Low, W., Blanquier, B., Marvel, J. (1999). "Role of PI3-kinase in Bcl-X induction and apoptosis inhibition mediated by IL-3 or IGF-1 in Baf-3 cells." Cell death and differentiation 6(3): 290-296.

Li, Y., Kong, D., Bao, B., Ahmad, A., Sarkar, FH. (2011). "Induction of cancer cell death by isoflavone: the role of multiple signaling pathways." Nutrients 3(10): 877-896.

Liang, J., Shao, SH., Xu, ZX., Hennessy, B., Ding, Z., Larrea, M., Kondo, S., Dumont, DJ., Gutterman, JU., Walker, CL., Slingerland, JM., Mills, GB. (2007). "The energy sensing LKB1-AMPK pathway regulates p27(kip1) phosphorylation mediating the decision to enter autophagy or apoptosis." Nature cell biology 9(2): 218-224.

Lichter, A., Lawrence, TS (1995). "Recent advances in radiation oncology." New England Journal of medicine 332: 371-379.

Liu, B., Fan, Z., Edgerton, SM., Deng, XS., Alimova, IN., Lind, SE., Thor, AD. (2009). "Metformin induces unique biological and molecular responses in triple negative breast cancer cells." Cell cycle 8(13): 2031-2040.

Lovejoy, C., Cortez, D. (2009). "Common mechanisms of PIKK regulation." DNA repair 8(9): 1004-1008.

Lukas, J., Bartek, J. (2004). "Watching the DNA repair ensemble dance." Cell 118(6): 666-668.

Maddocks, O., Vousden, KH. (2010). "Metabolic regulation by p53." Journal of molecular medicine 89(3): 237-245.

Mansi, L., Viel, E., Curtit, E., Medioni, J., Le Tourneau, C. (2011). "Targeting the RAS signalling pathway in cancer." Bulletin du Cancer 98(9): 1019-1028.

Massion, P., Carbone, DP. (2003). "The molecular basis of lung cancer: molecular abnormalities and therapeutic implications." Respiratory Research 4(12): 1-15.

Meier, F., Schittek, B., Busch, S., Garbe, S., Smalley, K., Satyamoorthy, K., Li, G., Herlyn, M. (2005). "The Ras/Raf/Mek/Erk and PI3K/AKT signaling pathways present molecular targets for the effective treatment of advanced melanoma". Frontiers in Bioscience (10): 2986-3001

McNamara, C., Degterev, A. (2011). "Small-molecule inhibitors of the PI3K signaling network." Future Medical Chemistry 3(5): 549-565.

Miliani de Marval, P., Zhang, Y. (2011). "The RP-Mdm2-p53 pathway and tumorigenesis." Oncotarget 2(3): 234-238.

Mogi, A., Kuwano, H. (2011). "TP53 mutations in nonsmall cell lung cancer." Journal of biomedicine and biotechnology 2011.

Natali, A., Ferrannini, E. (2006). "Effects of metformin and thiazolidinediones on suppression of hepatic glucose production and stimulation of glucose uptake in type 2 diabetes: a systematic review." Diabetologia 49(3): 434-441.

Nourse, J., Firpo, E., Flanagan, WM., Coats, S., Polyak, K., Lee, MH., Massague, J., Crabtree, GR., Roberts, JM. (1994). "Interleukin-2-mediated elimination of the p27Kip1 cyclin-dependent kinase inhibitor prevented by rapamycin." Nature 372(6506): 570-573.

Oakhill, J., Chen, ZP., Scott, JW., Steel, R., Castelli, LA., Ling, N., Macaulay, SL., Kemp, BE. (2010). "β-Subunit myristoylation is the gatekeeper for initiating metabolic stress sensing by AMP-activated protein kinase (AMPK)." Proceedings of the American Thoracic Society 107(45): 19237-19241.

O'Driscoll , M., Jeggo, PA. (2006). "The role of double-strand break repair - insights from human genetics." Nature Reviews. Genetics 7(1): 45-54.

Ollila, S., Mäkelä, TP. (2011). "The tumor suppressor kinase LKB1: lessons from mouse models." Journal of molecular cell biology 3(6): 330-340.

Padhani, A.R., Krohn, K.A., Lewis, J.S., Alber, M. (2007). “Imaging oxygenation of human tumours”. European Radiology 17(4): 861–872

Panka, D., Mano, T., Suhara, T., Walsh, K., Mier, JW. (2001). "Phosphatidylinositol 3-kinase/Akt activity regulates c-FLIP expression in tumor cells." The Journal of biological chemistry 276(10): 6893-6896.

Peters, L., Ang, KK (1986). "Unconventional fractionation schemes in radiotherapy." Important advances in oncology 1986: 269-286.

Pollard, T., Blanchoin, L., Mullins, RD. (2011). "Actin dynamics." Journal of cell science 114(1): 3-14.

Polyak, K., Weinberg, RA. (2009). "Transitions between epithelial and mesenchymal states: acquisition of malignant and stem cell traits." Nature reviews.Cancer 9(4): 265-273.

Pópulo, H., Lopes, JM., Soares, P. (2012). "The mTOR Signalling Pathway in Human Cancer." International Journal of Molecular Sciences 13(2): 1886-1918.

Pore, N., Gupta, AK., Cerniglia, GJ., Jiang, Z., Bernhard, EJ., Evans, SM., Koch, CJ., Hahn, SM., Maity A. (2006). "Nelfinavir down-regulates hypoxia-inducible factor 1alpha and VEGF expression and increases tumor oxygenation: implications for radiotherapy." Cancer Research 66(18): 9252-9259.

Reinhardt, H., Yaffe, MB. (2009). "Kinases that control the cell cycle in response to DNA damage: Chk1, Chk2, and MK2." Current opinion in cell biology 21(2): 245-255.

Riches, L., Lynch, AM., Gooderham, NJ. (2008). "Early events in the mammalian response to DNA double-strand breaks." Mutagenesis 23(5): 331-339.

Rocha, G., Dias, MM., Ropelle, ER., Osório-Costa, F., Rossato, FA., Vercesi, AE., Saad, MJ., Carvalheira, JB. (2011). "Metformin amplifies chemotherapy-induced AMPK activation and antitumoral growth." Clinical Cancer Research 17(12): 3993-4005.

Rogakou , E., Pilch, DR., Orr, AH., Ivanova ,VS., Bonner, WM. (1998). "DNA double-stranded breaks induce histone H2AX phosphorylation on serine 139." The Journal of biological chemistry 273(10): 5858-5868.

Romeo. Y/, Z. X., Roux. PP. (2012). "Regulation and function of the RSK family of protein kinases." Biochemical Journal 441(2): 553-569.

Rowell, N., Williams, C (2004). Radical radiotherapy for stage I/II non-small cell lung cancer in patients not sufficiently fit for or declining surgery (medically inoperable) (Review). The Cochrane Library 2009. C. L. C. Group., JohnWiley & Sons, Ltd.

Ruderman. N., P., M. (2004). "AMP kinase and malonyl-CoA: targets for therapy of the metabolic syndrome." Nature reviews. Drug Discovery 3(4): 340-351.

Sarbassov, D., Ali, SM., Kim, DH., Guertin, DA., Latek, RR., Erdjument-Bromage, H., Tempst, P., Sabatini, DM. (2004). "Rictor, a novel binding partner of mTOR, defines a rapamycin-insensitive and raptor-independent pathway that regulates the cytoskeleton." Current Biology 14(14): 1296-1302.

Sause, W., Turrisi, AT (1996). Principles and application of preoperative and standard radiotherapy for regionally advanced non-small cell lung cancer. Philadelphia, PA, Lippincott-Raven.

Schmidt-Ullrich , R., Mikkelsen, RB., Dent, P., Todd, DG., Valerie, K., Kavanagh, BD., Contessa, JN., Rorrer, WK., Chen, PB. (1997). "Radiation-induced proliferation of the human A431 squamous carcinoma cells is dependent on EGFR tyrosine phosphorylation." Oncogene 15(10): 1191-1197.

Schneider, M., Matsuzaki, H., Haorah, J., Ulrich, A., Standop, J., Ding, XZ., Adrian, TE., Pour, PM. (2001). "Prevention of pancreatic cancer induction in hamsters by metformin." Gastroenterology 120(5): 1263-1270.

Secko, D. (2006). “For mTOR, Clarification and Confusion”. The Scientist Magazine. LabX Media Group, Midland, Ontario. http://classic.the-scientist.com/?articles.view/articleNo/24534/title/For-mTOR--Clarification-and-Confusion/

Shackelford, D.B., Shaw, R.J. (2009). “The LKB1–AMPK pathway: metabolism and growth control in tumour suppression”. Nature Reviews Cancer 9: 563-575

Shaw RJ, K. M., Bardeesy N, Hurley RL, Witters LA, DePinho RA, Cantley LC. (2004). "The tumor suppressor LKB1 kinase directly activates AMP-activated kinase and regulates apoptosis in response to energy stress." Proceedings of the American Thoracic Society 101(10): 3329-3335.

Sheppard, K., Kinross, KM., Solomon, B., Pearson, RB., Phillips, WA. (2012). "Targeting PI3 kinase/AKT/mTOR signaling in cancer." Critical Reviews in oncogenesis 17(1): 69-95.

Shimuras, T. (2011). "Acquired radioresistance of cancer and the AKT/GSK3β/cyclin D1 overexpression cycle." Journal of radiation research 52(5): 539-544.

Shu, Y., Sheardown, SA, Brown, C, Owen, RP, Zhang, S, Castro, RA, Ianculescu, AG, Yue, L, Lo, JC, Burchard, EG, Brett, CM, Giacomini, KM. (2007). "Effect of genetic variation in the organic cation transporter 1 (OCT1) on metformin action." The Journal of clinical investigation 117(5): 1422-1431.

Stein, S., Woods, A., Jones, NA., Davison, MD., Carling, D. (2000). "The regulation of AMP-activated protein kinase by phosphorylation." The Biochemical journal 345(3): 437-443.

Steinberg, G., Kemp, BE. (2009). "AMPK in Health and Disease." Physiological reviews 89(3): 1025-1078.

Stucki, M. (2009). "Histone H2A.X Tyr142 phosphorylation: a novel sWItCH for apoptosis?" DNA repair 8(7): 873-876.

Suter, M., Riek, U., Tuerk, R., Schlattner, U., Wallimann, T., Neumann, D. (2006). "Dissecting the role of 5'-AMP for allosteric stimulation, activation, and deactivation of AMP-activated protein kinase." The Journal of biological chemistry 281(43): 32207-32216.

Suzuki, M., Kase, Y., Kanai, T., Ando, K (1998). "Residual chromatin breaks as biodosimetry for cell killing by carbon ions." Advances in Space Research 22(12): 1663-1671.

Tang, J., Greenberg ,RA. (2010). "Connecting the Dots: Interplay between Ubiquitylation and SUMOylation at DNA Double-Strand Breaks." Genes and cancer 1(7): 787-796.

Tichý, A., Vávrová, J., Pejchal, J., Rezácová, M. (2010). "Ataxia-telangiectasia mutated kinase (ATM) as a central regulator of radiation-induced DNA damage response." Astra Medica 53(1): 13-17.

Tomimoto, A., Endo, H., Sugiyama, M., Fujisawa, T., Hosono, K., Takahashi, H., Nakajima, N., Nagashima, Y., Wada, K., Nakagama, H., Nakajima, A. (2009). "Metformin suppresses intestinal polyp growth in ApcMin/+ mice." Cancer science 99(11): 2136-2141.

Toulany, M., Dittmann, K., Krüger, M., Baumann, M., Rodemann, HP. (2005). "Radioresistance of K-Ras mutated human tumor cells is mediated through EGFR-dependent activation of PI3K-AKT pathway." Radiotherapy and oncology 76(2): 143-150.

Toulany , M., Kasten-Pisula, U, Brammer, I, Wang, S, Chen, J, Dittmann, K, Baumann, M, Dikomey, E, Rodemann, HP. (2006). "Blockage of epidermal growth factor receptor-phosphatidylinositol 3-kinase-AKT signaling increases radiosensitivity of K-RAS mutated human tumor cells in vitro by affecting DNA repair." Clinical Cancer Research 12(13): 4119-4126.

Travis, W. (2011). "Pathology in Lung Cancer." Clinics in Chest Medicine 32(4): 669-692.

Upadhyay, S., Liu, C., Chatterjee, A., Hoque, MO., Kim, MS., Engles, J., Westra, W., Trink, B., Ratovitski, E., Sidransky D. (2006). "LKB1/STK11 suppresses cyclooxygenase-2 induction and cellular invasion through PEA3 in lung cancer." Cancer Research 66(16): 7870-7879.

Viollet, B., Horman, S., Leclerc, J., Lantier, L., Foretz, M., Billaud, M., Giri, S., Andreelli, F (2010). "AMPK inhibition in health and disease." Critical reviews in biochemistry and molecular biology 45(4): 276-295.

Webster, L., Hodgkiss, RJ., Wilson, GD. (1998). "Cell cycle distribution of hypoxia and progression of hypoxic tumour cells in vivo." British journal of cancer 77(2): 227-234.

Witters, L. (2001). "The blooming of French lilac." The Journal of clinical investigation 108(8): 1105-1107.

Woods, A., Johnstone, SR., Dickerson, K., Leiper, FC., Fryer, LG., Neumann, D., Schlattner, U., Wallimann, T., Carlson, M., Carling D. (2003). "LKB1 is the upstream kinase in the AMP-activated protein kinase cascade." Current Biology 13(22): 2004-2008.

Yang, J., Hung, MC. (2011). "Deciphering the role of forkhead transcription factors in cancer therapy." Current Drug Targets 12(9): 1284-1290.

Yokogami, K., Wakisaka, S., Avruch, J., Reeves, SA. (2000). "Serine phosphorylation and maximal activation of STAT3 during CNTF signaling is mediated by the rapamycin target mTOR." Current Biology 10(1): 47-50.

Zakikhani, M., Dowling, R., Fantus, IG., Sonenberg, N., Pollak, M. (2006). "Metformin is an AMP kinase-dependent growth inhibitor for breast cancer cells." Cancer Research 66(21): 10269-10273.

Zhang, Z., Wang, Z. (2011). "K-ras role in lung cancer therapy." Minerva Chirurhiga 66(3): 251-268.

Zheltukhin, A., Chumakov PM. (2010). "Constitutive and induced functions of the p53 gene." Biochemistry (Moscow) 75(13): 1692-1721.

Zhu, B., Zhou, X. (2010). "The study of PI3K/AKT pathway in lung cancer metastasis and drug resistance." Chinese Journal of Lung Cancer 14(8): 689-694.